PETROLOGY OF THE DEER PEAK VOLCANICS, COLORADO

by

Michael J. DiMarco

B.A. State University of New York at Buffalo, 1979

A MASTER'S THESIS

submitted in partial fulfillment of the

requirements for the degree

MASTER OF SCIENCE

Department of Geology

KANSAS STATE UNIVERSITY
Manhattan, Kansas

1983

Approved by:

Major Professor

CONTENTS

ILLUSTRATIONS

TABLES

THIS BOOK
CONTAINS
NUMEROUS PAGES
WITH THE ORIGINAL
PRINTING BEING
SKEWED
DIFFERENTLY FROM
THE TOP OF THE
PAGE TO THE
BOTTOM.

THIS IS AS RECEIVED
FROM THE
CUSTOMER.

I N T R O D U C T I O N

STATEMENT OF THE PROBLEM

The Deer Peak Volcanics, a newly identified formation of Oligocene age (Scott and Taylor, 1975), consist of deeply dissected exposures along the crest of the Wet Mountains about 35 miles southwest of Pueblo, Colorado (Figs. 1 and 2). These rocks represent the roots of a central-vent, intermediate-composition volcano and remnants of its associated volcanic field. The formation is in the central part of a belt of Tertiary volcanic rocks that extends from the Rosita Hills volcanic field (Siems, 1968; Smalley, 1981) southeasterly to the volcanic rocks that cap Greenhorn Peak (Fig. 2).

This investigation focuses on the petrology of the Deer Peak volcanic-rock suite. Major- and trace-element data are integrated with field and petrographic observations to describe and characterize the suite. Petrogenetic models are developed to: (1) establish possible sources, (2) estimate the degree of partial melting, and (3) investigate the extent of magma evolution by fractional crystallization or other processes.

This study contributes to an increased understanding of an extensive mid-Tertiary volcanic episode that occurred in south-central Colorado and adjacent areas (Steven, 1975). The results of this study should en-

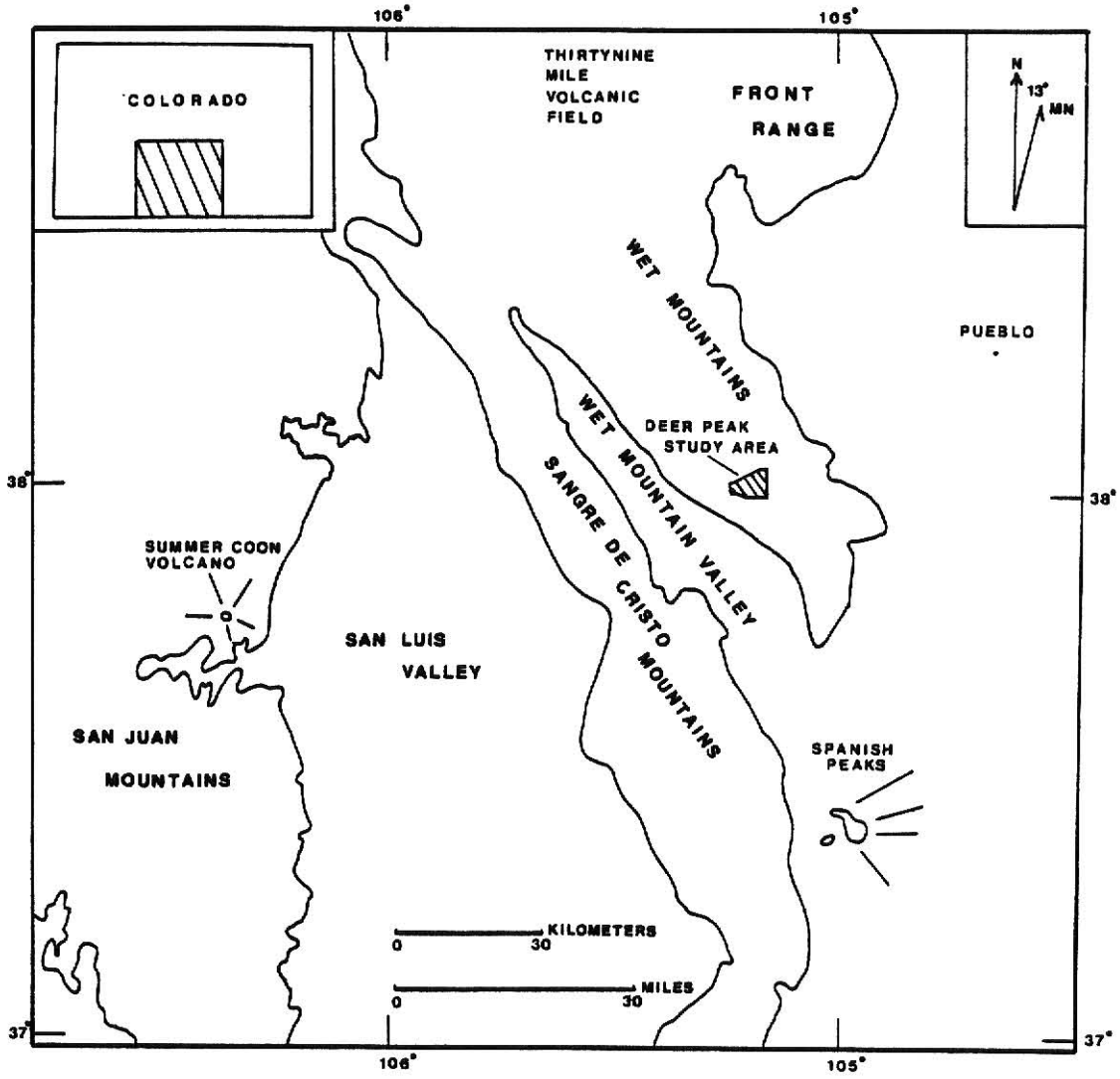

Figure 1: Index map of south-central Colorado (after Tweto, 1979).

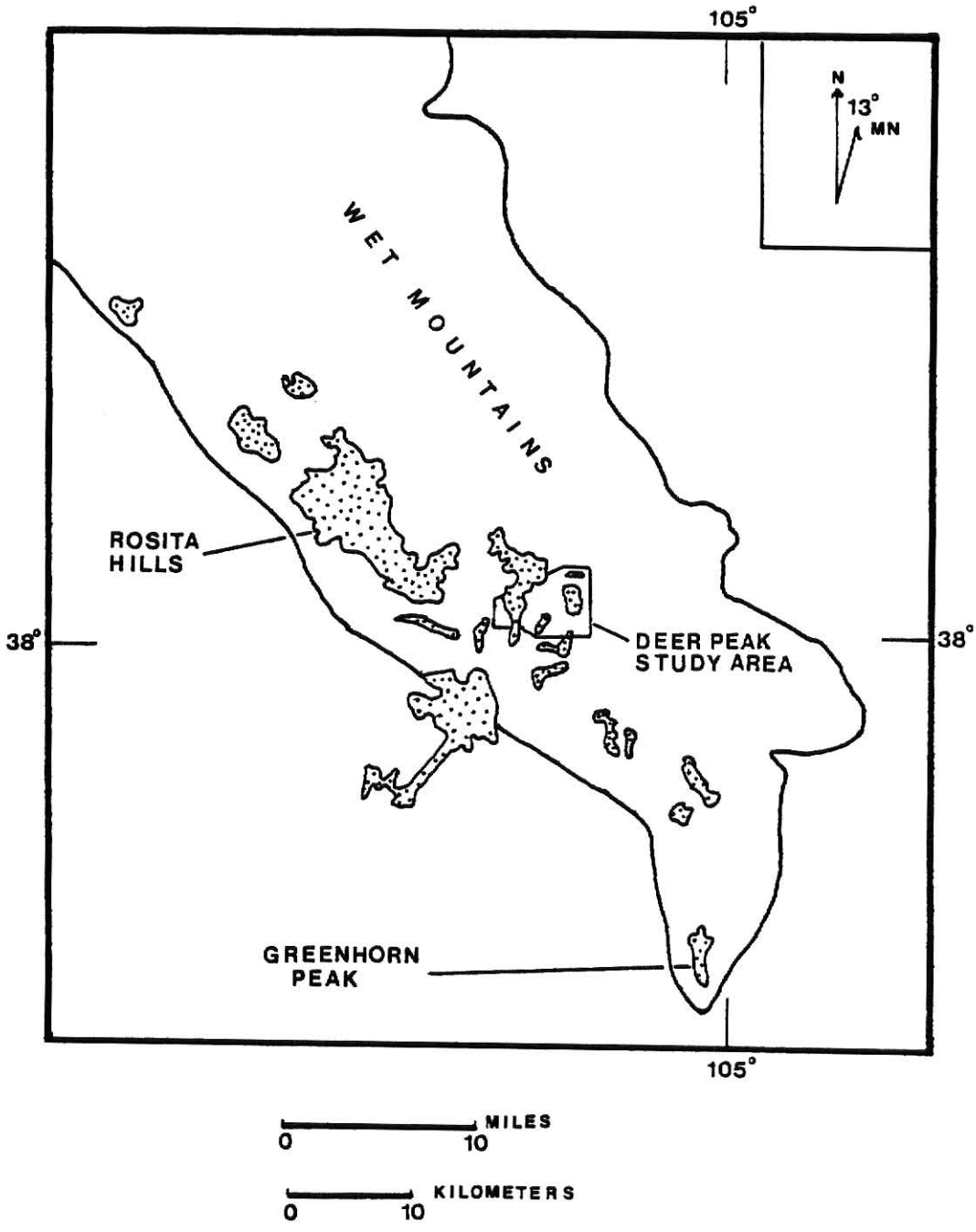

Figure 2: Distribution of Tertiary volcanic rocks (stippled) on the Wet Mountains block (after Tweto, 1979).

courage further geochemical investigations of volcanic rocks in the Wet Mountains.

ACKNOWLEDGMENTS

I would like to acknowledge the assistance of my major professor Robert L. Cullers, for his continued guidance throughout this research project. I would also like to thank Page C. Twiss, Ronald R. West, and James L. Copeland for serving on my supervisory committee and for their constructive criticism of this thesis. I also benefited from numerous discussions with the remaining members of the faculty of the Department of Geology at Kansas State University.

The assistance of the staff of the Department of Nuclear Engineering at Kansas State University is greatly appreciated. Jerry James, of the Kansas Geological Survey, provided analyses by X-ray fluorescence. Brad LaRue drafted many of the figures.

I reserve a special, heart-felt thanks for my wife, Ramona, who provided continued encouragement and inspiration throughout this project.

This research was partially supported by a Grant-in-Aid by Sigma Xi, the Scientific Research Society of North America.

PREVIOUS INVESTIGATIONS

Deer Peak Volcanics

The Deer Peak Volcanics (formation name and used in Lexicon of Geologic Names (Luttrell and others, 1981)) were named and described by Scott and

Taylor (1975) who identified andesite and latite lava flows, lahars, and other volcaniclastic sedimentary rocks that erupted from a central-vent volcano. Because of erosion, only patches of the volcanic field remain. Lava flows occur within 4 miles of the former vent, which is now represented by a composite stock. Scott and Taylor (1975) determined that 2,000 to 4,000 feet of rock have been eroded from the stock.

Rocks that are now part of the Deer Peak Volcanics were mapped by Boyer (1962) in a structural and petrologic survey of the southern Wet Mountains. Volcaniclastic rocks that originated at the Deer Peak volcano were considered part of the Rosita Formation by Siems (1968); similar rocks were designated as part of the Devils Hole Formation by Guyton and others (1960). Johnson (1969) included some of the southern-most lahars of the Deer Peak Volcanics on his map of the Devils Hole area.

Scott and Taylor (1975) stated that the Deer Peak Volcanics are Oligocene in age, and that the Deer Peak volcano erupted during an appreciable part of the Oligocene activity of the adjacent Rosita volcanic center. Briggs (in McCulloch, 1963; and in MacNish, 1966) obtained a potassium-argon date of 38.2 ± 1.5 m.y. from biotite in an andesite boulder embedded in the lower-most lahar at the type locality of the Deer Peak Volcanics. Scott and Taylor (1975) inferred that the andesite boulder originated at the Deer Peak volcano and that the age of the boulder would represent early eruptive activity at Deer Peak. MacNish (1966), however, suggested that reworked Precambrian biotite might constitute a small but significant fraction of biotite in Wet Mountains

volcaniclastic rocks; potassium-argon analysis of such biotite would result in anomalously old dates for the volcanic rocks. Consequently, Scott and Taylor (1975) believed that the 38.2 m.y. date is a few million years older than the age of early volcanic activity at Deer Peak.

Mid-Tertiary Volcanic Field

Volcanic rocks that are similar in age and composition to the Deer Peak Volcanics occur throughout south-central Colorado (Figs. 1 and 2). The Rosita Hills volcanic center, about 15 miles northwest of Deer Peak, was studied by Cross (1890, 1896), Siems (1968), and Smalley (1981). Epis and Chapin (1968) investigated the Thirtynine Mile volcanic field, about 40 miles north of the Deer Peak Volcanics. Petrology of the Spanish Peaks intrusive complex, about 50 miles south of Deer Peak, was studied by Jahn (1973), Jahn and others (1979), and Smith (1979). Thick sequences of volcanic rocks occur in the San Juan Mountains, about 60 miles west of the Wet Mountains (Lipman, 1968; Zielinski and Lipman, 1976).

Steven and Epis (1968) suggested that a widespread volcanic sheet covered south-central Colorado 40 to 25 million years ago. Steven (1975) concluded that this volcanic field represented a coalesence of volcanic rocks of smaller fields that completely covered an Eocene erosional surface. Steven (1975) stated that these volcanic rocks are predominantly calc-alkalic and intermediate in composition, although rocks along the eastern fringe of this field are distinctly more alkalic.

The Wet Mountain Valley and the San Luis Valley, which are fault-bounded troughs, occur near the eastern border of the mid-Tertiary

volcanic field. Scott and Taylor (1975) inferred that the Wet Mountain Valley began subsiding in the latest Cretaceous. Scott and Taylor (1975) and MacNish (1966) suggested that northwest-trending faults associated with the development of the Wet Mountain valley controlled the northwest trend of mid-Tertiary volcanism in the Wet Mountains region. The San Luis Valley is a northern extension of the Rio Grande Rift and began subsiding in the Miocene (Seager and Morgan, 1979).

Volcano-tectonic Setting

Suites of mainly andesitic rocks that occur in orogenic regions at or near continental margins were collectively referred to as the andesitic association (Dickenson and Hatherton, 1967). The andesitic association was also termed the orogenic suite (Taylor and White, 1965), the basalt-andesite-rhyolite association (Turner and Verhoogen, 1960), the hypersthenic series (Kuno, 1959), and the volcanic-rock series (Miyashiro, 1974). Dickenson and Hatherton (1967) noted that the andesitic association is geochemically polarized; rocks that occur farther from the continental margin are generally more alkalic than those that occur near the continental edge. As summarized by Green (1980): "Rocks once collectively termed the orogenic, calc-alkaline suite are now recognized as forming a continuum between tholeiitic, calc-alkaline, and alkalic suites." Kieth (1978) divided the andesitic association into five geochemical groups that correlate with increasing distance from the continental edge in southwestern North America: (1) calcic, (2) calc-alkaline, (3) high-potassic calc-alkaline, (4) alkali-calcic, and (5) alkalic. The relationship between alkali-rich suites that occur farthest from the continental margin and tectonic setting is poorly understood (Leeman, 1982).

The mid-Tertiary volcanic field in Colorado is about 1500 km inland from the Pacific margin and is part of a diffuse, north-south belt of moderately to strongly alkalic rocks on the eastern periphery of the North American cordillera. Tertiary volcanic rocks that are chemically and petrographically similar to those of the mid-Tertiary province in Colorado occur in Montana and Wyoming (Chadwick, 1970), in New Mexico (Thompson, 1972), and in the Trans-Pecos region of Texas (Barker, 1977). Except for the volcanic rocks in West Texas, this belt of alkali-rich volcanism is superimposed on the Colorado-Wyoming Rocky Mountain terrane (Burchfiel, 1980), which consists of uplifts of Precambrian crystalline rock. As in the case of alkali-rich, continental-interior volcanic rocks, the origin of the Colorado-Wyoming Rocky Mountain terrane is obscure, although Burchfiel (1980) believed its development is ultimately related to plate-boundry interaction.

Lipman and others (1972) recognized that variations in Cenozoic volcanism correlated closely with changes in tectonic style in the western United States. Early and mid-Cenozoic andesitic volcanism erupted through orogenic or fairly stable crust whereas late Cenozoic basaltic volcanism occurred concurrently with crustal extension. Elston and Bornhorst (1979) envisioned three volcano-tectonic stages in the volcanic history of the southwestern United States: (1) Modified Andean Arc stage, 40 to 29 m.y., with andesitic volcanism; (2) Modified back-arc extension stage, 30 to 18 m.y., with eruption of basaltic andesite; and (3) Intraplate block faulting, 21 m.y. to present, characterized by eruption of alkali and tholeiitic basalt.

Petrogenesis

Isotopic and trace-element studies (Lipman and others, 1978; Zielinski and Lipman, 1976) indicated that andesitic rocks in Colorado probably originated by partial melting of eclogite. Models involving an eclogite source for andesitic rocks can be divided into those that are related to a subduction system and those that are unrelated, at least directly, to plate tectonics.

Based on plate-tectonic reconstructions (Atwater, 1970; Atwater and Molnar, 1973) and K_2O-SiO_2 systematics (Dickenson and Hatherton, 1967), Lipman and others (1972) hypothesized that an imbricate subduction system provided the eclogite source for andesitic volcanism in the western United States; the innermost member of this pair of subducted oceanic slabs generated volcanism in Montana, Wyoming, Colorado, New Mexico, and West Texas. Other individuals (Coney and Reynolds, 1977; Cross and Pilger, 1978) suggested that increased rates of convergence during the early Cenozoic decreased the dip of an inferred subducted slab and thereby initiated andesitic volcanism in the eastern cordillera of the United States.

In many cases, simple direct models involving one-stage melting of subducted eclogite do not account for the observed abundances of trace elements in andesitic rocks. Complex models were proposed by many authors (e.g. Gill, 1981) for the petrogenesis of andesitic rocks; these models incorporate one or more of the following processes: magma mixing, assimilation, zone refining, multiple contributions from different sources, and various metasomatic processes.

Eclogite that is indigenous to the continental lithosphere and is

unrelated to plate tectonics was also considered a likely source for andesitic rocks in the western United States (Elston and Bornhorst, 1979), especially for alkali-rich andesitic rocks (Miller, 1978). Xenoliths of eclogite are commonly found in diatremes, as at the Moses Rock diatreme in Utah (McGetchen and Silver, 1972); these xenoliths apparently represent the subcontinental lithosphere. Brooks and others (1976) suggested that lower-crustal eclogite might originate from periodic melting episodes of upper-mantle peridotite. Smith (1979) suggested that deep-crustal faults associated with incipient stages of the development of the Rio Grande Rift generated magmatism at the Spanish Peaks.

The results of experimental petrology support an eclogite source for andesitic rocks (Green and Ringwood, 1967, 1968; Wyllie, 1973). Under hydrous conditions, low (< 10 percent) and intermediate (10 to 40 percent) percentages of melting produce dacitic and andesitic liquids respectively. Dry melting of eclogite produces only andesitic liquids, and only by low percentages of melting.

Kushiro and others (1972) claimed that partial melting of wet peridotite produced andesitic liquids at 1190° C. Other experimental groups, however, refuted this claim and reported that partial melting of peridotite produces basaltic, not andesitic liquids (Nicholls and Ringwood, 1973; Green, 1973; Ringwood, 1974). Consequently, basaltic rocks in the western United States probably originated by partial melting of upper-mantle peridotite. Alkali-rich basalts are generally produced by 5 percent of melting or less (Cullers and Graf, in press; Green, 1973).

Bowen (1928, p. 62-122) suggested that fractional crystallization is a dominant process in magma differentiation. Trace-element studies indicate that some silicic members (dacite, rhyodacite, and rhyolite) of the

andesitic association form from more mafic parents (andesite) by fractional crystallization (Fountain, 1979; Zielinski and Lipman, 1976). Experimental petrology shows that low-pressure fractional crystallization of a number of assemblages, which include olivine, magnetite, pyroxene, hornblende, or plagioclase, or combinations thereof, increases the silica content of both basaltic and andesitic liquids (Osborne, 1969; Nicholls and Ringwood, 1973; Green and Ringwood, 1968; Wyllie, 1971).

Hildreth (1981) summarized evidence that thermogravitational diffusion of elements is the dominant process of differentiation in very viscous, high-silica magmas. Hildreth (1981) believed that fractional crystallization is a minor process in these systems.

Trace-element Modeling

Trace elements are extremely sensitive indicators of magma-differentiation processes (e.g. Hanson, 1978). In most cases, trace elements do not form their own minerals, but instead may substitute for major elements in rock-forming minerals.

In recent years, the partitioning of trace elements in crystal-liquid equilibria has been investigated and quantified (e.g. Arth and Hanson, 1975; Schnetzler and Philpotts, 1968). The distribution coefficient (D.C.) is defined as the ratio of the concentration of a particular trace element in a crystal relative to its concentration in a coexisting liquid. An incompatible element has a D.C. less than one and partitions into the liquid phase during crystal-liquid equilibria; a compatible element has a D.C. greater than one, and concentrates in solid phases.

Several mathematical relationships that model trace-element behavior in petrologic systems have been proposed (e.g. Gast, 1968; Shaw, 1970).

In order to use such models effectively, several assumptions must be made:

(1) Mineralogy and mineral proportions in possible sources must be estimated. Xenoliths of crustal and upper-mantle rocks constrain such estimates.

(2) The relative contribution of each phase in the source to the melt must be assumed. These assumptions are supported by experimental data.

(3) Distribution coefficients must be estimated. These values are a function of temperature, pressure, and composition of the system. Thus, behavior of trace elements can vary widely in different silicate systems and at different depths.

(4) The trace-element concentration of the source must be assumed. This is constrained by published values of abundances of trace elements in rocks compositionally similar to the model source and by inferences generated by other petrologic studies.

(5) The physical situation governing the separation of the derivative phases (melt or phenocrysts) from the residual phases (source or unfractionated liquid) must be assumed. In partial-melting processes, two end-member situations may be considered, batch melting and aggregate melting. In batch melting, a discrete amount, i.e., "batch," of melt is produced and removed from equilibrium with the source when conditions become favorable. At the other

extreme, aggregate melting occurs when infinitesimally small amounts of liquid are continuously produced, removed from the source, and added together.

(6) The mathematical relationship must model all aspects of petrogenesis and must be assumed. This is perhaps the least constrainable assumption. Many complex models cannot be tested because chemical behavior in hypothesized processes is poorly understood or the processes themselves are undetectable. Also, trace-element modeling equations do not account for trace-element behavior in post-solidification processes such as weathering, hydrothermal alteration, and devitrification; large-ion-lithophile elements (LILE) are particularly mobile in such processes (Mason, 1966). Furthermore, post-solidification processes are not always detectable by petrographic methods.

Despite these assumptions, trace-element modeling has been used with success to investigate a variety of igneous processes. In most cases, such modeling does not provide unique solutions to petrogenetic hypotheses, but is most effective in limiting the range of possible magma sources and in imposing constraints on magma evolution by fractional crystallization.

CLASSIFICATION OF THE DEER PEAK VOLCANIC ROCKS

Classification of igneous rocks has traditionally been based on

mineralogy (Johannsen, 1939; Williams, Turner, and Gilbert, 1954). This method of classification, however, is difficult to apply to volcanic rocks, because much of the rock may be aphanitic or glassy. Moreover, moderately and strongly alkalic rocks of the andesitic association are not necessarily distinguishable by routine petrography from their less alkalic counterparts (Ewart, 1979).

Because of these problems, many current workers prefer a simpler classification scheme for andesitic rocks based on a plot of K_2O versus SiO_2. The Deer Peak Volcanics are classified in Figure 3. This classification is based on the scheme of Peccerillo and Taylor (1976) with minor modifications: (1) their "banakite" field was renamed "latite" in order to replace a rock name that is used mainly in the southwestern Pacific region with one commonly used in the western United States, and (2) their "rhyolite" field was subdivided into "high-silica rhyolite" and "low-silica rhyolite", based on petrogenetic differences inferred in this thesis.

In this classification scheme, a group of rocks straddles the divider between latite and high-potassium andesite, although most of the rocks are in the latite field. Henceforth in this report, this group will be termed the latite group.

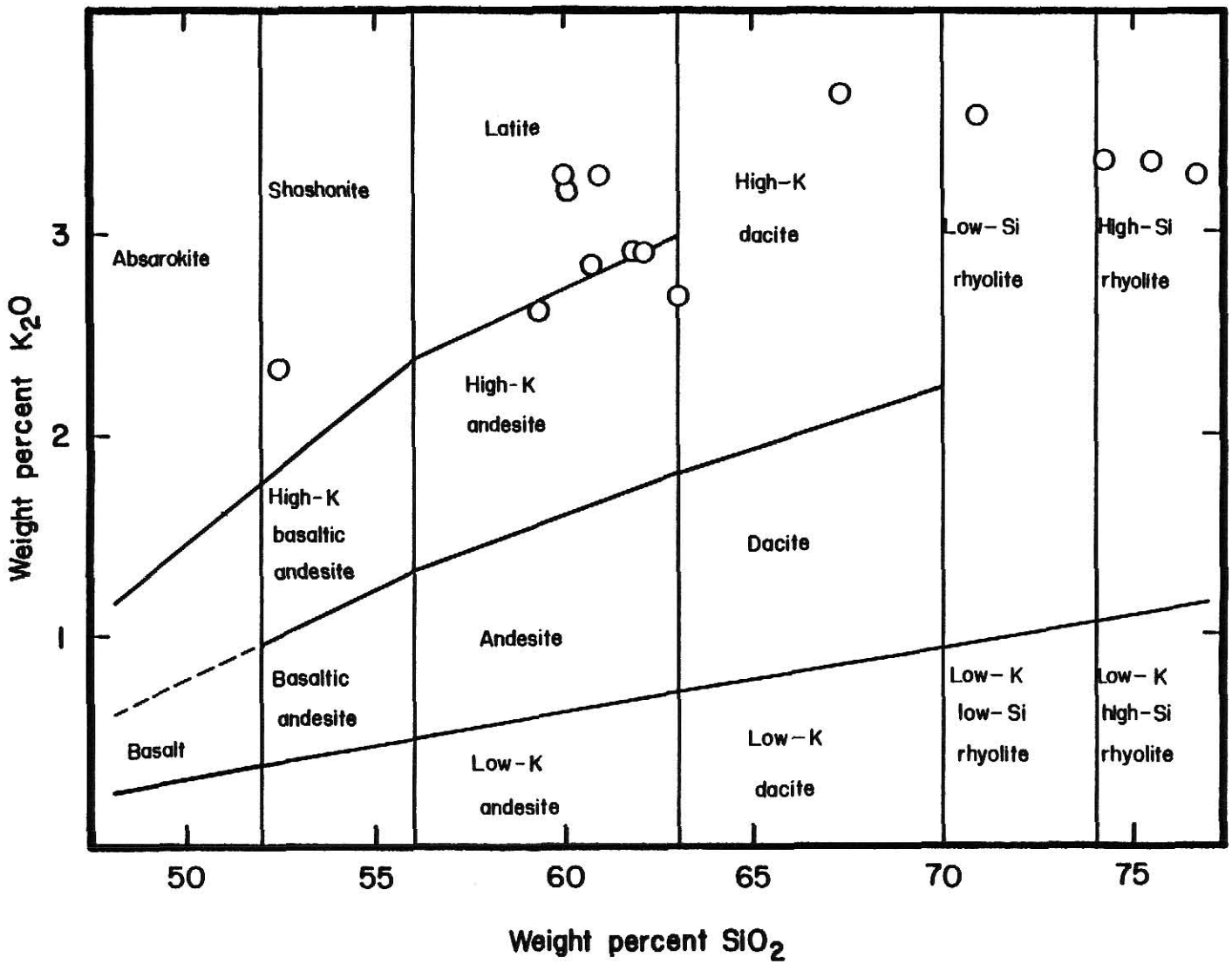

Figure 3: Classification of the Deer Peak volcanic rocks. (Modified from Peccerillo and Taylor, 1976.)

METHODS

FIELD AND MAPPING TECHNIQUES

The reconnaissance map of Taylor (1974) showed the general location of volcanic-rock exposures in the Deer Peak quadrangle. Geologic contacts were walked laterally, and numerous traverses were made across igneous bodies to: (1) define the aerial extent of each exposure as precisely as possible, (2) define the lithologic types in each exposure, and (3) establish age relationships among the rock types. In many cases, bedrock geology was inferred on the basis of float (Compton, 1962, p. 61) because of poor exposure.

Geologic data were plotted directly on 10 in. by 10 in. air photos of 1:18728 scale (Compton, 1962, p. 51). The geologic map was constructed by transferring data from the air photo to a U. S. Geological Survey 1:24000-scale topographic map of the Deer Peak quadrangle. Data points on the air photo that could be correlated precisely to locations on the topographic map were transferred by inspection; data points that could not be correlated precisely were transferred by resection (Compton, 1962, p. 86).

Samples of all lithologic types were collected. The least weathered of these were brought to the laboratory for petrographic and chemical analysis. Samples were coded in the field with two numerals separated by a dash. The first numeral refers to the date (in June, 1980); the second represents the number of samples that were collected up to that time on

that particular day. This system permitted ease of correlation among sample, air photo, and notebook.

PETROGRAPHIC TECHNIQUES

Thin sections were prepared from thirty-five of the most visibly unaltered samples. Mineral percentages were obtained by the Chayes (1949) point-count method. The color of unweathered rock was determined by comparison to the Geological Society of America rock-color chart (Goddard and others, 1948); color codes are reported in parentheses.

Composition of clinopyroxene was estimated by measuring Z ∧ C of longitudinal sections that had the highest order interference colors. Composition of plagioclase was estimated by the Michel-Lévy method (1877) and is expressed as the percentage of albite component (Ab). Many plagioclase crystals are zoned; the median composition was recorded for each crystal that was measured; the reported range represents the range of median plagioclase values that were measured in a particular rock. The composition of sanidine was approximated by estimating the 2V angle in acute bisectrix figures and is expressed as the percentage of orthoclase component (Or).

CHEMICAL TECHNIQUES

Fourteen of the freshest samples that spanned the range of composition within the suite were chosen for chemical analysis. These samples were broken with a sledge hammer to obtain fragments with unweathered surfaces. The fragments were pulverized in a steel ball-mill. Aliquots of powdered rock were analyzed chemically.

Major-element contents, except for P, were determined by atomic-absorption and flame-emission techniques. The method was adopted from the procedures of Medlin and others (1969) and Shapiro (1978). Details of the major-element analyses are in Appendix A.

Trace-element contents, except for Sr, were determined by instrumental neutron activation analysis (INAA). The method was adapted from Gordon and others (1968) and Jacobs and others (1977). Details of INAA techniques are in Appendix B.

Concentrations of Rb, Sr, Ba, and P were determined by James (1980) using X-ray fluorescence. Details of this technique are in Appendix C.

Certain elements were determined by two techniques; this served as a check on internal experimental consistency. Concentrations of Rb and Ba were determined by INAA and X-ray fluorescence. Abundances of Na and Fe were obtained by atomic absorption and INAA.

Total volatile content was measured gravimetrically. Details are in Appendix D.

TRACE-ELEMENT MODELING

In this investigation, the non-modal aggregate-melting relationship developed by Shaw (1970) is used to model partial-melting processes. The equation of Haskin and others (1970) is used to predict the chemical effects of fractional crystallization. These equations, and D.C. values used in the models are given in Appendices E and F.

G E O L O G Y

GENERAL

Field observations and geologic mapping of parts of the Deer Peak Volcanics were completed in June and July of 1980. This work served to: (1) refine Taylor's reconnaissance map, (2) provide a framework for appropriate selection of samples for laboratory analysis, and (3) provide background for formulation of petrogenetic hypotheses.

Field work focused on an area of approximately 11 square miles within the Deer Peak Quadrangle. This area includes the type locality of the Deer Peak Volcanics, the central stock, and five other smaller exposures within a radius of 1.5 miles of the stock (Fig. 4).

Precambrian rocks underlie all Oligocene volcanic and volcaniclastic rocks (Fig. 4). Latite, which is the most abundant rock in the suite, was the first volcanic rock that erupted in most localities, and continued to erupt throughout the time of emplacement of most of the volcanic sequence at Deer Peak. Minor amounts of high-potassium dacite and rhyolite erupted during the time in which latite was emplaced. During the waning stages of volcanism, masses of vitrophyre and of shoshonite, and a hydrothermal breccia pipe intruded latite and high-potassium dacite.

The area has rugged topography and ranges in elevation from about

Figure 4: Geology of the Deer Peak study area.

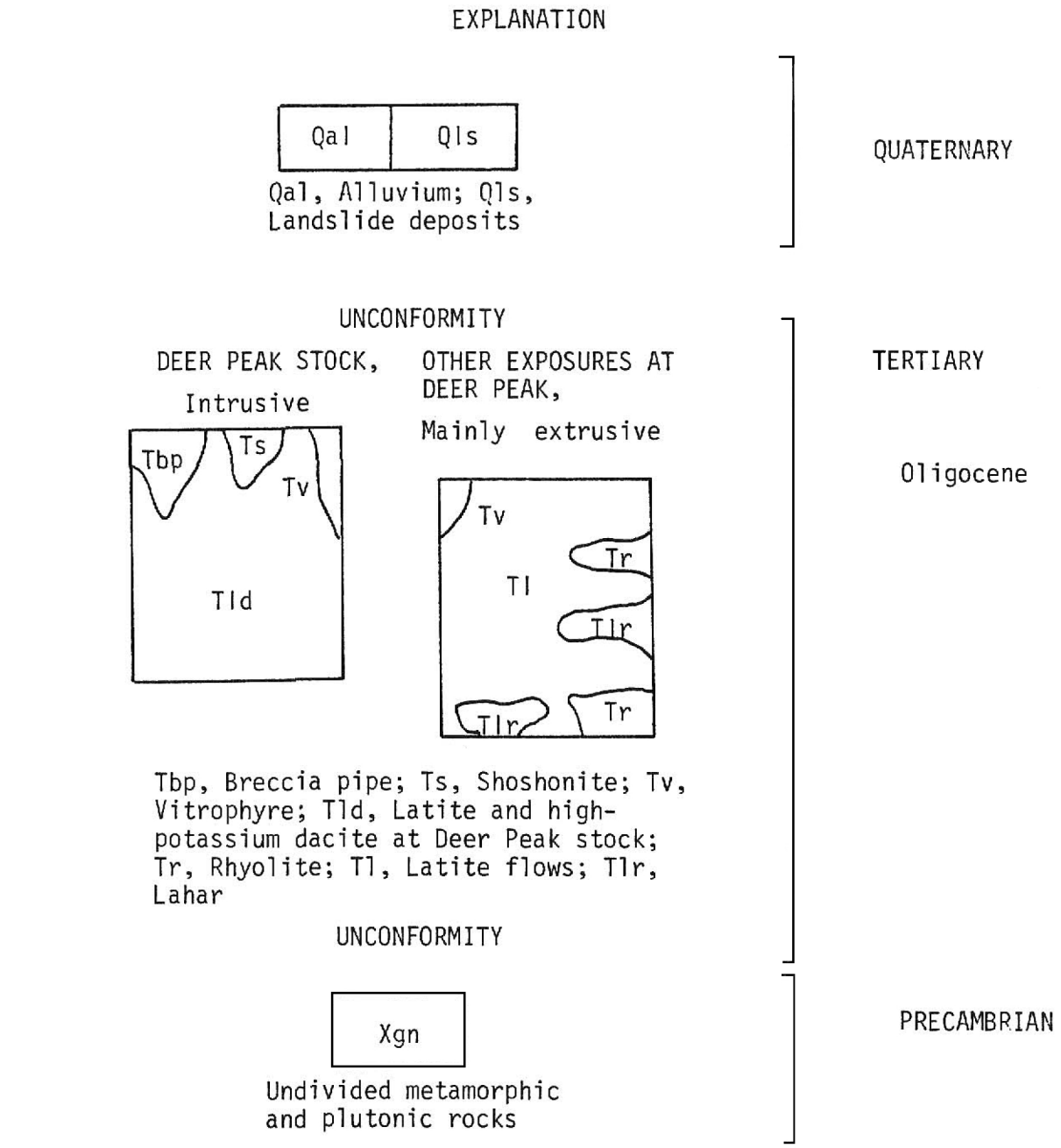

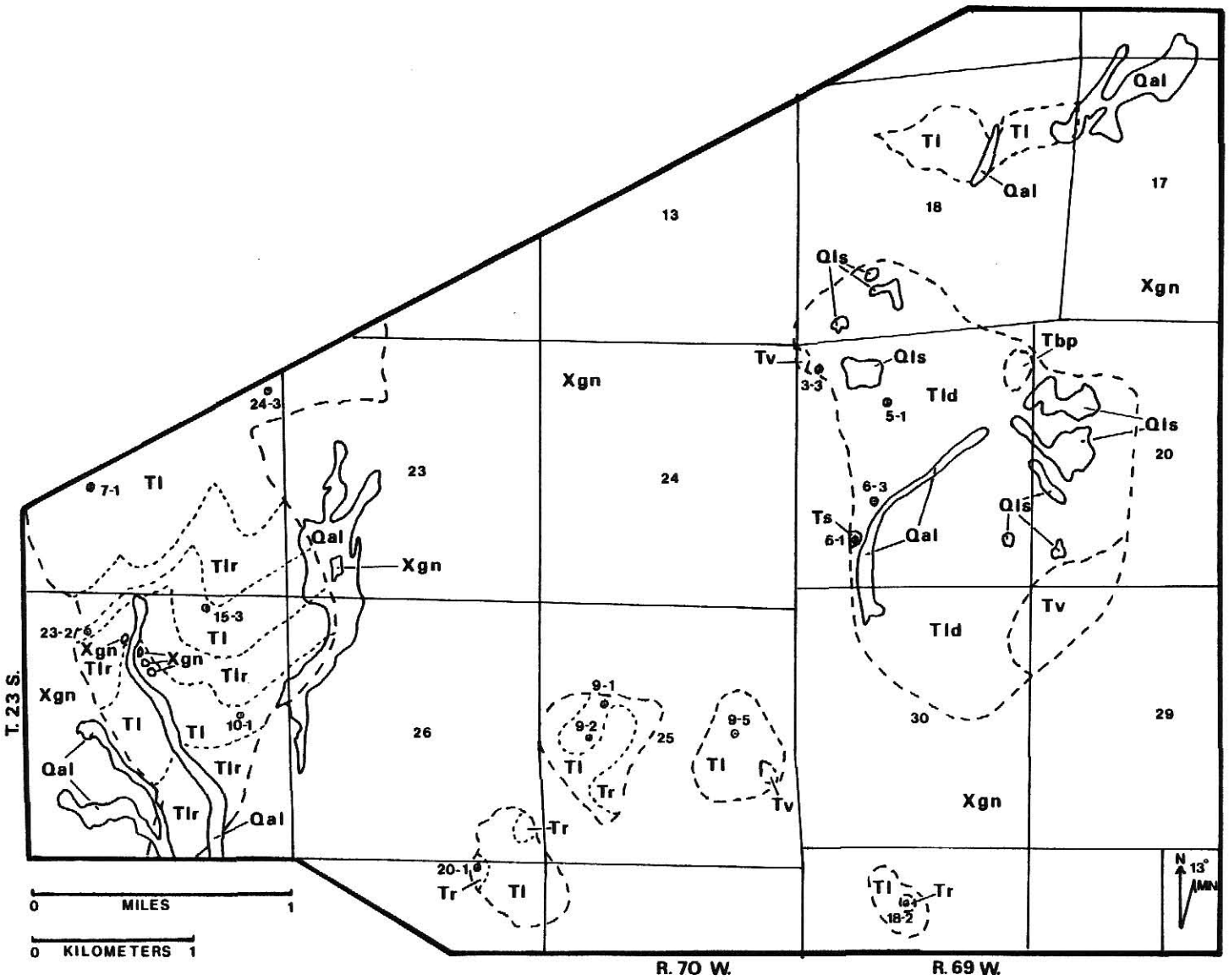
T. 23 S.
R. 70 W.
R. 69 W.
13
17
18
20
23
24
25
26
29
30
Qal
Tl
Tlr
Tld
Tv
Tbp
Qls
Xgn
Ts
Tr
7-1
24-3
15-3
23-2
10-1
3-3
5-1
6-3
6-1
9-1
9-2
9-5
20-1
18-2
0 MILES 1
0 KILOMETERS 1
N 13° MIN.

9,500 feet at the stock to more than 11,000 feet in the type locality. Outcrops are poor. South-facing slopes are grass covered; most other localities are covered by a forest of aspen and evergreen.

TYPE LOCALITY

The type locality of the Deer Peak Volcanics is near the head of Froze Creek drainage in secs. 22 and 27, T. 23 S., R. 70 W., Custer County. The type locality is extensively grass covered and consists of lava-flow rocks intercalated with lahars (Scott and Taylor, 1975). Rocks in the type locality constitute the best and most extensively preserved remnants of the Deer Peak Volcanics in the study area.

Scott and Taylor (1975) gave a general stratigraphic section of the rocks in the type locality; they referred to this section as the type section of the Deer Peak Volcanics. They reported that this section consists of 1,055 to 1,640 feet of poorly exposed rock that did not permit accurate measurement. Scott and Taylor (1975) determined that the lavas in the type locality flowed down a pre-Oligocene stream valley. Although the geometry of this valley-fill could not be determined accurately, consideration of measured thicknesses and areal extent suggests that approximately 0.5 cubic mile of latite and lahar filled the paleovalley.

The basal unit in the type locality is a lahar that contains many boulder- to cobble-sized clasts of porphyritic volcanic rocks and granitic gneiss in a poorly sorted, fine-grained matrix. Farther up-section, younger lahars are more difficult to locate; in most places they form gently sloping, boulder-strewn surfaces in contrast to the cliff-forming lava rocks. Presumably erosion preferrentially removed the poorly consolidated lahar matrix leaving the larger clasts behind.

Lava rocks are latite and contain prominent phenocrysts of plagioclase, biotite, and pyroxene. Lava rocks, which represent multiple lava flows, form knobby cliffs that are 10 to 30 feet high. Individual flow units have vesicular tops and grade downward into massive rock; the bases of flow units are brecciated.

EXPOSURES SOUTH AND NORTH OF THE STOCK

Exposures in sec. 18, and in sec. 31, T. 23 S., R. 69 W. and in sec. 25 and in sec. 35, T. 23 S., R. 70 W. also were examined. These exposures range in area from about 0.2 square mile to 0.05 square mile. Latite that is similar to that of the type locality is the principal rock type there, but a few flows of rhyolite and an intrusion of vitrophyre also occur. Rhyolite occurs only in exposures south of the stock. The thickness of the rocks in these exposures has not been measured.

In most of these exposures, latite lies unconformably on Precambrian rocks, which is in contrast to the sequence at the type section where a basal lahar is present. However, rhyolite underlies the eastern portion of, and occurs near the top of, the volcanic section in the western half of sec. 25, T. 23 S., R. 70 W. Rhyolite also occurs at the base of the volcanic exposure that is centered in the NE ¼, sec. 35, T. 23 S., R. 70 W. and near the top of the volcanic rocks in sec. 31, T. 23 S., R. 69 W. An intrusion of vitrophyre cuts the latite in the eastern half of sec. 25. T. 23 S., R. 70 W.

CENTRAL STOCK

The presumed vent of the volcano is a composite stock of about 2 square miles that is centered in sec. 19, T. 23 S., R. 69 W., Custer

County. Numerous prospect pits excavated in altered rock in the stock were an invaluable mapping aid.

Latite, which has phenocrysts of plagioclase, biotite, and pyroxene, is the dominant and oldest rock type at the stock. A subordinate volume of high-potassium dacite also occurs and is distinguished from latite in the field by an absence of pyroxene and presence of sanidine.

Latite and high-potassium dacite at the stock were intruded by three other units; age relationships among these late-stage units cannot be determined from field relationships. A vent-filling of waxy-looking vitrophyre, covering about 0.12 square mile and similar to that in sec. 25, T. 23 S., R. 70 W., intruded the southeast edge of the stock. A much smaller body of vitrophyre, covering about 0.05 square mile, cuts the northwest edge of the stock. A small, dike-like intrusion of shoshonite, coverning about 60,000 square feet, occurs at the western edge of the stock. Hydrothermal alteration, which was most intense around a breccia pipe that intruded the northeast edge of the stock, affected some latite and high-potassium dacite. Altered latite and high-potassium dacite are commonly silicified, pyritized, and argillized.

Erosion has cut deeply into the stock. Landslide deposits, some of which might be active, cover many of the steeper slopes.

P E T R O G R A P H Y

GENERAL STATEMENT

Fourteen of the freshest samples that span the range of composition in the Deer Peak volcanic-rock suite were examined petrographically for: (1) percentages of minerals, (2) types of textures, and (3) signs of weathering and alteration. All samples that were examined are porphyritic (11 to 41 percent phenocrysts). Plagioclase (oligoclase to labradorite) predominates in shoshonite, latite, and high-potassium dacite; sanidine predominates in rhyolite. The groundmass ranges from pilotaxitic to felty to hyalophitic in shoshonite, latite, and high-potassium dacite; rhyolite has a hypohyaline to holohyaline groundmass. Glomeroporphyritic clusters occur commonly in latite and high-potassium dacite. A summary of petrographic characteristics is in Table 1. Individual petrographic descriptions are in Appendix G.

LATITE

Eight specimens of latite were examined (samples 5-1, 6-3, 7-1, 9-5, 10-1, 15-3, 23-2, and 24-3). Latite occurs at the stock, in the type locality, and in exposures north and south of the stock. Fresh latite ranges from olive black (5 Y 2/1) to very light gray (N 8).

Table 1: Summary of petrographic characteristics of the Deer Peak volcanic rocks

Differentiation index	Location	Sample number	Classification	Modal Composition (in percent)	Groundmass texture	Other features
49.3	stock	6-1	shoshonite	7 clinopyroxene 5 plagioclase 4 olivine 84 groundmass	pilotaxitic	secondary calcite and hematite
67.7	type locality	10-1	latite	13 Na-plagioclase 5 hornblende 4 clinopyroxene 2 biotite 76 groundmass	pilotaxitic	relatively unaltered
69.6	type locality	7-1	latite	22 Na-plagioclase 4 clinopyroxene 4 biotite 70 groundmass	felty	relatively unaltered
70.4	type locality	24-3	latite	17 Na-plagioclase 6 clinopyroxene 5 biotite 72 groundmass	felty	relatively unaltered
71.2	type locality	15-3	latite	24 Na-plagioclase 6 clinopyroxene 5 biotite 65 groundmass	pilotaxitic	relatively unaltered
73.7	section 25, T. 23 S., R. 70 W.	9-5	latite	27 Na-plagioclase 3 clinopyroxene 70 groundmass	hyalophitic	relatively unaltered

Table 1: Summary of petrographic characteristics of the Deer Peak volcanic rocks (continued)

Differentiation index	Location	Sample number	Classification	Modal Composition (in percent)	Groundmass texture	Other features
73.9	stock	5-1	latite	30 Na-plagioclase 6 clinopyroxene 5 biotite 59 groundmass	felty	moderately altered
75.3	type locality	23-2	latite	11 Na-plagioclase 10 oxyhornblende 79 groundmass	felty	relatively unaltered
76.2	stock	6-3	latite	25 Na-plagioclase 4 clinopyroxene 3 biotite 68 groundmass	felty	moderately altered
85.6	stock	3-3	high-potassium dacite	17 Na-plagioclase 6 sanidine 4 biotite 73 groundmass	felty	microfaults, relatively unaltered
93.6	section 25, T. 23 S., R. 70 W.	9-2	low-silica rhyolite	25 sanidine 2 plagioclase 1 oxyhornblende 72 groundmass	felty	relatively unaltered, sanidine mantles plagioclase
95.0	section 31, T. 23 S., R. 69 W.	18-2	high-silica rhyolite	11 sanidine 89 groundmass	flow-banded, hematitic, felty	glomerocrysts of sanidine

Table 1: Summary of petrographic characteristics of the Deer Peak volcanic rocks (continued)

Differentiation index	Location	Sample number	Classification	Modal Composition (in percent)	Groundmass texture	Other features
96.0	section 35, T. 23 S., R. 70 W.	20-1	high-silica rhyolite	24 sanidine 3 plagioclase 73 groundmass	felty	sanidine mantles plagioclase
97.8	section 25, T. 23 S., R. 70 W.	9-1	high-silica rhyolite	13 sanidine 4 quartz 83 groundmass	flow-banded, hematitic, devitrified	secondary quartz sanidine glomerocrysts

Phenocryst minerals consist of 11 to 30 percent plagioclase (Ab_{79} to Ab_{48}), 0 to 10 percent hornblende and oxyhornblende, 0 to 6 percent clinopyroxene (augite to diopsidic augite), and 0 to 5 percent biotite. Plagioclase occurs as euhedral to subhedral laths, 0.1 to 5.0 mm long, and is characteristically zoned and twinned; it may be unaltered, or may be corroded or sericitized or both. Hornblende and oxyhornblende occur as elongate prisms, 0.2 to 2.2 mm long. Clinopyroxene occurs as stubby prisms, 0.1 to 1.8 mm long. Biotite forms euhedral pseudohexagonal plates, 0.2 to 1.8 mm across. Glomeroporphyritic clusters that consist of all phenocryst phases occur up to 4.0 mm across.

The groundmass consists of pilotaxitic, felty, or hyalophitic mixtures of feldspar, $\leqslant$ 0.05 mm long; anisotropic microlites, $\leqslant$ 0.04 mm long; opaque minerals, $\leqslant$ 0.02 mm across; apatite, $\leqslant$ 0.2 mm long, crystallites, and glass. In samples 5-1 and 6-3, opaque minerals mantle or replace biotite and pyroxene and are finely disseminated throughout the groundmass; these textural characteristics probably are related to hydrothermal alteration associated with the breccia pipe at the Deer Peak stock.

HIGH-POTASSIUM DACITE

High-potassium dacite (sample 3-3) occurs at the stock. In contrast to latite, high-potassium dacite has sanidine and lacks clinopyroxene and amphibole. The fresh rock is light gray (N 7).

Phenocryst minerals consist of 17 percent plagioclase (Ab_{76} to Ab_{64}), 6 percent sanidine (Or_{80} to Or_{70}), and 4 percent biotite. Euhedral to

subhedral plagioclase laths, 0.5 to 5.0 mm long, are zoned, twinned, and altered similarly to plagioclase in latite. Sanidine occurs as relatively unaltered euhedral to subhedral laths, 0.5 to 2.0 mm long. Biotite, 0.2 to 1.0 mm across, has a crystal habit similar to biotite in latite. Glomeroporphyritic clusters occur up to 8.0 mm across. The groundmass consists of a felty mixture of anisotropic microlites, $\leqslant$ 0.02 mm long; opaque minerals, $\leqslant$ 0.1 mm across; and apatite, $\leqslant$ 0.4 mm long.

RHYOLITE

Rhyolite is restricted to exposures south of the stock. The fresh rock ranges from grayish red (5 R 4/2) to brownish gray (5 YR 4/1). Chemically, rhyolite there is divided into two types: low-silica (sample 9-2) and high-silica (samples 9-1, 18-2, and 20-1). Sanidine predominates over plagioclase, and ferromagnesian minerals are scarce in rhyolite.

Phenocryst minerals consist of 11 to 25 percent sanidine (Or_{85} to Or_{75}), 0 to 4 percent quartz, 0 to 3 percent plagioclase, and traces of clinopyroxene and oxyhornblende. Sanidine occurs as euhedral to subhedral laths, 0.1 to 3.0 mm long, in samples 9-1 and 18-2, and as glomerocrysts, 0.2 to 4.0 mm long, in samples 9-1 and 20-1. Plagioclase occurs as subhedral laths, 0.5 to 2.5 mm long, and is characteristically mantled by sanidine. Quartz occurs as aggregates of equant crystals, $<$0.02 mm across, in sample 9-1 and appears to be secondary.

Samples 9-2 and 20-1 have a felty groundmass that consists of anisotropic microlites, $\leqslant$ 0.02 mm long; opaque minerals, $\leqslant$ 0.2 mm long,

crystallites, and glass. The devitrified groundmass in samples 9-1 and 18-2 is flow banded, hematitic, and includes feldspar laths, ⩽ 0.2 mm long.

SHOSHONITE

Shoshonite (sample 6-1) represents a late-stage episode of intrusion at the stock. Fresh shoshonite is grayish black (N 2). Shoshonite differs from other rocks in the Deer Peak volcanic-rock suite because it has olivine and lacks hydrous ferromagnesian minerals.

Phenocryst minerals consist of 7 percent clinopyroxene (augite), 5 percent plagioclase (Ab_{52} to Ab_{47}), and 4 percent olivine. Clinopyroxene occurs as euhedral prisms, 0.5 to 1.5 mm long. Plagioclase occurs as euhedral to anhedral laths, 0.5 to 1.0 mm long. Olivine occurs as subhedral to anhedral resorbed crystals, 0.5 to 1.0 mm long.

The groundmass consists of a pilotaxitic mixture of feldspar laths, ⩽ 0.2 mm long; anisotropic microlites, ⩽ 0.02 mm long; and opaque minerals, ⩽ 0.05 mm across. Secondary calcite and hematite form scaly masses that constitute about 3 percent of the rock.

G E O C H E M I S T R Y

MAJOR ELEMENTS

Major-element data of the fourteen petrographically analyzed samples are in Table 2. Shoshonite has 52.4 percent SiO_2. Latite, the most abundant rock type, ranges from 59.3 to 64.7 percent SiO_2. High-potassium dacite has 66.7 percent SiO_2. Low-silica rhyolite has 71.4 percent SiO_2 and high-silica rhyolite ranges from 74.1 to 76.7 percent SiO_2. The alkali content ($Na_2O + K_2O$) ranges from 6.7 to 9.9 percent in the Deer Peak volcanic-rock suite, which is high compared to the alkali content of most orogenic suites (Ewart and LaMaitre, 1980); abundances of MgO, CaO, and Fe_2O_3 are correspondingly low. Major-element contents of latite (Table 3) are: (1) similar to latite at Rosita Hills and syenodiorite (coarse-grained equivalent of latite) at Spanish Peaks, (2) more silicic and alkalic than andesite at the Summer Coon volcano in the San Juan Mountains, and (3) more alkalic than average high-potassium andesite. Major-element contents of shoshonite are very similar to average shoshonite and less alkalic than syenodiorite at Rosita Hills (Table 4).

The Cross, Iddings, Pirsson, and Washington (C.I.P.W.) norms (Table 5) reflect the high alkali content. In the samples that were

Table 2: Major-element contents (in weight percent oxide) of the Deer Peak volcanic rocks.

Classification	Shoshonite	Latite	Latite	Latite	Latite	Latite	Latite	Latite
Sample	6-1	10-1	7-1	24-3	15-3	9-5	5-1	23-2
D. I.	49.3	67.7	69.6	70.4	71.2	73.7	73.9	75.3
SiO_2	52.4	59.3	60.5	61.8	62.1	61.6	60.9	64.7
Al_2O_3	16.0	15.3	16.6	16.2	16.0	16.3	16.5	16.5
$Fe_2O_3^*$	9.0	4.4	5.7	5.6	5.0	4.5	5.8	5.5
MgO	5.3	2.1	2.3	2.3	2.3	1.6	2.0	1.3
CaO	7.8	6.4	4.5	4.4	4.1	4.0	4.3	3.6
Na_2O	3.6	4.0	4.2	4.3	4.0	4.5	5.5	4.5
K_2O	3.1	3.5	4.4	3.9	3.9	3.8	4.4	3.7
TiO_2	1.0	0.4	0.8	0.7	0.7	0.4	0.6	0.8
P_2O_5	0.6	0.4	0.4	0.4	0.4	0.3	0.5	0.4
Ignit.	0.88	3.40	1.50	1.53	1.51	2.67	0.90	1.56
Sum	99.7	99.2	100.9	101.1	100.0	99.7	101.4	102.6

* Representing Fe as Fe_2O_3

Table 2: Major-element contents (in weight percent oxide) of the Deer Peak volcanic rocks (continued).

Classification	Latite	High-potassium dacite	Low-silica rhyolite	High-silica rhyolite	High-silica rhyolite	High-silica rhyolite
Sample	6-3	3-3	9-2	18-2	20-1	9-1
D. I.	76.2	85.6	93.6	95.0	96.0	97.8
SiO_2	60.5	66.7	71.4	75.5	74.1	76.7
Al_2O_3	17.8	16.7	14.6	13.0	14.0	11.6
Fe_2O_3*	4.8	2.6	2.1	1.0	1.3	1.2
MgO	1.5	0.7	0.2	0.5	tr.	0.1
CaO	3.4	1.4	0.8	0.5	0.5	0.2
Na_2O	5.2	4.1	5.0	3.9	5.0	4.3
K_2O	4.4	4.9	4.8	4.5	4.5	4.4
TiO_2	0.5	0.3	0.1	tr.	0.2	tr.
P_2O_5	0.3	0.2	0.1	tr.	tr.	tr.
Ignit.	1.00	1.33	1.49	1.82	0.69	1.01
Sum	99.4	99.1	100.6	100.7	100.3	99.5

*Representing Fe as Fe_2O_3

Table 3: Comparison of average Deer Peak latite to rocks of similar composition at Rosita Hills, Spanish Peaks, the Summer Coon volcano, and to average high-potassium andesite (major elements in weight percent oxide, trace elements in ppm).

Deer Peak average latite	Rosita Hills[1] latite	Spanish Peaks[2] syenodiorite	Summer Coon[3] andesite	Average[4] high-potassium andesite
SiO_2 61.4	60.5	59.4	54.3	60.8
Al_2O_3 16.4	15.8	16.4	16.4	16.8
Fe_2O_3			4.5	
FeO			2.7	
Fe as Fe_2O_3 5.2	6.12	6.11		5.7
MgO 1.9	0.87	2.4	4.2	2.2
CaO 4.3	3.41	4.2	7.5	5.6
Na_2O 4.5	4.69	4.5	3.8	4.10
K_2O 4.0	4.34	3.3	2.1	3.25
La 63.9	75.3	57.9	32	13
Ce 100.9	120.4	102	78	23
Sm 7.9	6.4	6.29	6.7	4.5
Eu 1.8	1.5	1.72	1.9	1.4
Yb 2.0	2.2	1.63	1.8	3.2
Lu 0.36	0.34	0.28	0.28	
Rb 119	107		37	90
Ba 1455	1430		1100	400
Sr 897	740		930	620
Hf 7.9	6.4			

Table 3: Comparison of average Deer Peak latite to rocks of similar composition at Rosita Hills, Spanish Peaks, the Summer Coon Volcano, and to average high-potassium andesite (major elements in weight percent oxide, trace elements in ppm). (Continued)

	Deer Peak average latite	Rosita Hills[1] latite	Spanish Peaks[2] syenodiorite	Summer Coon[3] andesite	Average[4] high-potassium andesite
Sc	8.8	3.6			
Cr	42.7				3
Th	12.5	17.7		3.9	5.5

[1] Smalley, 1981; [2] Cullers, personal communication, 1981; [3] Zielinski and Lipman, 1976; [4] Condie, 1976.

Table 4: Comparison of shoshonite at Deer Peak to syenodiorite at Rosita Hills and to average shoshonite (major elements in weight percent oxide, trace elements in ppm).

	Deer Peak shoshonite	Rosita Hills[1] syenodiorite	Average[2] shoshonite
SiO_2	52.4	49.3	52.9
Al_2O_3	16.0	16.5	17.2
Fe as Fe_2O_3	9.0	9.28	8.4
MgO	5.3	3.67	3.6
CaO	7.8	8.39	6.4
Na_2O	3.6	4.44	3.50
K_2O	3.1	3.43	3.69
La	46.9	73.0	15
Ce	96.2	180.2	32
Sm	8.5	11.4	3.2
Eu	2.2	2.6	0.95
Yb	2.3	2.8	1.7
Rb	84	84	100
Ba	1140	1170	850
Sr	950	1353	850
Cr	219		30

(1) Smalley, 1981; (2) Condie, 1976

Table 5: Normative mineralogy (C.I.P.W.) of the Deer Peak volcanic rocks.[1]

Classification	Shoshonite	Latite	Latite	Latite	Latite	Latite	Latite	Latite
Sample	6-1	10-1	7-1	24-3	15-3	9-5	5-1	23-2
D. I.	49.3	67.7	69.6	70.4	71.2	73.7	73.9	75.3
Q		10.7	8.3	10.6	13.7	11.7	1.5	16.1
C								
Or	18.4	21.3	26.0	23.4	23.2	23.1	25.7	21.7
Ab	30.9	35.7	35.3	36.4	34.3	38.9	46.7	37.5
An	18.5	14.0	13.9	13.5	14.5	13.6	7.1	13.9
Di	10.6	11.6	2.6	2.7	0.8	2.9	6.9	
Hy	3.7		4.6	4.5	5.4	2.7	1.8	3.1
Wo		0.4						
Ac								
Ol	6.8							
Hm	9.1	4.6	5.6	5.7	5.1	4.6	5.7	5.5
Sp	2.6	0.9	1.9	1.6	1.7	0.9	1.5	0.9
Ru								0.4
Ap	1.3	0.8	0.9	0.9	0.9	0.7	1.1	0.9

(1) Determined using Fe as Fe_2O_3

Table 5: Normative mineralogy (C.I.P.W) of the Deer Peak volcanic rocks[1] (continued)

Classification	Latite	High-potassium dacite	Low-silica rhyolite	High-silica rhyolite	High-silica rhyolite	High-silica rhyolite
Sample	6-3	3-3	9-2	18-2	20-1	9-1
D. I.	76.2	85.6	93.6	95.0	96.0	97.8
Q	5.1	20.3	22.0	34.3	26.9	35.2
C		2.3				
Or	26.4	29.7	28.6	26.9	26.9	26.9
Ab	44.7	35.6	43.0	33.8	42.2	35.7
An	12.4	7.2	2.9	2.3	2.5	
Di	0.9	1.0				
Hy	3.2	1.8		1.3		
Wo						0.4
Ac						1.0
Ol						
Hm	4.9	2.6	2.2	1.0	1.3	0.9
Sp	1.2					
Ru		0.3				
Ap	0.8					

(1) Determined using Fe as Fe_2O_3

analyzed, normative orthoclase is always greater than 18 percent, even though phenocrysts of sanidine are not present in rocks with less than about 66 percent SiO_2. Normative anorthite is always subordinate to normative albite. All rocks have normative quartz, except shoshonite, which has normative (and modal) olivine.

Major-element contents are plotted versus differentiation index (D.I.) in Figures 5a, b, and c. Differentiation index (Thornton and Tuttle, 1960) is defined as the sum of normative quartz, orthoclase, albite, nepheline, leucite, and potassium metasilicate. In effect, it represents late-forming, salic minerals in a suite of igneous rocks that evolved by magma differentiation. Thus, major elements plotted against D.I. would portray fractional-crystallization trends better than if plotted against SiO_2.

Percentages of SiO_2, K_2O, and Na_2O increase with increasing D.I.; Fe_2O_3, MgO, and CaO are depleted in the felsic members of the suite. Cox and others (1979) pointed out that sharp inflections on chemical variation diagrams are the dominant characteristic of a suite of rocks evolving by fractional crystallization in which minerals suddenly commence or stop crystallizing. However, in intermediate and felsic suites, in which many phases are simultaneously crystallizing, such inflections tend to cancel one another.

Alkali enrichment relative to CaO in the Deer Peak volcanic-rock suite is shown in a plot of K_2O - Na_2O - CaO (Fig. 6), and is due to equal enrichment in Na_2O and K_2O, rather than strong enrichment of one relative to the other. An AFM plot of the suite (Fig. 7) shows a lack of Fe enrichment relative to MgO; this indicates that the Deer Peak

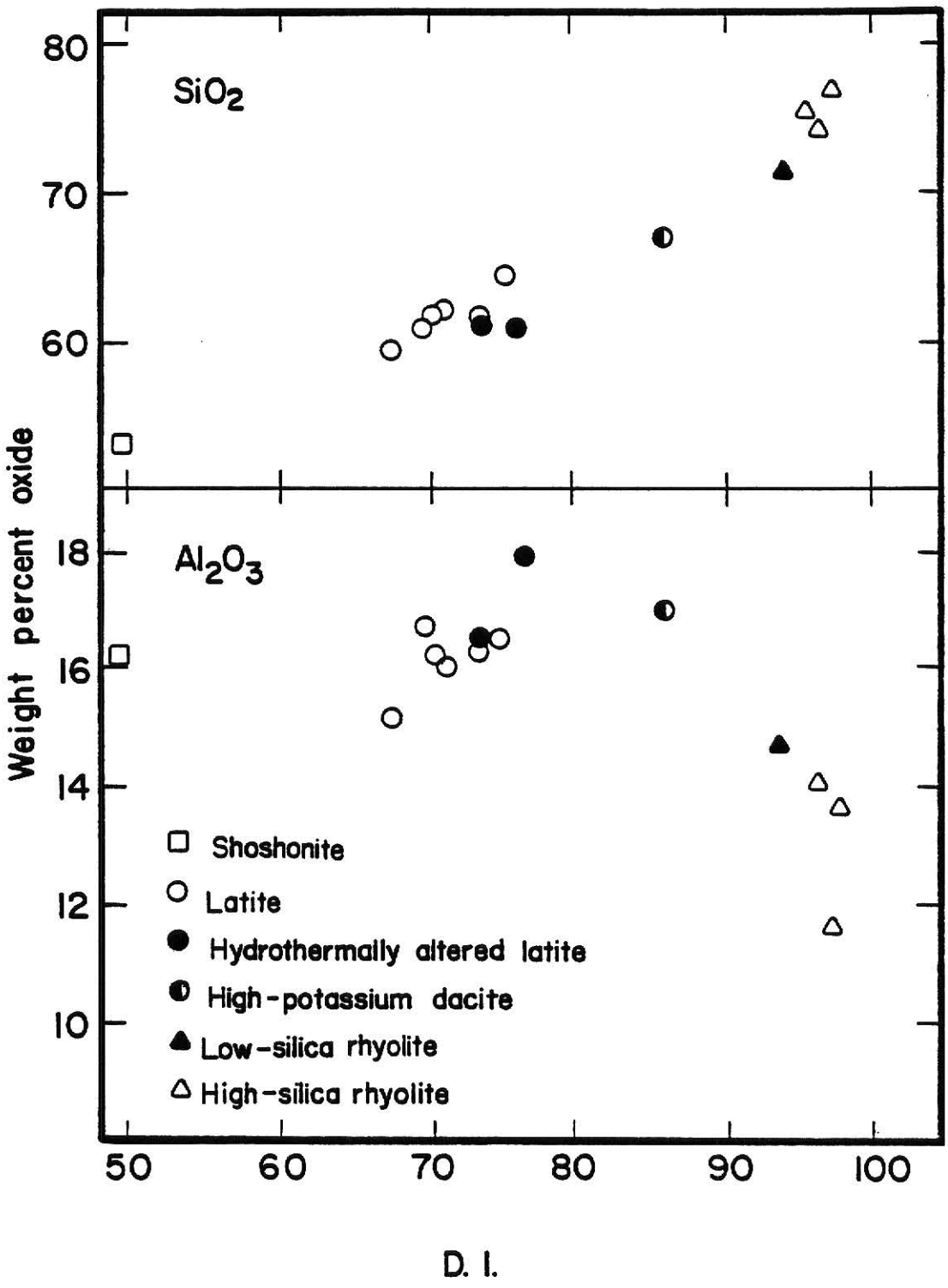

Figure 5a: Plot of SiO_2 and Al_2O_3 versus differentiation index for the Deer Peak volcanic rocks.

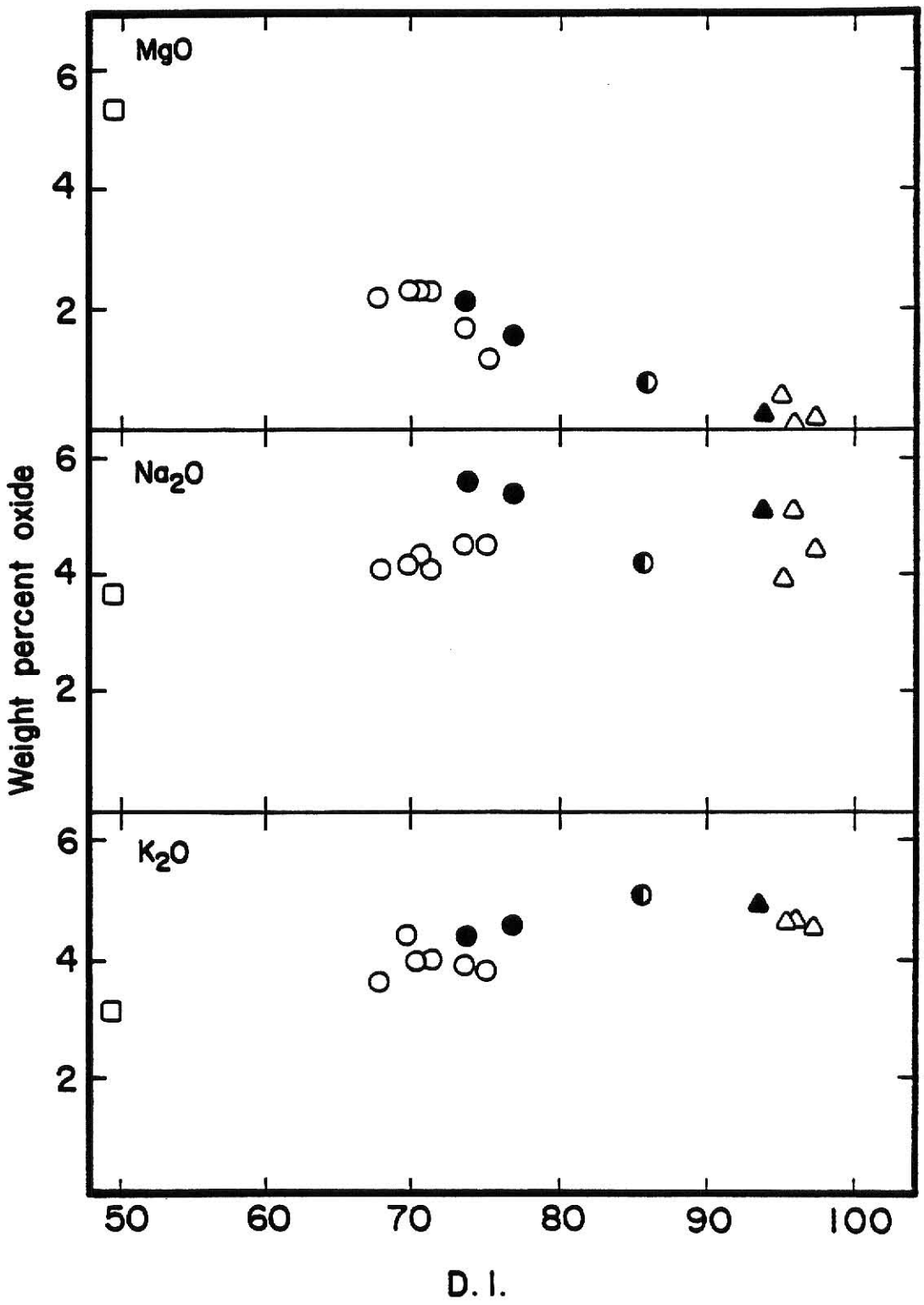

Figure 5b: Plot of MgO, Na_2O, and K_2O versus differentiation index for the Deer Peak volcanic rocks (symbols as in Fig. 5a).

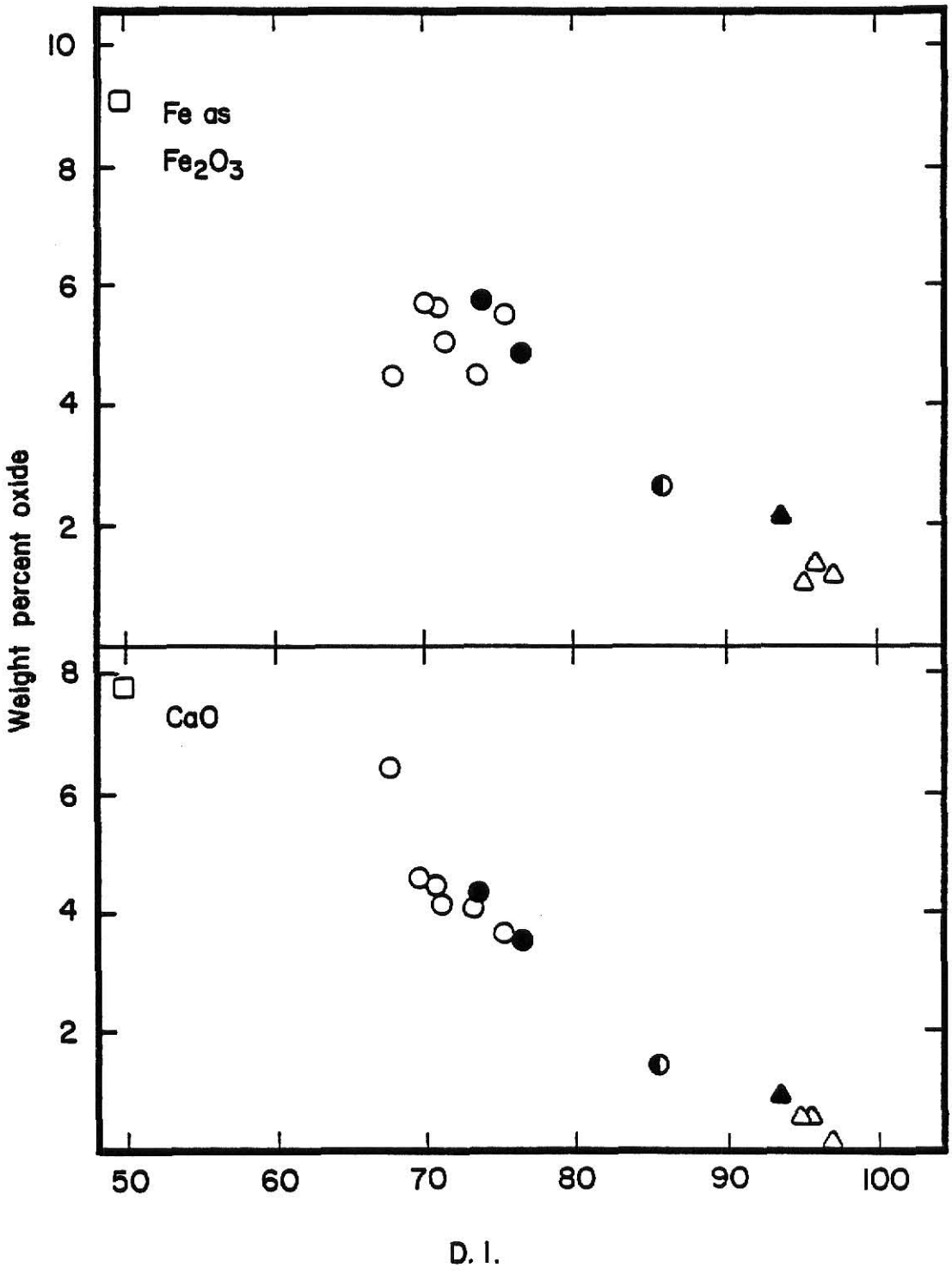

Figure 5c: Plot of Fe as Fe_2O_3 and CaO versus differentiation index for the Deer Peak volcanic rocks (symbols as in Fig. 5a).

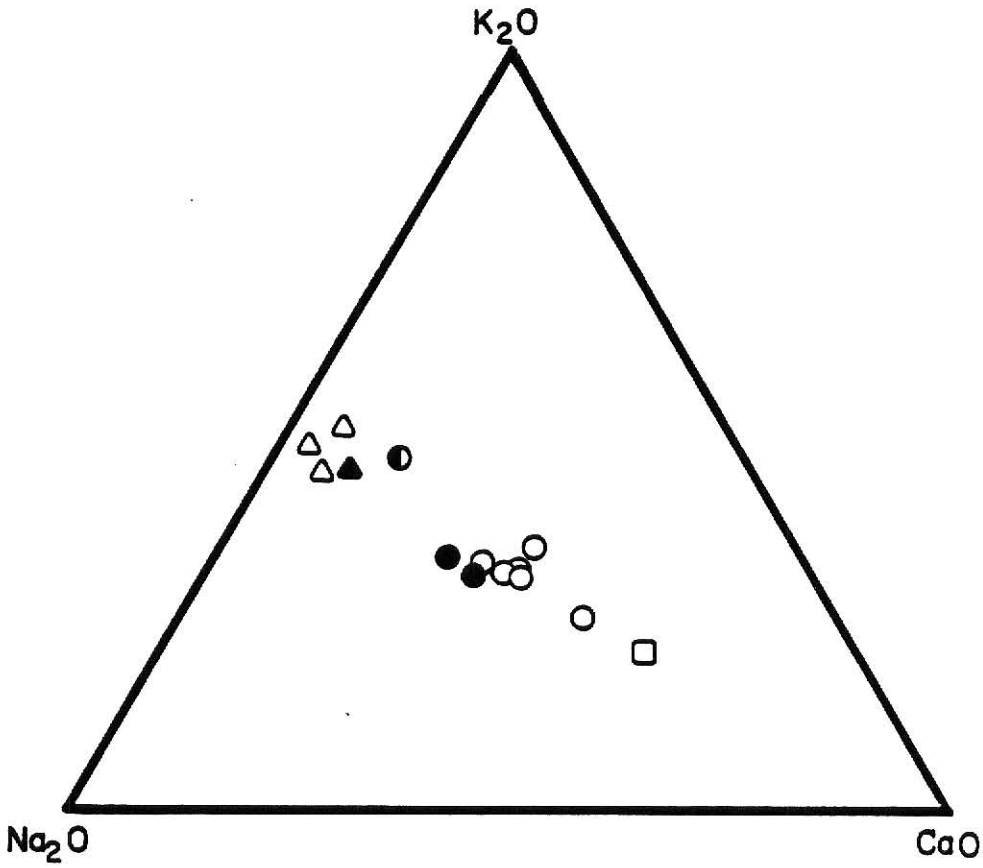

Figure 6: Plot of K_2O-Na_2O-CaO for the Deer Peak volcanic rocks (symbols as in Fig. 5a).

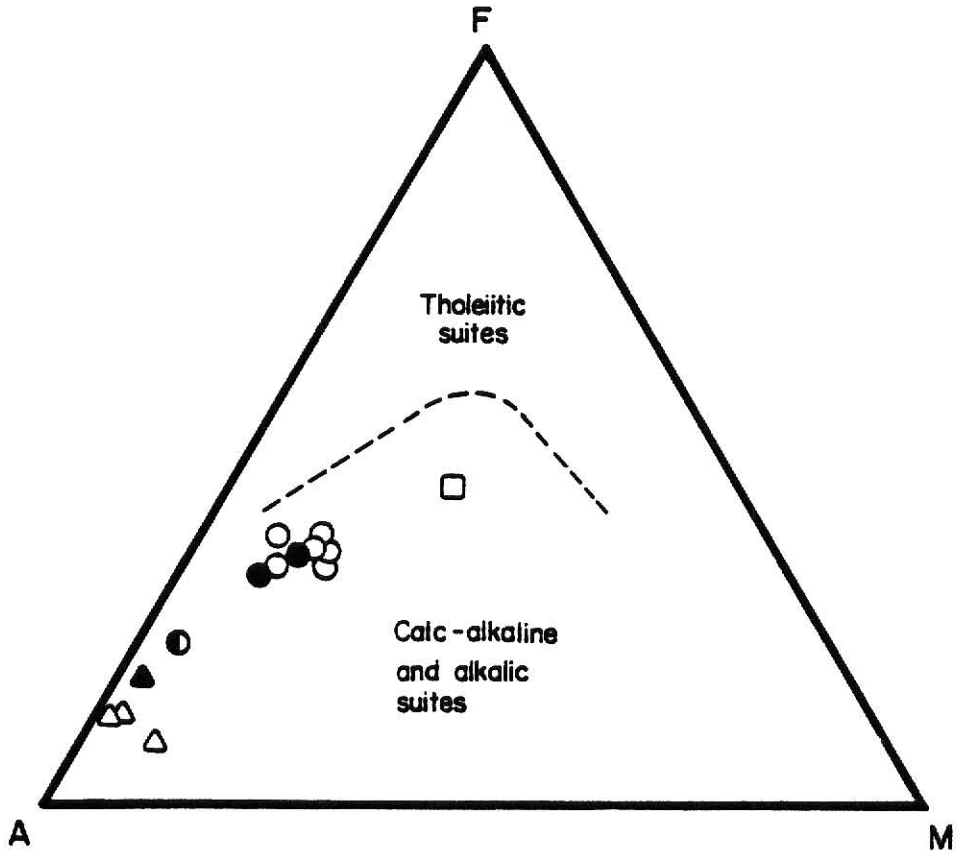

Figure 7: AFM plot of the Deer Peak volcanic rocks. A equals alkali ($Na_2O + K_2O$), F equals Fe as FeO, M equals MgO. Divider line from Irvine and Baragar (1971) (symbols as in Fig. 5a).

Volcanics are not tholeiitic, but are calc-alkaline, alkali-calcic, or alkalic. The Peacock plot (Fig. 8) shows that the suite is probably alkali-calcic, although only one sample was found with less than about 60 percent SiO_2. Consequently, the alkali-lime index cannot be determined precisely.

The degree of alumina saturation (Hyndman, 1972) is determined by comparing molecular Al_2O_3 to molecular K_2O, Na_2O, and CaO. Shoshonite and latite are metaluminous ($Al_2O_3 > Na_2O + K_2O$ but $Al_2O_3 < Na_2O + K_2O + CaO$). High-potassium dacite and rhyolite (sample 18-2) are slightly peraluminous ($Al_2O_3 > Na_2O + K_2O + CaO$), which reflects the lower CaO content in these rocks than in latite and shoshonite. Rhyolite (samples 9-2 and 20-1) is metaluminous, their lower CaO contents are counterbalanced by Al_2O_3 greater than 14 percent by weight. The most differentiated sample, 9-1, is slightly peralkaline ($Al_2O_3 < Na_2O + K_2O$); the excess alkali is reflected by normative acmite in this rock.

TRACE ELEMENTS

Trace-element contents and trace-element ratios of the Deer Peak volcanic-rock suite are listed in Table 6. Abundances of Rb, Sr, Ba, Th, and the light rare-earth elements (LREE), all of which have large ionic radii, are characteristically high compared to orogenic rocks of lower alkali contents (Ewart and LeMaitre, 1980). This distribution reflects the major-element contents because alkali-rich suites tend to be enriched in LILE.

The Sr, Cr, and Sc contents and Sr/Ba and K/Ba ratios tend to de-

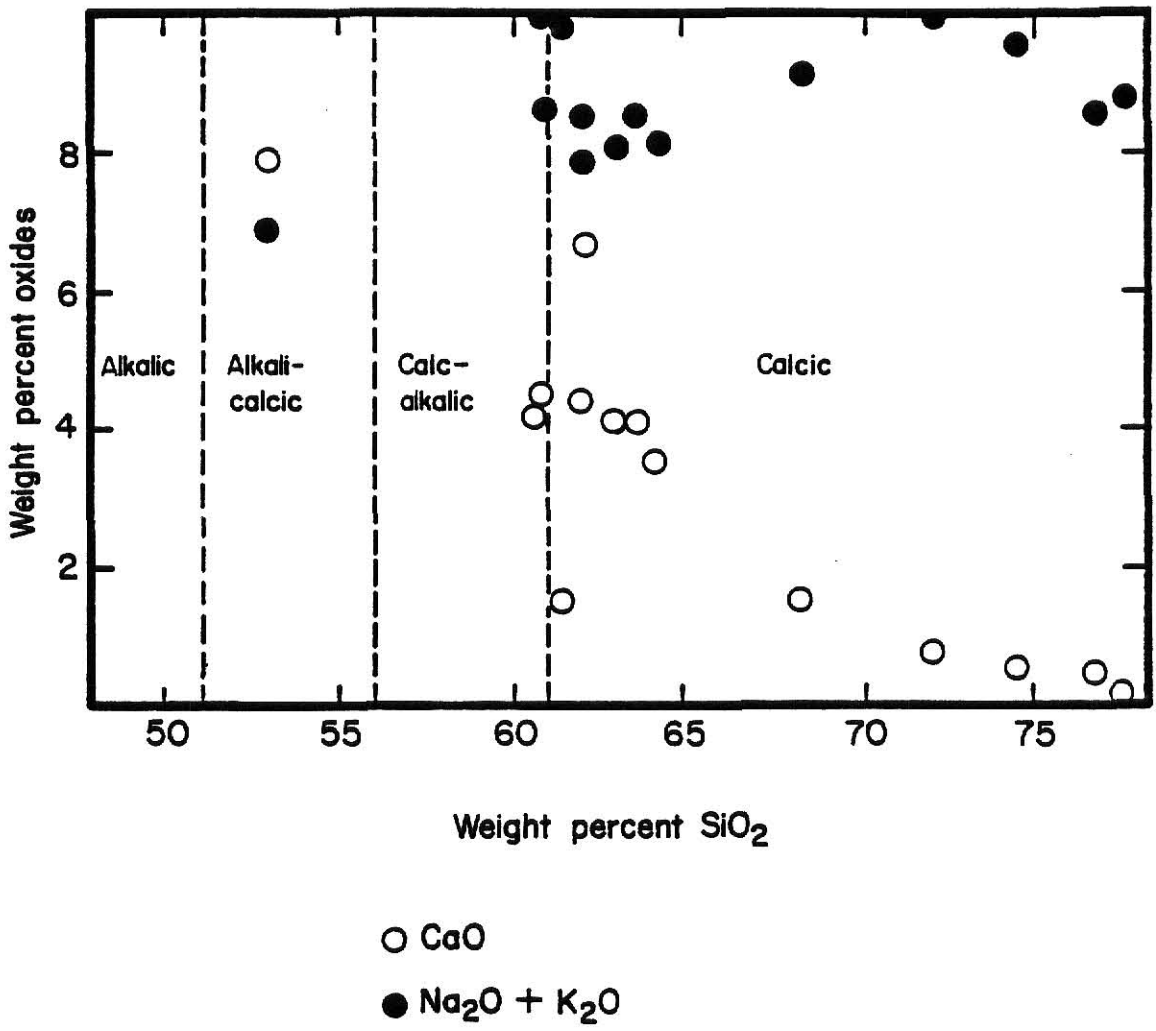

Figure 8: Peacock plot of the Deer Peak volcanic rocks.

Table 6: Trace-element contents (in ppm) of the Deer Peak volcanic rocks.

Classification	Shoshonite	Latite	Latite	Latite	Latite	Latite	Latite	Latite
Sample	6-1	10-1	7-1	24-3	15-3	9-5	5-1	23-2
D. I.	49.3	67.7	69.6	70.4	71.2	73.7	73.9	75.3
La	46.9	51.4	66.6	66.4	59.6	56.1	79.5	69.4
Ce	96.2	90.7	116	129	113	98.0	139	128
Sm	8.5	6.8	8.5	8.3	7.6	7.2	9.8	8.4
Eu	2.2	1.6	1.9	2.0	1.8	1.5	2.3	2.1
Yb	2.3	2.5	2.4	2.4	1.7	2.5	2.3	2.2
Lu	0.38	0.39	0.42	0.37	0.31	0.40	0.37	0.32
Rb	84	100	130	130	100	130	130	100
Ba	1140	1290	1490	1370	1330	1240	2130	1520
Sr	954	835	854	840	875	851	1050	923
Hf	5.1	5.3	7.4	7.4	6.4	6.1	12.1	6.3
Sc	20.4	7.8	10.3	10.3	9.3	6.0	8.1	10.8
Cr	219	64.8	35.6	26.8	43.3	35.8	38.6	45.6
Th	6.6	9.7	13.6	14.2	12.2	12.6	13.6	11.6
La/Lu_n	13	14	17	19	20	15	22	21
ΣREE	245	234	290	353	274	228	339	309
K/Rb	305	286	286	252	309	252	270	310
Rb/Sr	0.09	0.12	0.15	0.15	0.12	0.15	0.13	0.11
K/Ba	22.3	22.2	24.3	23.8	24.2	25.5	17.0	20.3
Sr/Ba	0.83	0.65	0.57	0.64	0.63	0.69	0.49	0.61

(1) La/Lu_n = chondrite-normalized La/Lu ratio

Table 6: Trace-element contents (in ppm) of the Deer Peak volcanic rocks (continued).

Classification	Latite	High-potassium dacite	Low-silica rhyolite	High-silica rhyolite	High-silica rhyolite	High-silica rhyolite
Sample	6-3	3-3	9-2	18-2	20-1	9-1
D. I.	76.2	85.6	93.6	95.0	96.0	97.8
La	62.1	55.9	45.8	32.0	55.0	26.1
Ce	93.5	88.3	97.3	58.8	95.1	52.2
Sm	6.9	5.4	4.7	3.7	5.0	3.5
Eu	1.5	1.3	0.78	0.27	0.71	0.22
Yb	1.9	1.6	2.0	2.3	2.8	2.4
Lu	0.31	0.29	0.32	0.43	0.46	0.40
Rb	130	190	170	290	190	200
Ba	1270	1490	750	64	630	61
Sr	950	647	607	31	181	21
Hf	12.1	8.2	10.9	6.9	9.6	6.5
Sc	8.1	4.2	1.2	13.9	4.4	1.1
Cr	51.6	29.4	41.2	1.3	2.5	28.5
Th	12.2	13.4	19.8	28.8	24.2	26.9
La/Lu_n	21	20	15	7.7	12	6.8
ΣREE	245	234	222	139	225	127
K/Rb	291	215	236	128	197	184
Rb/Sr	0.13	0.29	0.23	9.3	0.30	9.4
K/Ba	28.7	27.7	52.7	58.0	59.5	59.7
Sr/Ba	0.74	0.45	0.80	0.49	0.29	0.34

(1) La/Lu_n = chondrite-normalized La/Lu ratio

crease with increasing D.I. (Figs. 9a, b, and c). Concentrations of Ba are highest in latite and high-potassium dacite, lower in shoshonite, and lowest in rhyolite. The Rb and Hf contents and K/Ba and Rb/Sr ratios increase with increasing D.I. Thus, shoshonite has the lowest LILE content in the suite. The latite group forms a well-defined array in all of these plots, characterized by abundant LILE. High-potassium dacite is even more enriched in Ba, Rb, and Rb/Sr than latite. Rhyolite has a wide range of trace-element contents; except for Rb and Sr, it is depleted in trace elements relative to the rest of the suite. High-silica rhyolite generally has lower Sr, Ba, Cr, and Hf contents and Sr/Ba and K/Rb ratios and higher Rb and Sc contents and K/Ba and Rb/Sr ratios than low-silica rhyolite.

Because of systematic variation caused by lanthanide contraction, rare-earth elements (REE) are treated separately. Concentrations of REE are normalized to concentrations of REE in chondritic meteorites and plotted in variation diagrams in Figures 10 a, b, and c. Such plots are used to eliminate the saw-tooth effect that results because even-atomic-numbered REE are naturally more abundant than adjacent odd-atomic-numbered REE.

Shoshonite, latite, and high-potassium dacite are characterized by highly fractionated REE patterns; chondrite-normalized La/Lu ratios range from 14 to 22 in latite, equal 20 in high-potassium dacite, and equal 13 in shoshonite. Negative Eu anomalies are small to absent in these rocks. Total REE contents are generally higher in latite (234 to 353 ppm) than in shoshonite (245 ppm) and in high-potassium dacite (234 ppm).

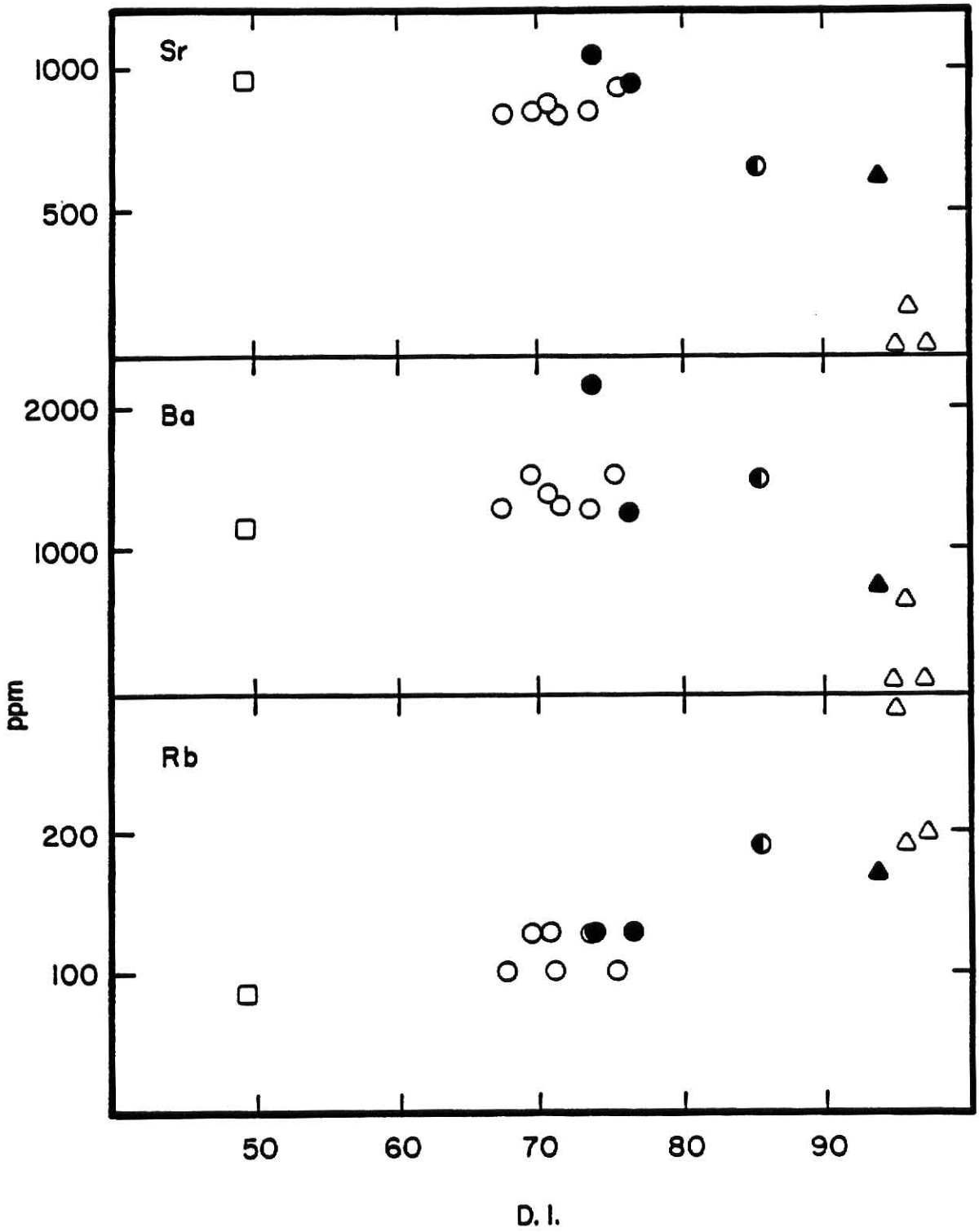

Figure 9a: Plot of Sr, Ba, and Rb versus differentiation index for the Deer Peak volcanic rocks (symbols as in Fig. 5a).

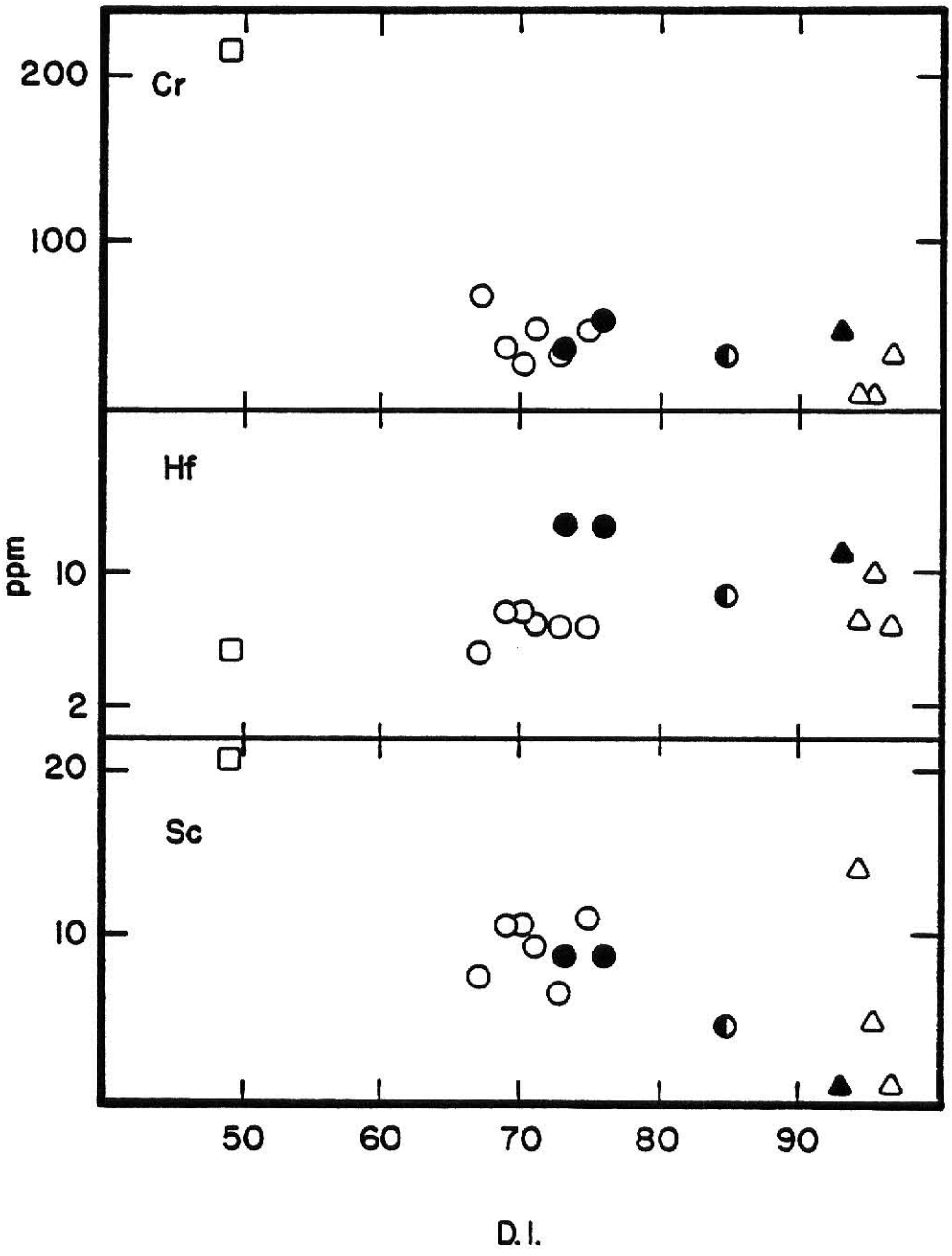

Figure 9b: Plot of Cr, Hf, and Sc versus differentiation index for the Deer Peak volcanic rocks (symbols as in Fig. 5a).

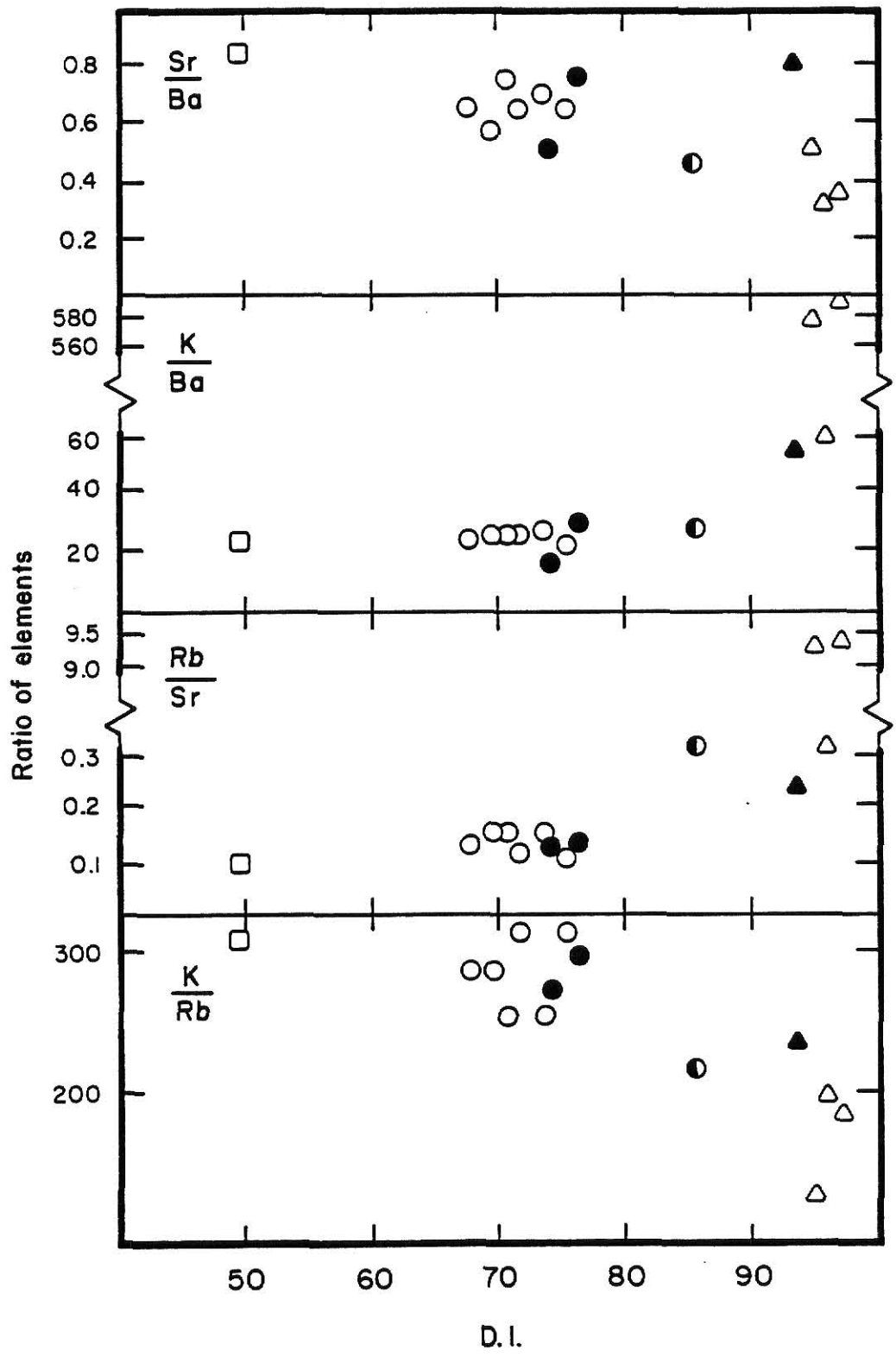

Figure 9c: Plot of Sr/Ba, K/Ba, Rb/Sr, and K/Rb versus differentiation index for the Deer Peak volcanic rocks (symbols as in Fig. 5a).

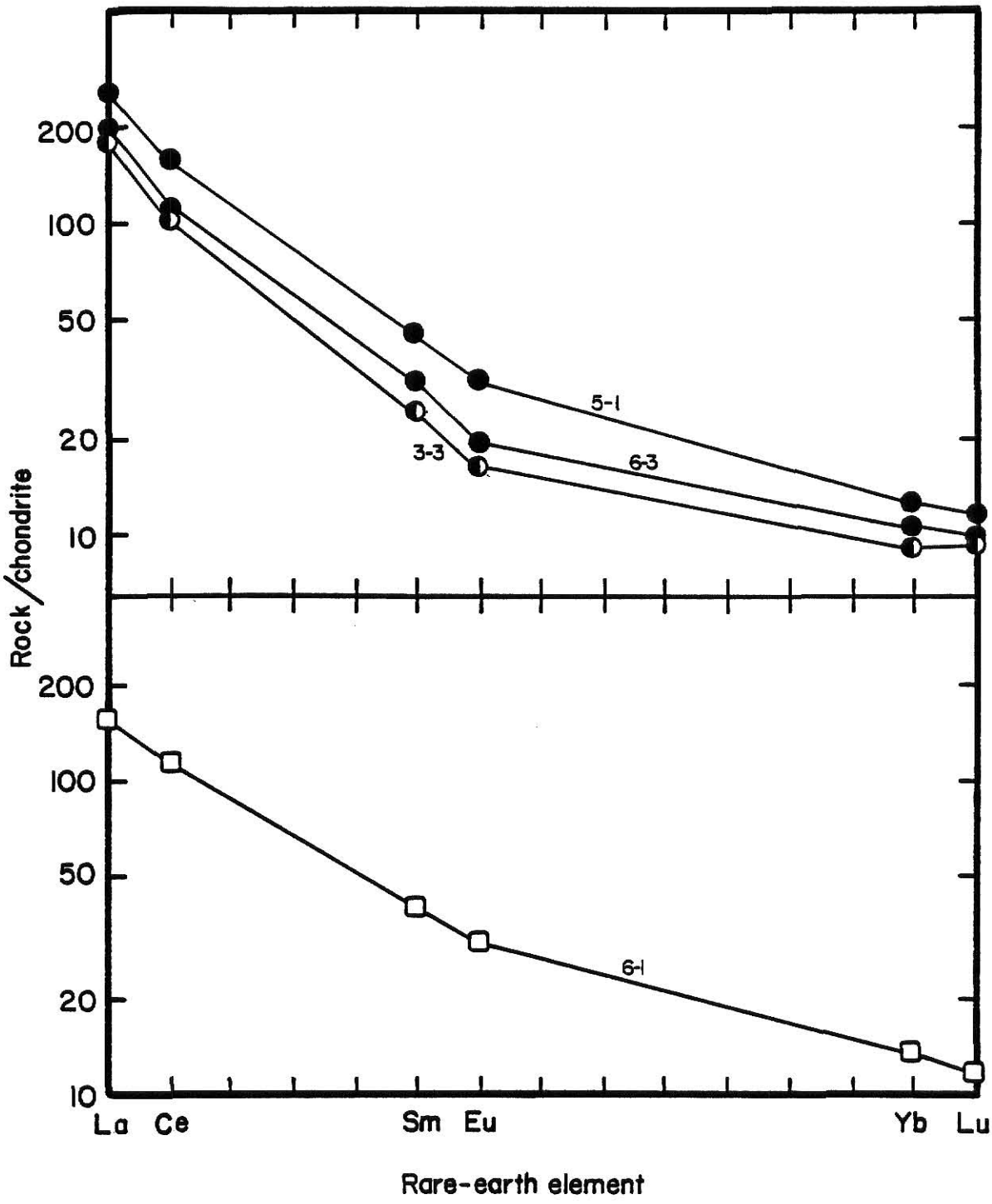

Figure 10a: Variation of REE in latite, high-potassium dacite, and shoshonite at the Deer Peak stock (symbols as in Fig. 5a).

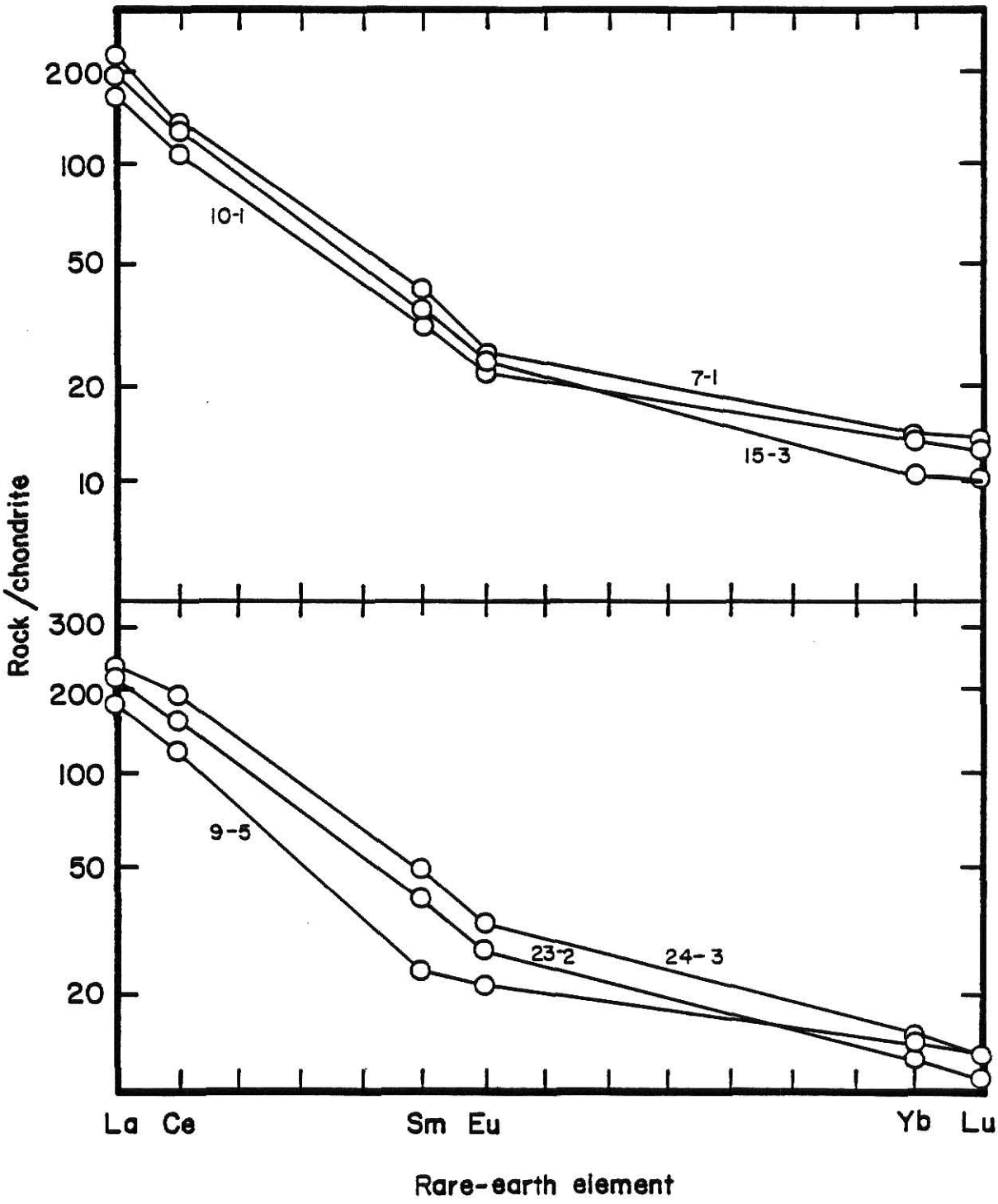

Figure 10b: Variation of REE in latite from lava flows (symbols as in Fig. 5a).

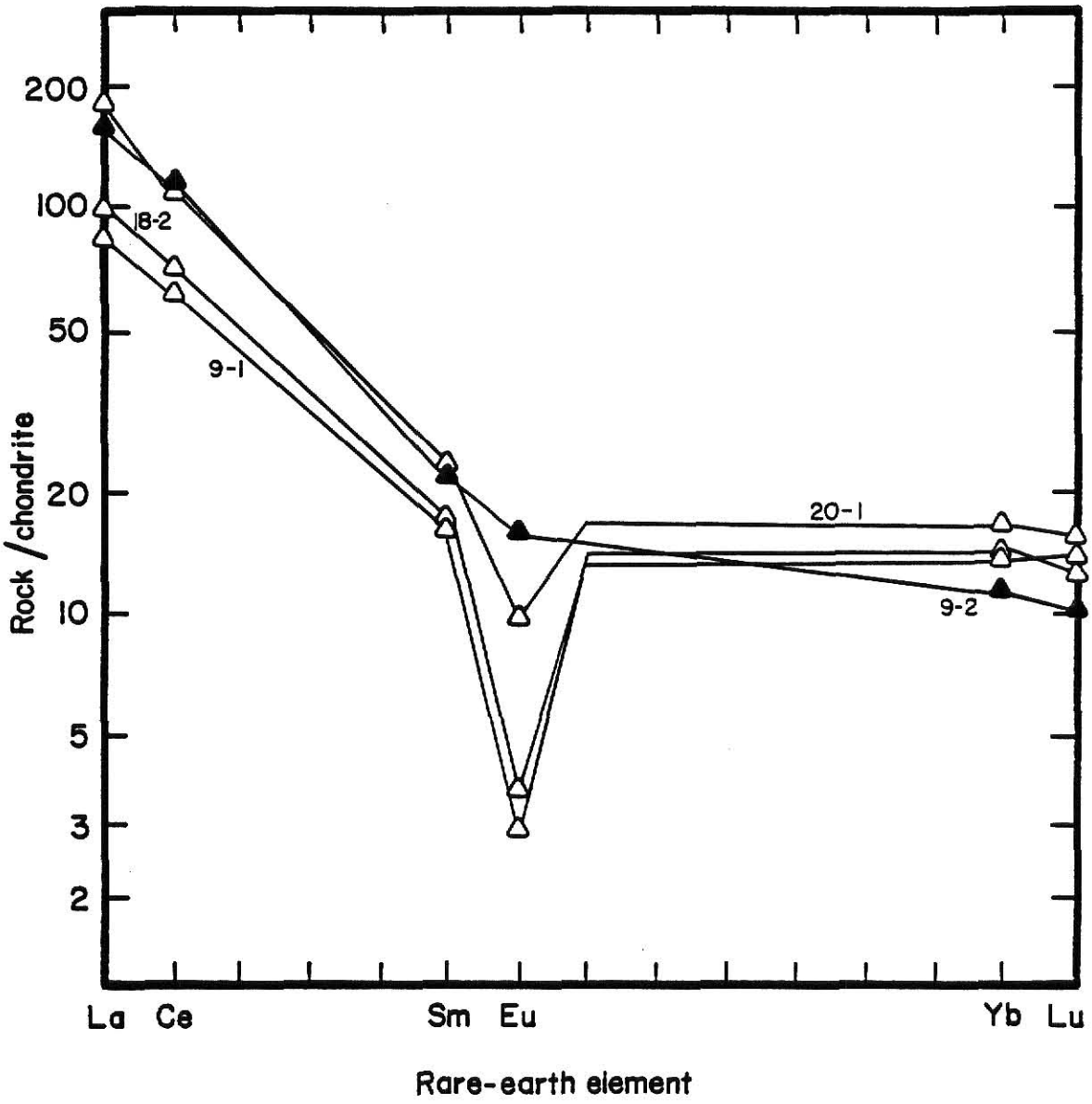

Figure 10c: Variation of REE in rhyolite (symbols as in Fig. 5a).

Rhyolite also has fractionated REE patterns, although samples 9-1 and 18-2 are depleted in LREE compared to the rest of the suite; chondrite-normalized La/Lu ratios in rhyolite range from 6.8 to 15. Rhyolite has progressively larger Eu anomalies with increasing SiO_2. Total REE contents (127 to 222 ppm) are lower in rhyolite than in the rest of the suite.

P E T R O G E N E S I S

EVIDENCE FOR ORIGIN

Field Evidence

Latite is the most abundant rock type that erupted from the Deer Peak volcano. Rhyolite and high-potassium dacite are subordinate in volume and erupted within or near the time interval in which latite erupted. Shoshonite is restricted to one late-stage intrusion.

Field relationships suggest that latite could represent the parent of high-potassium dacite and rhyolite but do not rule out the possibility that latite, high-potassium dacite, and rhyolite originated independently. Even though shoshonite has the lowest D.I., this rock probably does not represent the parent of more differentiated rocks in the Deer Peak volcanic-rock suite. Parent magmas often erupt early in the volcanic sequence, and rock that represents the parent is usually more abundant than comagmatic rocks originating by fractional crystallization (e.g. Fountain, 1979).

Petrographic Evidence

Petrographic evidence supports the hypotheses that shoshonite is

unrelated to latite, high-potassium dacite, and rhyolite and that latite, high-potassium dacite, and rhyolite might be comagmatic. Elston and Bornhorst (1979) stated that petrography can distinguish between basaltic andesite of the younger, back-arc, volcano-tectonic stage and andesitic rocks of the older, modified Andean-arc stage. The basaltic andesite suite is characterized by phenocrysts of olivine, augite, and plagioclase (andesine to labradorite); andesitic rocks are characterized by augite, amphibole, biotite, and plagioclase (andesine). Thus, shoshonite, which is an alkali-rich type of basaltic andesite (Fig. 3), is petrographically distinct from the rest of the suite.

Latite and high-potassium dacite are petrographically similar to andesitic rocks in the modified Andean-arc stage that was described by Elston and Bornhorst (1979). Fractionation of pyroxene and hornblende or pyroxene from a latitic magma would produce a rock that is petrographically similar to high-potassium dacite.

Sanidine mantles plagioclase in rhyolite. Compared to sanidine in high-potassium dacite, sanidine in rhyolite is slightly enriched in the orthoclase component. These observations suggest that rhyolite might also be a product of fractional crystallization.

Despite a careful search, no xenoliths of granitic rock were found in latite. Therefore, assimilation of granitic rock by a mafic magma, unless very efficient as a homogenizing agent, did not play a major role in the petrogenesis of latite.

TRACE-ELEMENT MODELING

General Statement

Trace-element modeling can test petrogenetic hypotheses that were developed from field and petrographic evidence. Even though all rocks in the suite are phenocryst-rich, it will be shown that the different rock types probably are not related by fractional crystallization. Trace-element contents in these rocks suggest that shoshonite, latite, high-potassium dacite, and rhyolite probably originated independently. Preferred models for the genesis of these rocks (Fig. 11) represent simple, one-stage solutions that account for the observed trace-element data and are compatible with field, petrographic, and major-element observations. A qualitative reference list of minerals into which trace elements concentrate is in Table 7.

Latite

Any model for the origin of latite must account for the following characteristics:

(1) high concentrations of LILE, such as Rb, K, Ba, and LREE, compared to oceanic tholeiite, island-arc basalt and andesite, and most continental-margin andesitic rocks (Condie, 1976);

(2) strongly light-element-enriched REE patterns, with small or nonexistent Eu anomalies; and

(3) low concentrations of compatible elements, especially Cr and Mg, compared to tholeiitic and calc-alkaline rocks (Condie, 1976).

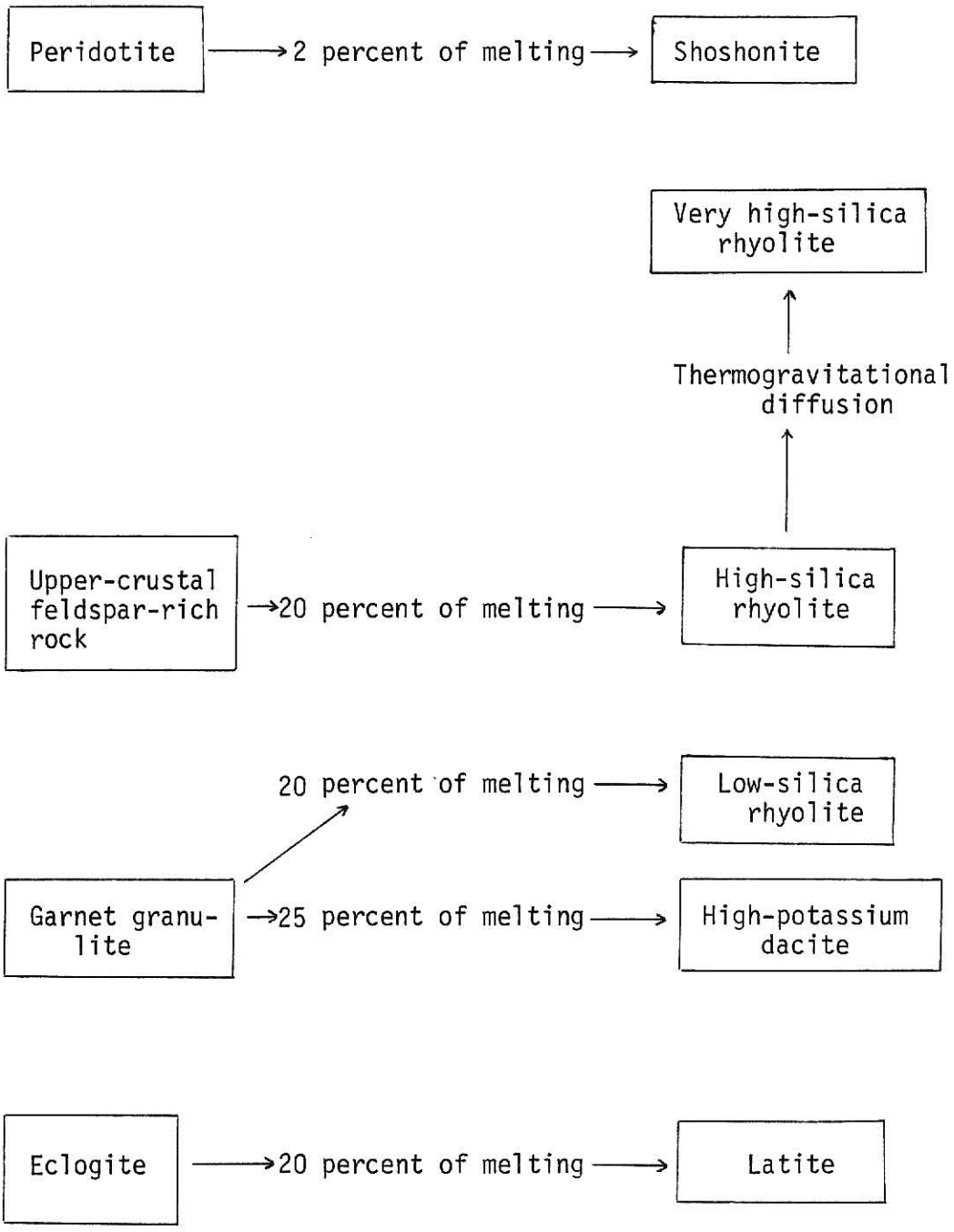

Figure 11: Schematic illustration of the petrogenesis of the Deer Peak Volcanics

Table 7: Trace elements that are concentrated in minerals and in the silicate melt during crystal-melt equilibria.

	Elements concentrated in the mineral	Elements concentrated in the melt
Quartz	none	Rb, Sr, Ba, REE, Cr, Sc
Alkali feldspar	Sr, Ba, Eu	Rb, REE (except Eu), Cr, Sc
Plagioclase	Sr, Eu	Rb, Ba, REE (except Eu), Cr, Sc
Biotite	Rb, Ba, Sc, Cr	Sr, REE
Hornblende	intermediate and HREE, Cr, Sc	Rb, Sr, Ba, LREE
Clinopyroxene	HREE, Cr, Sc	Rb, Sr, Ba, LREE
Orthopyroxene	Cr, Sc	Rb, Sr, Ba, REE, Sc
Olivine	Cr	Rb, Sr, Ba, REE, Sc
Garnet	HREE, Sc, Cr	Rb, Sr, Ba, LREE
Allanite	REE, especially LREE	Rb, Sr, Ba, Cr, Sc
Apatite	REE, especially Eu	Rb, Sr, Ba, Cr, Sc
Zircon	REE, especially HREE	Rb, Sr, Ba, Cr, Sc

After Cullers and others, 1981

Based on a blend of petrologic reasoning, including the results of experimental petrology, possible sources for latitic magma include: (1) upper-mantle peridotite, (2) feldspar-rich rocks, and (3) lower-crustal or upper-mantle eclogite.

Melting of upper-mantle peridotite. -- Even if partial melting of peridotite can produce intermediate-composition magma (experimental evidence is inconclusive), low abundances of Mg and Cr suggest that latite magma at Deer Peak did not equilibrate with peridotite or any other source with magnesian olivine. In addition, abundant LILE in latite at Deer Peak would imply that the mantle source region was incredibly enriched in these elements, or that the percentage of melting was very low. A low percentage of partial melting, however, would unlikely produce the vast volumes of intermediate-composition magma that erupted in the mid-Tertiary volcanic province.

Partial melting of mantle peridotite that produces a basaltic magma, which is then followed by fractional crystallization, has been proposed for the generation of intermediate-composition rocks (e.g. Bowen, 1928). As previously mentioned, the principal minerals that are capable of effecting this transition include plagioclase, pyroxene, hornblende, magnetite, and olivine, all of which could crystallize solely or in combination. Plagioclase strongly concentrates Eu and Sr, and thus would result in negative Eu anomalies and low concentrations of Sr in residual magmas. However, these conditions are not observed in latite. Fractionation of hornblende strongly depletes residual magmas in Sc and Cr; these elements occur in low abundance in latite at Deer Peak. However, significant fractionation of hornblende produces

concave-upward REE patterns in residual magmas, and these patterns are not observed in latite. Fractionation of clinopyroxene or olivine would produce the REE patterns observed in latite if the parent basalt had a lower REE content and a smaller La/Lu ratio than latite. Shoshonite meets these criteria, but chronologic and petrographic evidence discredits this hypothesis. In addition, Eggler and Burnham (1973) stated that observed liquidus phases that crystallized in experimental runs are incapable of effecting the transition from basalt to continental andesite.

Melting of feldspar-rich rock. -- Most rocks in the upper crust contain appreciable proportions of feldspar. Lack of Eu anomalies and high concentrations of Sr in latite would be produced only if most or all feldspar in a feldspar-bearing source melts. Miller (1978) estimated that 50 percent of melting would be required to eliminate feldspar from a source that originally had 50 percent feldspar. Such large percentages of melting would result in low abundances of LILE in the melt, yet LILE are very abundant in latite at Deer Peak. Therefore, at most, feldspar was a minor phase in the source of latite. In addition, lack of appreciable Eu anomalies in latite suggests that fractionation of feldspar did not significantly modify any initial melt and produce latitic magma, despite the abundance of plagioclase phenocrysts in latite.

Melting of eclogite. -- Twenty percent of melting of lower-crustal or upper-mantle eclogite (85 percent clinopyroxene, 15 percent garnet) that is chemically similar to continental tholeiite, but not oceanic tholeiite, could have produced the concentrations of trace elements in latite at Deer Peak (Fig. 12 and Tables 8a and b). Consistent with experimental

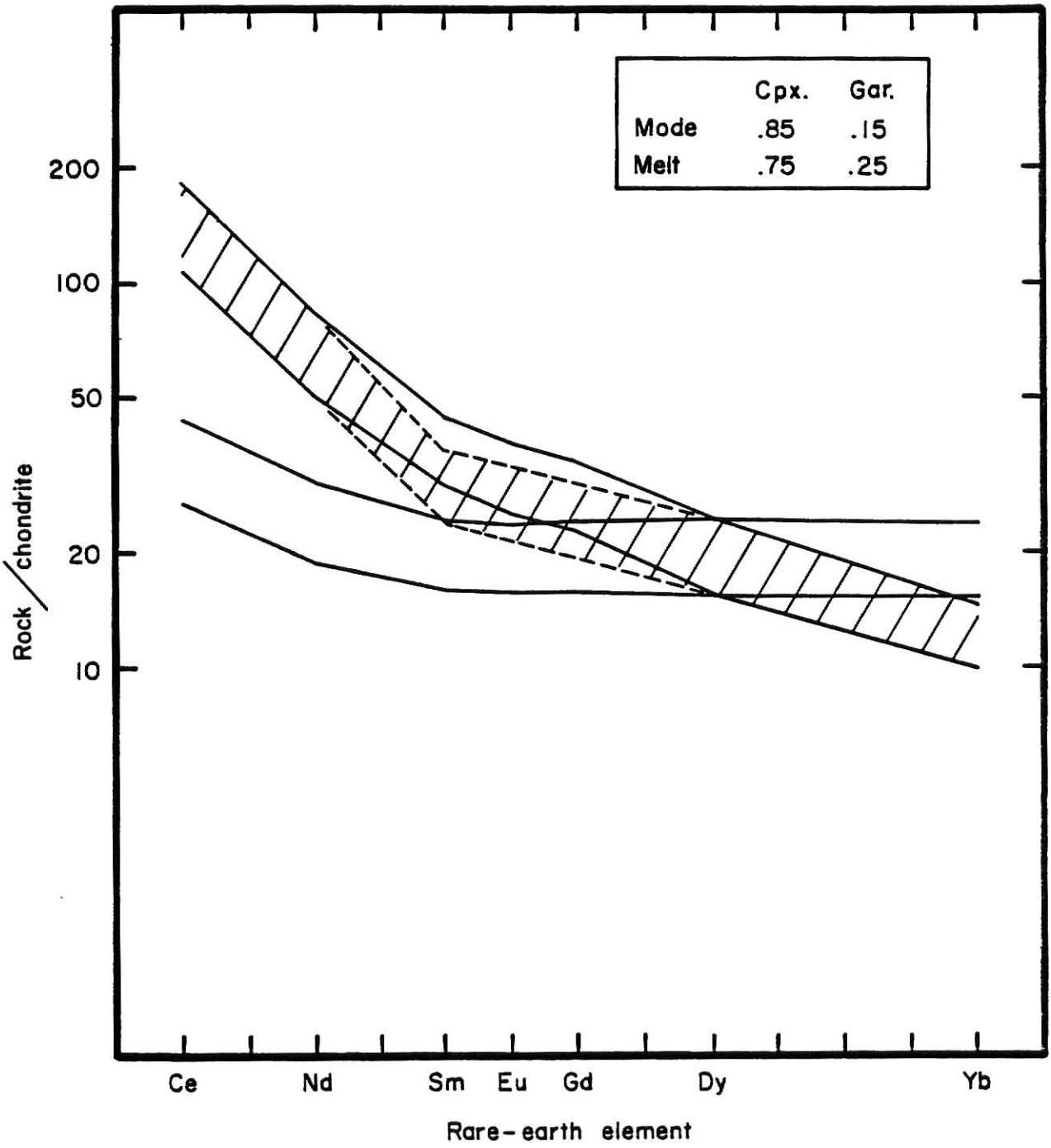

Figure 12: Twenty percent of melting of eclogite that produces latite. Range of eclogite source, lower solid lines; range of observed latite, cross-hatched pattern; range predicted by 20 percent of melting, upper solid lines (becomes coincident with predicted range at either end). The mode of the source is clinopyroxene/garnet = .85/.15 that melts in the ratio .75/.25.

Table 8a: Trace-element contents in naturally occurring tholeiitic rocks and in hypothetical eclogite source of latite at Deer Peak (data in ppm).

	Oceanic tholeiite[1]	Continental tholeiite[2]	Hypothetical source of latite
Rb	1.0 - 9.5	7.5 - 51	23
Sr	103 - 180	154 - 375	200
Ba	3 - 46	20 - 1160	270
Th	0.2 - 0.5	1 - 1.9	-- [3]
Hf	0.9 - 5.9	2.3 - 8.0	2.3
Sc	36 - 52	31 - 70	31
Cr	230 - 410	115 - 303	200

Table 8b: Trace-element contents in latite at Deer Peak and in hypothetical latite that is produced by 20 percent of melting of eclogite (data in ppm).

	Observed values in latite at Deer Peak	Predicted values in hypothetical latite
Rb	100 - 130	115
Sr	835 - 1050	880
Ba	1240 - 2130	1350
Th	9.7 - 14.2	--
Hf	5.3 - 12.1	11.5
Sc	6.0 - 10.8	9.6
Cr	26.8 - 64.8	52

(1) After Condie, 1976; Reitz, 1980; and Wedepohl, 1978

(2) After Condie, 1976; Leeman and Vitaliano, 1976; Lipman and Mehnert, 1975; McDougall, 1976; and Wedepohl, 1978

(3) D. C. for Th is poorly known in this system

evidence (Ringwood, 1975), garnet preferentially enters the melt during fusion. Garnet in the source causes low Cr, Sc, and heavy rare-earth element (HREE) contents in the melt; clinopyroxene also supresses Cr and Sc contents in the melt. In this system, LREE, Rb, Sr, Ba, Th, and Hf are incompatible and are enriched in the melt because eclogite has no residual minerals that concentrate these elements.

High concentrations of LILE in latite alternatively suggest that potassium-rich, minor phases existed in the source of latite. At least a dozen minor phases have been reported in eclogite xenoliths (e.g. Kushiro and Aoki, 1968). Included among these are phlogopite and sanidine, both of which are enriched in LILE. Additionally, the breakdown of phlogopite would provide a high water pressure that would favor melting. There is no experimental data concerning the melting behavior of phlogopite or sanidine in eclogite. Miller (1978) stated that these minerals probably enter the melt preferentially and release LILE into the liquid.

High-potassium Dacite

Fractional crystallization. -- In comparison to latite, high-potassium dacite has: (1) much higher Rb contents; (2) slightly lower REE contents, but a similar high La/Lu ratio; and (3) lower concentrations of Sr, Sc, and Cr. Removal of pyroxene or pyroxene and hornblende from a latitic magma would produce a rock petrographically similar to high-potassium dacite and would also explain the decrease in Sc and Cr contents. The decrease in Sr content, without a simultaneous decrease in Ba content, suggests that fractional crystallization of plagioclase also occurred.

However, a hypothesis involving fractional crystallization cannot explain REE and Rb data. Removal of clinopyroxene or plagioclase from a latitic magma would increase REE in the resulting liquid. Ten percent of fractionation of an extract consisting of subequal proportions of hornblende and plagioclase would produce the observed REE contents but does not explain the high Rb content in high-potassium dacite; about 30 percent of fractionation of a hornblende-plagioclase assemblage is required to produce the observed Rb content. If a minute proportion (about 0.05 percent) of allanite, which strongly concentrates LREE, existed in the hornblende-plagioclase assemblage, then 30 percent of fractionation of this assemblage could have produced both the REE and Rb contents that are observed in high-potassium dacite. However, this is an unlikely hypothesis because allanite was not observed in thin section.

Melting of the lower crust. -- Because fractional crystallization models fail, melting of crustal rocks probably produced high-potassium dacite. Similar high La/Lu ratios in high-potassium dacite and latite suggest that these rocks originated from the same source. However, this is unlikely because garnet has a much greater affinity for HREE when it equilibrates with a silicic liquid than with a more mafic liquid. Partial melting of a source that was petrographically and chemically equivalent to the source of latite would result in lower HREE contents than are observed in high-potassium dacite.

A high La/Lu ratio and possible small negative Eu anomaly in high-potassium dacite suggest that the source contained garnet and feldspar. Based on seismic evidence and experimental investigations, Ringwood (1975) suggested that silicic and intermediate-composition rocks in the

lower crust are converted to an eclogite-facies assemblage that consists of quartz, alkali feldspar, garnet, and clinopyroxene. In this transformation, plagioclase is converted to clinopyroxene and quartz.

In the preferred model, 25 percent of melting of garnet granulite can generate the trace-element contents in high-potassium dacite at Deer Peak (Fig. 13 and Tables 9a and b). Garnet granulite (58 percent clinopyronene, 25 percent alkali feldspar, 10 percent quartz, 5 percent biotite, and 2 percent garnet) is a lower-crustal equivalent of an upper-crustal, plagioclase-bearing rock. Garnet and clinopyroxene in the source produce low Cr, Sc, and HREE contents in the melt. Biotite and alkali feldspar, which melt preferentially, release LILE into the magma. Alkali feldspar produces a small negative Eu anomaly in the melt.

Low-silica Rhyolite

Fractional crystallization. -- Field and petrographic evidence suggest that fractional crystallization from a latitic or high-potassium dacitic magma might have produced low-silica rhyolite. In comparison to latite and high-potassium dacite, low-silica rhyolite has a similar highly fractionated REE pattern and has decreased abundances of REE. Fractionation of clinopyroxene or biotite would increase REE contents; fractionation of hornblende would increase La and strongly decrease HREE contents. Crystallization and removal of clinopyroxene, hornblende, or biotite would decrease Cr content. Fractional crystallization of feldspar would increase REE contents; significant fractionation of feldspar would produce a large negative Eu anomaly. However, none of these chemical characteristics are observed in low-silica rhyolite when compared to

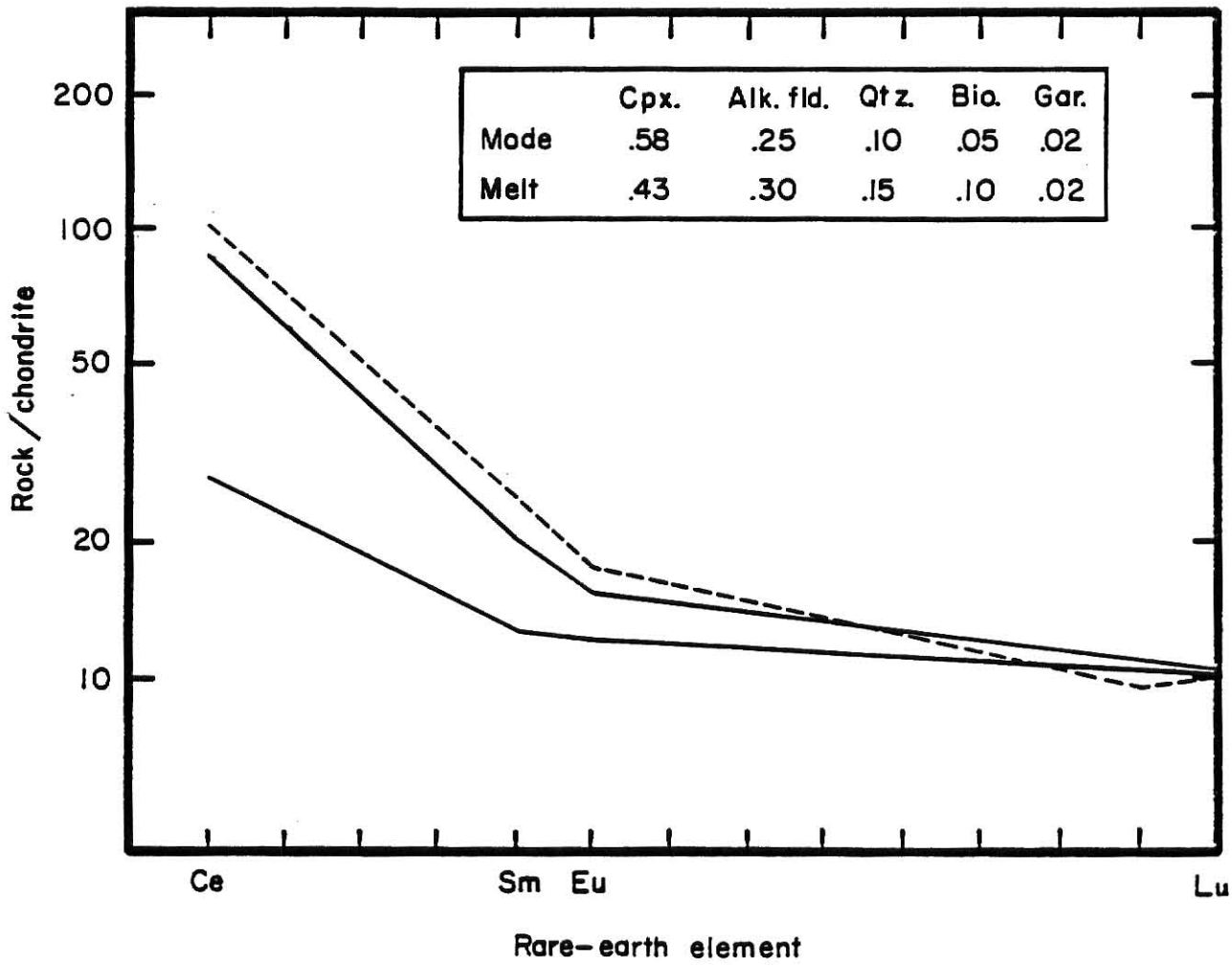

Figure 13: Twenty-five percent of melting of garent granulite that produces high-potassium dacite. Garnet granulite source, lower solid line; predicted high-potassium dacite, upper solid line; observed high-potassium dacite (3-3), dashed line. The mode of the source is clinopyroxene/alkali feldspar/quartz/biotite/garnet = .58/.25/.10/.05/.02 that melts in the ratio .43/.30/.15/.10/.02.

Table 9a: Trace-element contents in naturally occurring, feldspar-bearing crustal rocks and in hypothetical garnet granulite source of high-potassium dacite at Deer Peak (data in ppm).

	Feldspar-bearing[1] crustal rocks	Hypothetical source of high-potassium dacite
Rb	9 - 380	125
Sr	20 - 1100	805
Ba	22 - 18000	3900
Th	1 - 25	3.5
Hf	0.8 - 29	--[2]
Sc	1 - 34	30
Cr	< 1 - 90	50

Table 9b: Trace-element contents in high-potassium dacite at Deer Peak and in hypothetical high-potassium dacite that is produced by 25 percent of melting of garnet granulite (data in ppm).

	Observed in values in high-potassium dacite at Deer Peak	Predicted values in hypothetical high-potassium dacite
Rb	190	186
Sr	647	644
Ba	1490	1482
Th	13.4	14
Hf	8.2	--
Sc	4.2	4.2
Cr	29.4	30

(1) After Arth and Hanson, 1975; Bateman and Chappell, 1979; Cullers and others, 1981; Kistler and Peterman, 1973; Robinson and others, 1976; Spaid-Reitz, 1980; and Wedepohl, 1978

(2) D. C. for Hf is poorly known in this system.

latite or high-potassium dacite. Therefore, low-silica rhyolite probably did not originate by fractional crystallization.

Melting of the lower crust. -- The close similarity of REE contents and patterns between low-silica rhyolite and high-potassium dacite suggests that these rocks originated by partial melting of a similar lower-crustal source. In the preferred model, 20 percent of melting of garnet granulite can produce the abundance of trace elements in low-silica rhyolite at Deer Peak (Fig. 14, Tables 10a and b). This garnet granulite is mineralogically identical and chemically similar to the proposed source of high-potassium dacite. A lower percentage of melting is required than in the petrogenesis of high-potassium dacite, because low-silica rhyolite is the more silicic of the two volcanic rocks.

High-silica Rhyolite

Fractional crystallization. -- Petrographic evidence suggests that fractionation of sanidine or plagioclase from low-silica rhyolitic magma could have produced high-silica rhyolite. Fractionation of plagioclase, however, would produce higher Ba concentrations in high-silica rhyolite than in low-silica rhyolite, and this is not observed. Fractionation of sanidine or plagioclase and sanidine would produce the decrease in Sr, Ba, and Eu contents that are observed in high-silica rhyolite compared to low-silica rhyolite. Hanson (1978), however, pointed out that fractionation of sanidine results in a higher Sr/Ba ratio in the residual liquid, but the Sr/Ba ratio is lower in high-silica rhyolite than in low-silica rhyolite. Consequently, fractionation of sanidine alone probably did not produce high-silica rhyolite. In addition, high-silica rhyolite

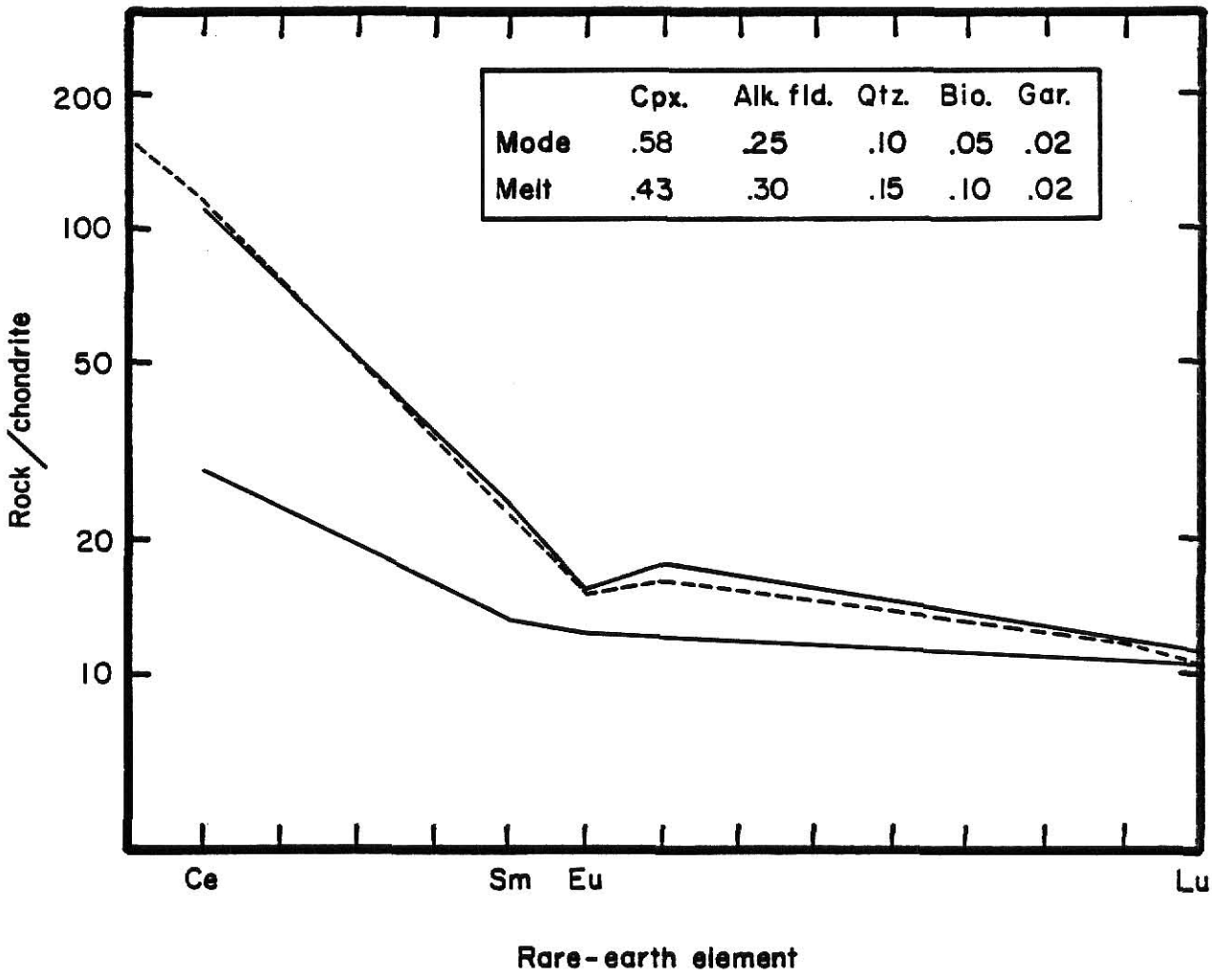

Figure 14: Twenty percent of melting of garnet granulite that produces low-silica rhyolite. Garnet granulite source, lower solid line; predicted low-silica rhyolite, upper solid line; observed low-silica rhyolite (9-2), dashed line. The mode of the source is clinopyroxene/alkali/feldspar/quartz/biotite/garnet = .58/.25/.10/.05/.02 that melts in the ratio .43/.30/.15/.10/.02.

Table 10a: Trace-element contents in naturally occurring, feldspar-bearing crustal rocks in comparison to hypothetical garnet granulite source of low-silica rhyolite at Deer Peak (data in ppm).

	Feldspar-bearing[1] crustal rocks	Hypothetical source of low-silica rhyolite
Rb	9 - 381	115
Sr	20 - 1100	280
Ba	22 - 18000	2000
Th	1 - 25	4
Hf	0.8 - 29	--[2]
Sc	1 - 34	8
Cr	< 1 - 90	70

Table 10b: Trace-element contents in low-silica rhyolite at Deer Peak and in hypothetical low-silica rhyolite that is produced by 20 percent of melting of garnet granulite (data in ppm).

	Observed values in low-silica rhyolite at Deer Peak	Predicted values in hypothetical low-silica rhyolite
Rb	170	176
Sr	607	624
Ba	750	760
Th	19.8	20
Hf	10.9	--
Sc	1.2	1.1
Cr	41.2	41

[1] After Arth and Hanson, 1975; Bateman and Chappell, 1979; Cullers and others, 1981; Kistler and Peterman, 1973; Robinson and others, 1976; Spaid-Reitz, 1980; and Wedepohl, 1978

[2] D. C. for Hf is poorly known in this system

has a wide range of Sc contents that cannot be explained by fractional crystallization of sanidine or plagioclase and sanidine. Therefore, fractional crystallization from a low-silica rhyolite magma probably did not produce high-silica rhyolite at Deer Peak.

Compositional differences that occur within the high-silica rhyolite group might be explained by fractional crystallization. Samples 9-1 and 18-2 are the most silicic rocks in the Deer Peak volcanic-rock suite. Fractionation of sanidine from a liquid represented by sample 20-1 would produce the: (1) increase in Si; (2) decrease in Na, K, Ba, and Sr; and (3) larger negative Eu anomalies that are observed in samples 9-1 and 18-2 compared to sample 20-1. Quantitative modeling of Ba and Sr suggests that about 45 percent of fractionation of sanidine would produce the required depletions of Ba and Sr in the residual liquid. However, mass-balance calculations of even very silica-rich alkali feldspar result in a liquid with SiO_2 in excess of 80 percent by weight. In addition, the wide range of Sc within the high-silica rhyolite group suggests that samples 9-1 and 18-2 did not originate by fractional crystallization from a magma represented by sample 20-1.

Melting of feldspar-rich rock. -- Partial melting of a feldspar-rich source in which feldspar remains in the residue would produce rhyolitic melts with very low concentrations of Ba, Sr, and Eu similar to sample 20-1. In the preferred model, 20 percent of melting of an upper-crustal source that contains mostly alkali feldspar, plagioclase, hornblende, and quartz produces a melt with REE characteristics that are similar to sample 20-1 (Fig. 15). The concentrations of REE in the hypothetical source are similar to many granodiorites and quartz monzonites with small

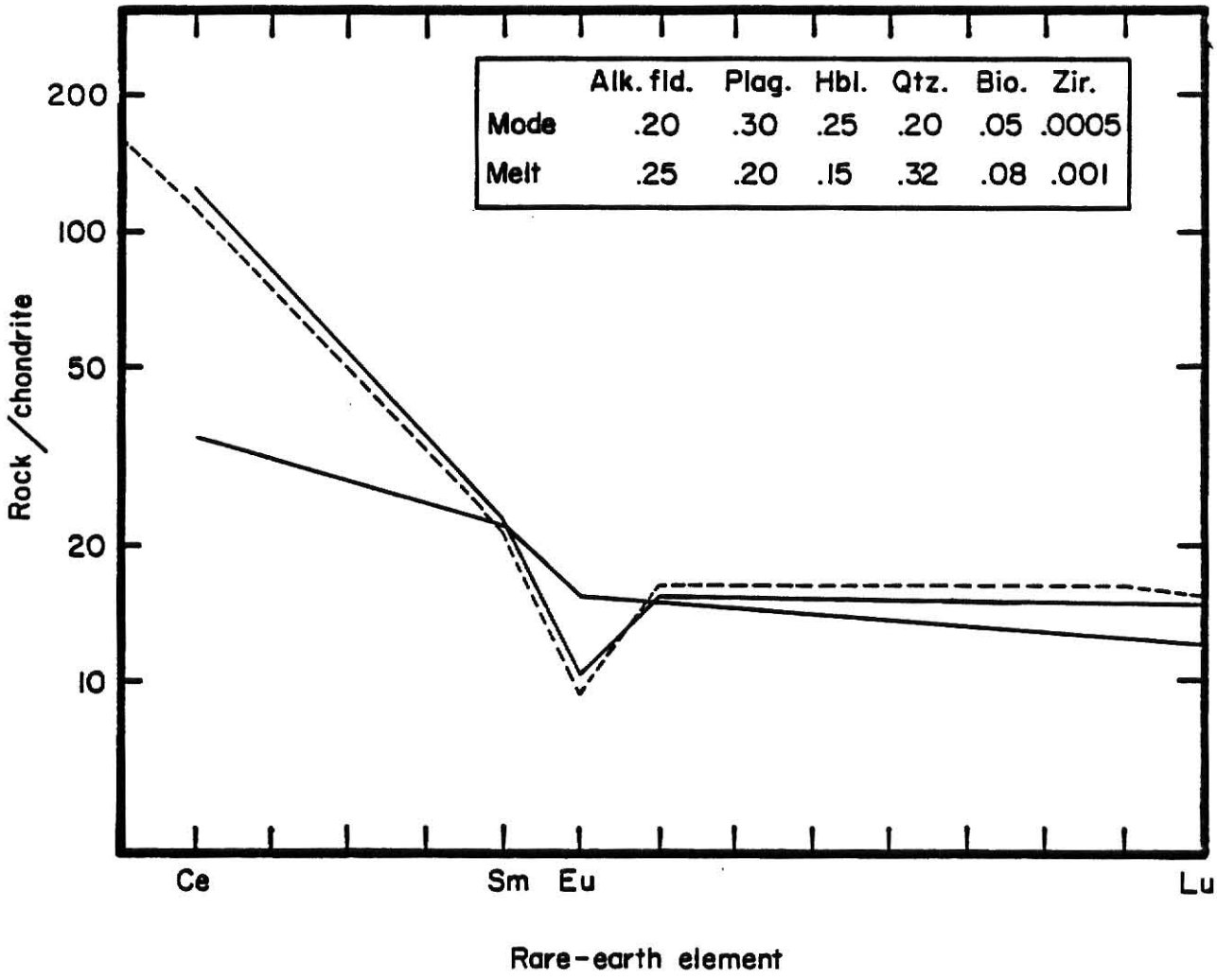

Figure 15: Twenty percent of melting of a feldspar-rich source that produces high-silica rhyolite similar to sample 20-1. Source, solid line with lower LREE and HREE; predicted high-silica rhyolite, solid line with higher LREE; sample 20-1, dashed line. The mode of the source is alkali feldspar/plagioclase/hornblende/quartz/biotite/zircon = .20/.30/.25/.05/.0005 that melts in the ratio .25/.20/.15/.32/.08/.001.

negative Eu anomalies (Cullers and Graf, in press). Proposed abundances of Rb, Sr, Ba, Th, Sc, and Cr in the hypothetical source are well within the range of these elements that are observed in feldspar-bearing crustal rocks (Table 11a). Data in Table 11b show that the abundances of Rb, Sr, Ba, Th, Sc, and Cr that are predicted in the melt by this model are very similar to the observed abundances of these elements in high-silica rhyolite (sample 20-1) at Deer Peak.

Partial melting might also produce very high-silica rhyolite represented by samples 9-1 and 18-2. McCarthy and Kable (1978) suggested that a source with a negative Eu anomaly, which was originally produced by igneous processes, could remelt and form a magma with a larger Eu anomaly. The model in Figure 16 shows that a quartz monzonite source could undergo 5 percent of melting and produce a REE pattern similar to those of samples 9-1 and 18-2. The hypothetical REE distribution in this source is similar to the observed abundances of REE in granitic rocks with negative Eu anomalies (Cullers and Graf, in press). However, the elements Rb, Sc, and Cr have markedly different concentrations in samples 9-1 and 18-2; this discrepancy suggests that partial melting of a single source cannot fully explain the range in chemical behavior that is observed in very high-silica rhyolite at Deer Peak.

Thermogravitational diffusion. -- The preferred model for the origin of very high-silica rhyolite at Deer Peak is by thermogravitational diffusion of elements in a silicic magma chamber. Field and laboratory studies of compositionally zoned ash-flow tuffs, such as the Bishop Tuff, California (Hildreth, 1979) suggest that they represent rapid eruption, from top to bottom, of compositionally zoned magma chambers. Hildreth

Table 11a: Trace-element contents in naturally occurring, feldspar-bearing crustal rocks in comparison to hypothetical source of high-silica rhyolite (sample 20-1) at Deer Peak (data in ppm).

	Feldspar-bearing[1] crustal rocks	Hypothetical source of high-silica rhyolite (sample 20-1)
Rb	9 - 381	115
Sr	20 - 1100	280
Ba	22 - 18000	2000
Th	1 - 25	5
Hf	0.8 - 29	--[2]
Sc	1 - 34	12
Cr	1 - 90	28

Table 11b: Trace-element contents in high-silica rhyolite (sample 20-1) and in hypothetical high-silica rhyolite that is produced by 20 percent of melting of an upper-crustal source (data in ppm).

	Observed values in sample 20-1	Predicted values in hypothetical high-silica rhyolite
Rb	190	186
Sr	181	180
Ba	630	611
Th	24.3	25
Hf	9.6	--
Sc	4.4	4.3
Cr	2.5	2.6

(1) After Arth and Hanson, 1975; Bateman and Chappell, 1979; Cullers and others, 1981; Kistler and Peterman, 1973; Robinson and others, 1976; Spaid-Reitz, 1980; and Wedepohl, 1978

(2) D. C. for Hf is poorly known in this system

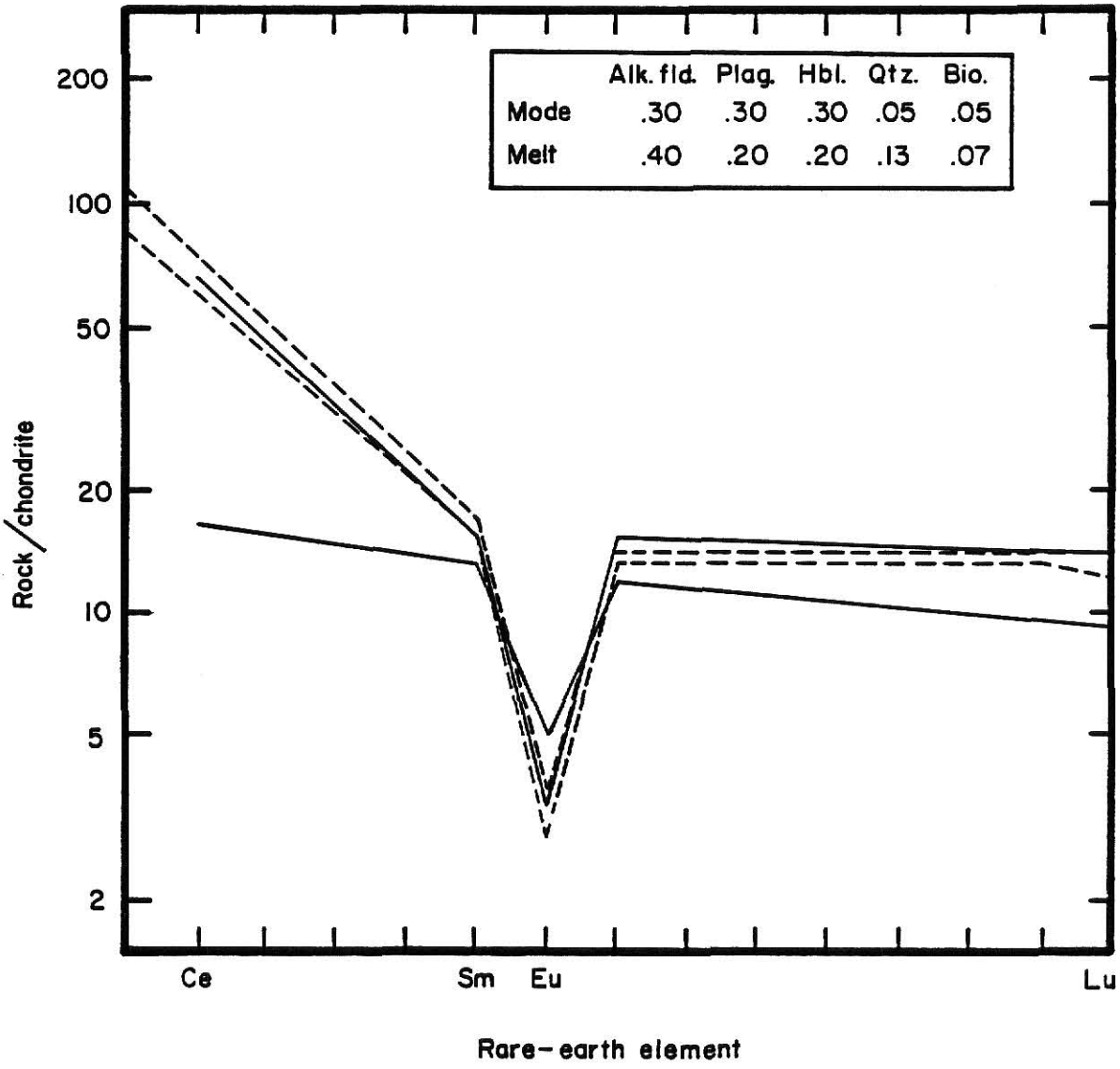

Figure 16: Five percent of melting of a feldspar-rich source that produces high-silica rhyolite similar to samples 9-1 and 18-2. Source, solid line with lower LREE and HREE; predicted high-silica rhyolite, solid line with higher LREE; samples 9-1 and 18-2, dashed lines. The mode of the source is alkali feldspar/plagioclase/hornblende/quartz/biotite = .30/.30/.30/.05/.05 that melts in the ratio .40/.20/.20/.13/.07.

(1981) summarized evidence for thermogravitational diffusion of elements through viscous, silicic magma bodies that causes the otherwise enigmatic wide range of many trace elements among the individual ash-flows of a single eruption.

Selected elements in more differentiated (higher SiO_2) and less differentiated (lower SiO_2) high-silica rhyolite pairs from the Bishop Tuff, the Lava Creek Tuff, Yellowstone, and the Deer Peak Volcanics are compared in Table 12. The following trends, which Hildreth (1981) believed are characteristic of thermogravitational diffusion, are observed in all three pairs:

(1) major-element gradients are low;

(2) Sr, Ba, Eu, and K/Rb are severely depleted in the most silicic rocks;

(3) Ce/Yb ratios decrease with increasing SiO_2; and

(4) Rb, Rb/Sr, and volatile components such as H_2O, F, and Cl increase with increasing SiO_2.

Hildreth (1981) observed that K_2O varies antithetically with Na_2O in the Bishop Tuff and the Lava Creek Tuff; this behavior is not observed in high-silica rhyolite at Deer Peak. However, in other compositionally zoned extrusions, such as those from the 1912 eruption at Katmai, Alaska, both Na_2O and K_2O decrease with increasing SiO_2 (Hildreth, 1981); this trend is observed at Deer Peak. Therefore, thermogravitational diffusion of elements best explains the origin of very high-silica rhyolite at Deer Peak, although it was not possible, because of poor exposure, to demonstrate that high-silica rhyolite represents a single, rapid eruption.

Table 12: Comparison of more differentiated (very high-silica rhyolite) and less differentiated (high-silica rhyolite pairs in high-silica rhyolite suites (major-element oxides, H_2O, and ignition in percent; others in ppm).

	Bishop Tuff[1]		Lava Creek Tuff[2]		Deer Peak Volcanics	
	Higher SiO_2	Lower SiO_2	Higher SiO_2	Lower SiO_2	Higher SiO_2	Lower SiO_2
SiO_2	77.7	75.5	77.0	75.5	75.5 - 76.7	74.1
Al_2O_3	13.3	13.0	12.5	13.1	11.6 - 13.0	14.0
K_2O	4.8	5.5	4.8	5.2	4.4 - 4.5	4.5
Na_2O	3.9	3.35	3.8	3.6	3.9 - 4.3	5.0
H_2O	4.9	2.8	--	--	-----	--
Ignit.	--	--	--	--	1.01 - 1.82	0.69
Rb	190	95	300	150	200 - 290	190
Sr	4.8	110	< 5	> 5	21 - 31	181
Ba	9.5	580	70	400	61 - 64	630
Eu	0.04	0.38	0.1	0.8	0.22 - 0.27	0.71
F	560	340	1600	650	-----	--
Cl	670	280	1100	500	-----	--
Ce/Yb	17.3	89	9.5	44.4	22.9 - 24.5	33.9
Rb/Sr	39.6	0.86	> 60	> 30	9.3 - 9.4	0.30
K/Rb	106	243	67.2	146	128 - 184	197

[1] Hildreth, 1979; [2] After Hildreth, 1981

Shoshonite

Melting of eclogite. -- Compared to latite, shoshonite has a slightly lower La/Lu ratio and has similar high contents of Ba and Sr. These data suggest that the source of shoshonite was similar to the eclogite source that was proposed for latite. However, very large percentages of partial melting of eclogite are required to produce basaltic magma. Such large percentages of melting would result in low abundances of LILE in the magma and should result in large volumes of shoshonite at the surface. These characteristics are not observed and partial melting of eclogite probably did not produce shoshonite at Deer Peak.

Melting of upper-mantle peridotite. -- In the preferred model, about 2 percent of melting of garnet peridotite (60 percent olivine, 25 percent orthopyroxene, 13 percent clinopyroxene, and 2 percent garnet) can produce the trace-element contents in shoshonite at Deer Peak (Fig. 17, Tables 13a and b). The peridotite source is enriched in LILE compared to typical undepleted peridotite (Yoder, 1976; Kay and Gast, 1973). Consistent with experimental evidence (Green, 1973), garnet and clinopyroxene preferentially enter the melt. Heavy rare-earth elements, Cr, and Sc are compatible with the mineralogy of peridotite and exist in low abundance in the melt. The melt is enriched in LREE, Rb, Ba, Sr, Th, and Hf because these elements are not concentrated in olivine, pyroxene or garnet.

Two alternative models for the origin of shoshonite can be considered. Partial melting of typical peridotite, which has much lower LILE contents than peridotite in the preferred model, could melt and form a basaltic liquid. However, 0.5 percent of melting or less of typical peridotite

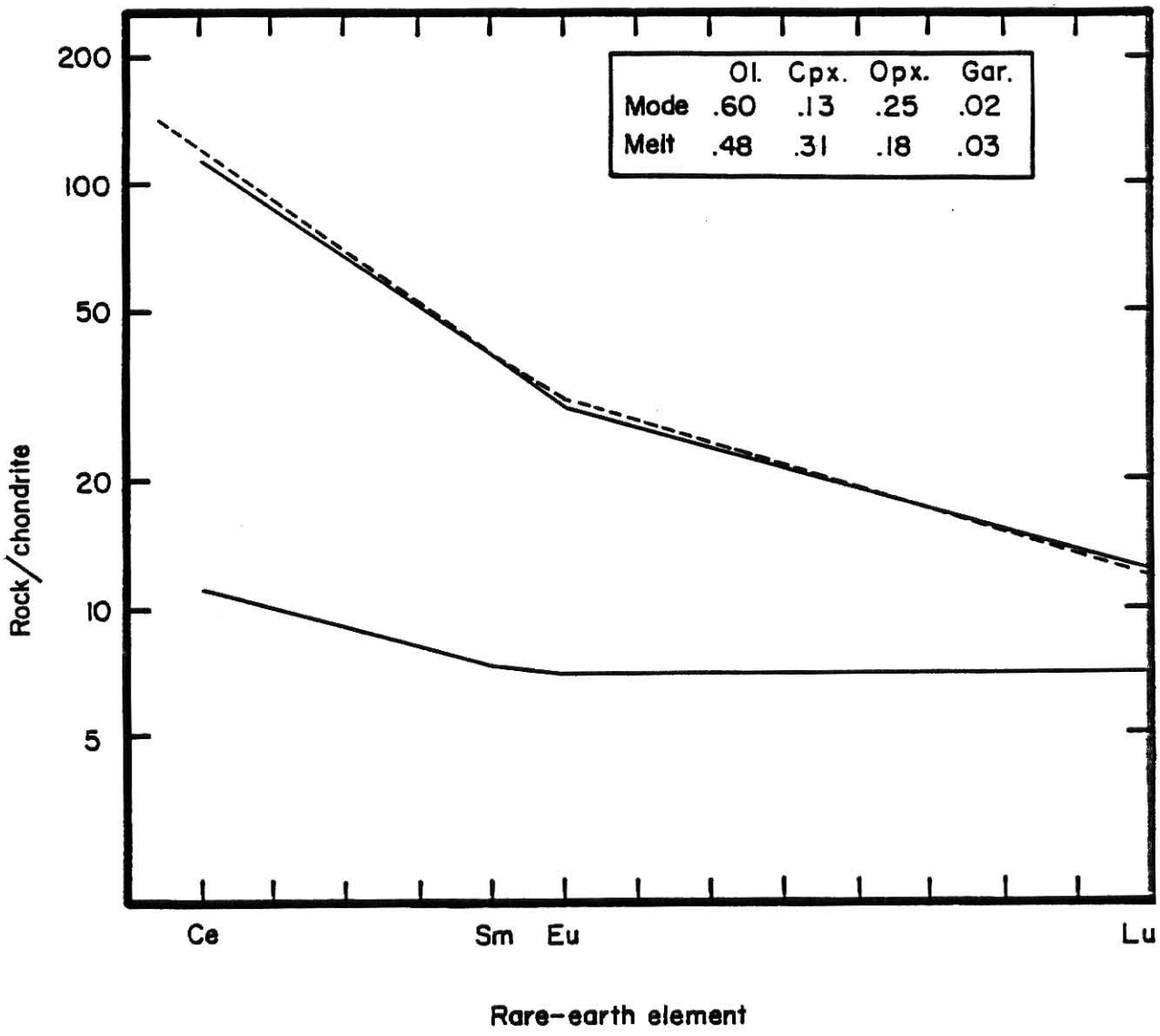

Figure 17: Two percent of melting of peridotite that produces shoshonite. Peridotite source, lower solid line; predicted shoshonite, upper solid line; observed shoshonite (6-1), dashed line. The mode of the source is olivine/clinopyroxene/orthopyroxene/garnet = .60/.13/.25/.02 that melts in the ratio .48/.31/.18/.03.

Table 13a: Trace-element contents in naturally occurring peridotite and in hypothetical peridotite source of shoshonite at Deer Peak (data in ppm).

	Undepleted peridotite[1]	All peridotites[2]	Hypothetical peridotite source of shoshonite
Rb	2 - 8	0.07 - 8	2.3
Sr	10 - 40	0.4 - 104	53
Ba	4 - 5	1 - 70	22
Th	0.004 - 0.006	-----	--[3]
Hf	0.5 - 1.0	0.5 - 1.0	0.5
Sc	5 - 15	1 - 52	38
Cr	2800 - 3400	150 - 18000	625

Table 13b: Trace-element contents in shoshonite at Deer Peak and in hypothetical shoshonite that is produced by 2 percent of melting of peridotite (data in ppm).

	Observed values in shoshonite at Deer Peak	Predicted values in hypothetical shoshonite
Rb	84	85
Sr	954	938
Ba	1140	1100
Th	6.6	--
Hf	5.1	5.7
Sc	20.4	20
Cr	219	219

(1) After Reitz, 1980; (2) After Wedepohl, 1978; (3) D. C. for Th is poorly known in this system.

would produce the concentrations of REE that are observed in shoshonite at Deer Peak. Such a small percentage of melting poses physical problems for extraction of the minute, liquid fraction from the source.

Alternatively, typical undepleted peridotite might melt and equilibrate with basaltic magma and H_2O-rich vapor. Wendtlandt and Herrington (1979) and Mysen (1979) suggested that REE (particularly LREE) partition from peridotite into H_2O-rich vapor at high pressure; with decreasing pressure, REE move from the vapor into the melt. Thus basaltic melts may become enriched in REE by this mechanism.

MECHANISMS OF MAGMA GENERATION

Many individuals (Lipman and others, 1972; Coney and Reynolds, 1977; Cross and Pilger, 1978) inferred that a shallow-dipping subduction system extended inland from the Pacific margin as far as Colorado during the early and middle Cenozoic. They proposed that melting within this system resulted in the generation of andesitic magmas.

The geochemical results of this thesis suggest that the source of latite at Deer Peak was eclogite of continental-tholeiitic rather than oceanic-tholeiitic affinity. Thus, chemical data would preclude a simple model in which direct melting of subducted oceanic tholeiite produced latite at Deer Peak.

Additional factors discredit the imbricate subduction hypothesis of Lipman and others (1972). No surface expression, such as melange or blueschist-facies assemblages, has been found for the hypothetical easternmost member of the imbricate subduction system. Also, Lipman and others (1972) hypothesized that the depth of melting of the subducted

slab under Colorado would be about 300 to 400 km. Experimental studies indicate that andesitic magma is probably not generated at depths below 150 km (Wyllie, 1973).

The development of deep-crustal fault zones associated with subsidence of the Wet Mountain Valley probably caused magmatism at Deer Peak and in the Wet Mountains area. Movement along these faults began in the late Cretaceous and continued throughout the early and middle Cenozoic (Scott and Taylor, 1975), and controlled the location of eruptive centers in the Wet Mountains area (Scott and Taylor, 1975; MacNish, 1966). Smith (1979) suggested a similar origin for magmatism at Spanish Peaks. Movement along deep-crustal faults might have provided one or more of the following conditions that favor melting: (1) decrease of lithostatic pressure, (2) increase in fugacity of H_2O because of migration of vapor along fault zones, and (3) movement of rocks across the geothermal gradient.

Although direct partial melting of a subducted slab probably did not produce volcanism in the Wet Mountains area, convergence at the Pacific margin could have resulted in favorable conditions for the generation of magma along deep-crustal fault zones. For example, Barazangi and Isacks (1976) suggested that low-angle subduction results in efficient transmission of compressive stress between descending and overriding plates. Burchfiel and Davis (1975) and Brewer and others (1980) applied this relation to explain the origin of basement-rooted structure and volcanic activity in the eastern cordillera. Alternatively, oblique subduction, which is required in the plate-tectonic reconstructions of Atwater (1970) and Atwater and Molnar (1973), could have provided a significant component of tensional or shearing stress, which may have favored the development of intermontane troughs such as the Wet Mountain Valley.

The beginning of Basin-and-Range style tectonics (Elston and Bornhorst, 1979; Lipman, 1980) might have extended deep-crustal faults into the upper mantle. Dry mantle conditions, perhaps reflected by the anhydrous phenocryst assemblage of shoshonite, favored a low percentage of melting and produced late-stage shoshonite at Deer Peak.

S U M M A R Y

Field and petrographic observations were integrated with major- and trace-element data to investigate the petrology of the Oligocene Deer Peak Volcanics, Colorado. The investigation focused on the central stock, which represents the eroded neck of the Deer Peak volcano, the type locality, and five other exposures near the stock. Five igneous-rock types are recognized: (1) latite, (2) high-potassium dacite, (3) low-silica rhyolite, (4) high-silica rhyolite, and (5) shoshonite. Latite is the most abundant rock type and erupted early in the volcanic sequence. Small volumes of high-potassium dacite and rhyolite erupted within the time interval that latite erupted. Shoshonite occurs as a small, late-stage intrusion at the stock.

The Deer Peak Volcanics are alkali-calcic and are characterized by high concentrations of LILE in comparison to most other orogenic rock suites. Although the volcanic rocks at Deer Peak have a high phenocryst content, trace-element modeling shows that the different rock types are probably not related by fractional crystallization but that they originated independently by partial melting.

Generation of magma by movement along deeply penetrating faults explains the diversity and order of eruption of the Deer Peak Volcanics. Development of these faults is related to subsidence of the Wet Mountain Valley. The following magmatic history of the Deer Peak Volcanics is

compatible with field, petrographic, and chemical data:

(1) Approximately 20 percent of melting of eclogite similar in composition to continental tholeiite produced latitic magma that erupted as the oldest lavas at Deer Peak. Latite probably did not originate by melting of upper-mantle peridotite or by fractional crystallization from a more mafic parent.

(2) Approximately 25 and 20 percent of melting of lower-crustal garnet granulite produced high-potassium dacitic and low-silica rhyolitic magmas, respectively. Models involving fractional crystallization do not fully account for the observed abundances of trace elements in high-potassium dacite and low-silica rhyolite. Both of these rocks were emplaced during the time interval in which latite erupted.

(3) Rising volumes of magma fused parts of the upper crust and generated high-silica rhyolite by about 20 percent of melting. Some high-silica rhyolite magma erupted after its formation, but some formed subsurface bodies that differentiated by thermogravitational diffusion and produced very high-silica rhyolite. Fractional crystallization does not explain the origin of high-silica rhyolite nor does it explain compositional differences within the high-silica rhyolite group.

(4) The beginning of Basin-and-Range style tectonics extended deep-crustal faults into the upper mantle and produced late-stage shoshonite by about 2 percent of melting of peridotite.

Melting of eclogite is an unlikely origin for shoshonite. The lower percentage of melting that is required for shoshonite in comparison to the other magma types could reflect drier mantle conditions or the high-melting point of peridotite.

The inferred source of latite is enriched in LILE in comparison to oceanic tholeiite. Consequently, a simple model involving partial melting of subducted oceanic tholeiite probably did not produce magmatism at Deer Peak. However, oblique subduction at the Pacific margin, or a shallow-dipping subduction geometry, or both, could have provided a stress field that favored the development of deep-crustal faults and associated volcanism.

REFERENCES

Anderson, J. L., and Cullers, R. L., 1978, Geochemistry and Evolution of the Wolf River Batholith, a late Precambrian rapakivi massif in north Wisconsin, U.S.A: Precambrian Research, v. 7, p. 284-324.

Arth, J. G., and Hanson, G. N., 1975, Geochemistry and origin of the early Precambrian crust of northeast Minnesota: Geochemica et Cosmochemica Acta, v. 39, p. 325-362.

Atwater, T., 1970, Applications of plate tectonics for the Cenozoic tectonic evolution of western North America: Geological Society of America Bulletin, v. 81, p. 3513-3535.

Atwater, T., and Molnar, P., 1973, Relative motion of the Pacific and North American plates deduced from sea-floor spreading in the Atlantic, Indian, and South Pacific oceans, in Kovach, R. L., and Amos, N., eds., Proceedings of the conference on tectonics problems of the San Andreas fault system: Stanford University Publications in the Geological Sciences, v. 13, p. 136-148.

Barazangi, M., and Isacks, B. L., 1976, Spatial distribution of earthquakes and subduction of the Nazca plate beneath South America: Geology, v. 4, p. 686-692.

Barker, D. S., 1977, Northern Trans-Pecos magmatic province: Introduction and comparison with the Kenya Rift: Geological Society of America Bulletin, v. 88, p. 1421-1427.

Bateman, P. C., and Chappell, B. W., 1979, Crystallization, fractionation, and solidification of the Toulumne instrusive series, Yosemite National Park: Geological Society of America Bulletin, v. 90, p. 465-482.

Bowen, N. L., 1928, The evolution of igneous rocks: Princeton, N. J., Princeton University Press, 332 p.

Boyer, R. E., 1962, Petrology and structure of the southern Wet Mountains, Colorado: Geological Society of America Bulletin, v. 73, p. 1047-1069.

Brewer, J. A., Smithson, S. B., Oliver, J. E., and Brown, L. D., 1980, The Laramide orogeny: Evidence from COCORP deep crustal seismic profiles in the Wind River Mountains, Wyoming: Tectonophysics, v. 62, p. 165-189.

Brooks, C., James, D. E., and Hart, S. R., 1976, Ancient lithosphere: Its role in young continental volcanism: Science, v. 193, p. 1086-1094.

Burchfiel, B. C., 1980, Tectonics of noncollisional regimes - the modern Andes and the Mesozoic cordilleran orogen of the western United States, in Burchfiel, B. C., Oliver, J. E., and Silver, L. T., chm., Continental Tectonics: National Academy of Sciences, p. 410-450.

Burchfiel, B. C., and Davis, G. A., 1975, Nature and controls of cordilleran orogenesis, western United States: Extensions of an earlier synthesis: American Journal of Science, v. 275-A, p. 363-396.

Chadwick, R. A., 1970, Belts of eruptive centers in the Absaroka-Gallatin volcanic province, Wyoming-Montana: Geological Society of America Bulletin, v. 81, p. 267-274.

Chayes, F., 1949, Simple point counter for thin section analysis: American Mineralogist, v. 34, p. 1-11.

Compton, R. R., 1962, A manual of field geology: New York, John Wiley, 378 p.

Condie, K. C., 1976, Plate tectonics and crustal evolution (1st ed.): New York, Pergammon Press, 284 p.

Coney, P. J. and Reynolds, S. J., 1977, Cordilleran Benioff zones: Nature, v. 270, p. 403-405.

Cox, K. G., Bell, J. D., and Pankhurst, R. J., 1979, The interpretation of igneous rocks: London, George Allen and Unwin, 450 p.

Cross, T. A. and Pilger, R. H. Jr., 1978, Constraints on absolute motion and plate interaction inferred from Cenozoic igneous activity in the western United States: American Journal of Science, v. 278, p. 865-902.

Cross, W., 1890, Geology of the Rosita Hills, Custer County, Colorado: Colorado Science Society Proceedings, v. 3, p. 269-279.

———— 1896, Geology of Silver Cliff and the Rosita Hills, Colorado: U. S. Geological Survey 17th Annual Report, pt. 2, p. 263-403.

Cullers, R. L., and Graf, in press, Rare earth elements in igneous rocks of the continental crust: Intermediate and silicic rocks, in Henderson, P., ed., Rare earth element geochemistry: Amsterdam, Elsiever Scientific Publishing Co.

Cullers, R. L., Kock, R., and Bickford, M. E., 1981, Chemical evolution of magmas in the Proterozoic terrane of the St. Francois Mountains, southeastern Missouri, 2. Trace element data: Journal of Geo physical Research, v. 86, p. 10388-10481.

Dickenson, D. H., and Hatherton, T., 1967, Andesitic volcanism and seismicity around the Pacific: Science, v. 157, p. 801-803.

Elston, W. E., and Bornhorst, T. J., 1979, The Rio Grande Rift in context of regional post-40 m.y. volcanic and tectonic events, in Reiker, R. E., ed., Rio Grande Rift: Tectonics and magmatism: American Geophysical Union, p. 416-438.

Eggler, D. H., and Burnham, C., 1973, Crystallization and fractionation trends in the system andesite-H_2O-CO_2-O_2 at pressures to 10 kb: Geological Society of American Bulletin, v. 84, p. 2517-2532.

Epis, R. K., and Chapin, C. E., 1968, Geologic history of the Thirty-nine Mile volcanic field, central Colorado: Colorado School of Mines Quarterly, v. 63, p. 51-85.

Ewart, A., 1979, A review of the mineralogy and chemistry of Tertiary-Recent dacitic, latitic, rhyolitic, and related volcanic rocks, in Barker, F., ed., Trondhjemites, dacites, and related rocks: Amsterdam, Elsiever Scientific Publishing Co., p. 12-112.

Ewart, A., and LeMaitre, R. W., 1980, Some regional compositional differences within Tertiary-Recent orogenic magmas: Chemical Geology, v. 63, p. 51-85.

Flanagan, F. J., 1976, Compilation of data on U.S.G.S. standards: U. S. Geological Survey Professional Paper 840, p. 131-183.

Fountain, J. C., 1979, Geochemistry of Brokeoff volcano, California: Geological Society of American Bulletin, v. 90, p. 294-300.

Gast, P. W., 1968, Trace element fractionation and the origin of tholeiitic and alkaline magma: Geochemica et Cosmochemica Acta, v. 32, p. 1057-1086.

Gill, J. B., 1981, Orogenic andesites and plate tectonics: Berlin, Springer-Verlag, 390 p.

Goddard, E. N., chm., and others, 1948, Rock-color chart: National Research Council; reprinted by Geological Society of America, 1951, 1963, 1970, 1975, 6 p.

Gordon, G. E., Randle, K., Goles, G., Corliss, J., Beeson, M. H., and Olsey, S. S., 1968, Instrumental neutron activation analysis of standard rocks with high resolution gamma ray detectors: Geochemica et Cosmochemica Acta, v. 32, p. 369-396.

Green, D. H., 1973, Experimental melting studies on a model upper-mantle composition at high pressure under water-saturated conditions and water-undersaturated conditions: Earth and Planetary Science Letters, v. 19, p. 37-58.

Green, D. H., and Ringwood, A. E., 1967, The genesis of basaltic magmas: Contributions to Mineralogy and Petrology, v. 15, p. 103-190.

Green, T. H., 1980, Island arc and continent-building magmatism - a review of petrogenic models based on experimental petrology and geochemistry: Tectonophysics, v. 63, p. 367-385.

Green, T. H., and Ringwood, A. E., 1968, Genesis of the calc-alkaline igneous rock suite: Contributions to Mineralogy and Petrology, v. 18, p. 105-162.

Guyton, J. S., Hutton, J. R. and Sokolsky, G. E., 1960, Geology of the Devils Hole area, Custer and Huerfano Counties, Colorado: Michigan University M. S. dissertation, 81 p.

Hanson, G. N., 1978, The application of trace elements to the petrogenesis of igneous rocks of granitic composition: Earth and Planetary Science Letters, v. 38, p. 26-43.

Haskin, L. A., Allen, R. O., Helmke, P. A., Pastor, T. R., Anderson, M. R., Kortev, R. S., and Zweifel, K. A., 1970, Rare earths and other trace elements in Apollo II lunar samples: Proceedings of the Apollo II Lunar Science Conference, suppliment 1, v. 2, p. 1213-1231.

Higuchi, H., and Nagasawa, H., 1969, Partition of trace elements between rock-forming minerals and the host volcanic rocks: Earth and Planetary Science Letters, v. 7, p. 281-289.

Hildreth, W., 1979, The Bishop Tuff: Evidence for the origin of compositional zonation in silicic magma chambers: Geological Society of America Special Paper 180, p. 43-75.

———— 1981, Gradients in silicic magma chambers: Implications for lithospheric magmatism: Journal of Geophysical Research, v. 86, p. 10153-10192.

Hyndman, D. W., 1972, Petrology of igneous and metamorphic rocks: New York, McGraw-Hill, 533 p.

Irvine, T. N., and Baragar, W. R. A., 1971, A guide to the chemical classification of the common volcanic rocks: Canadian Journal of Earth Sciences, v. 8, p. 523-548.

Jacobs, J. W., Korstev, R. L., Blanchard, D. P., and Haskin, L. A., 1977, A well-tested procedure for instrumental neutron activation analysis of silicate rocks and minerals: Journal of Radioanalytical Chemistry, v. 40, p. 93-114.

Jahn, B., 1973, A petrogenic model for the igneous complex in the Spanish Peaks region, Colorado: Contributions to Mineralogy and Petrology, v. 41, p. 241-258.

Jahn, B., Sun, S. S., and Nesbitt, R. W., 1979, REE distribution of the Spanish Peaks igneous complex, Colorado: Contributions to Mineralogy and Petrology, v. 70, p. 281-298.

James, G. W., 1980, Determination of Rb, Sr, Ba, and P_2O_5 in Wet Mountain volcanics: Kansas Geological Survey Report 80:11-1, 1 p.

Johannsen, A., 1939, A descriptive petrography of the igneous rocks (2nd ed.), v. 1: Chicago, The University of Chicago Press, 318 p.

Johnson, R. B., 1969, Geologic map of the Trinidad quadrangle, south-central Colorado: U. S. Geological Survey Misc. Geol. Inv. Map I-558.

Kay, R. W., and Gast, P. W., 1973, The rare earth content and origin of alkali-rich basalts: Journal of Geology, v. 81, p. 653-683.

Kieth, S. B., 1978, Paleosubduction geometries inferred from Cretaceous and Tertiary magmatic patterns in southwestern North America: Geology, v. 6, p. 516-521.

Kilbane, N. A., 1978, Petrogenesis of the McClure Mountain mafic-ultramafic and alkalic complex, Fremont County, Colorado: Kansas State University M. S. thesis, 158 p.

Kistler, P. W., and Peterman, Z. E., 1973, Variations in Sr, Rb, K, Na, and initial Sr87/Sr86 in Mesozoic granitic rocks and intruded wall rocks in central California: Geological Society of America, v. 84, p. 3489-3512.

Koch, R., 1978, Petrogenesis of the Precambrian Bevos and Musco groups, St. Francois Mountains igneous complex, Missouri: Kansas State University M. S. thesis, 102 p.

Kuno, H., 1959, Origin of Cenozoic petrographic provinces of Japan and surrounding areas: Bulltin Volcanologique, ser. 2, v. 20, p. 37-76.

Kushiro, I., and Aoki, K., 1968, Origin of some eclogitic inclusions in kimberlite: American Mineralogist, v. 53, p. 1347-1367.

Kushiro, I., Shimizu, N., Nakamura, Y., and Akimoto, S., 1972, Composition of coexisting liquid and solid phases formed upon melting of natural garnet and spinel lherzolites at high pressures: A preliminary report: Earth and Planetary Science Letters, v. 14, p. 19-25.

Leeman, W. P., 1982, Tectonic and magmatic significance of strontium isotopic variations in Cenozoic volcanic rocks from the western United States: Geological Society of America Bulletin, v. 93, p. 487-503.

Leeman, W. P., and Vitaliano, C. J., 1976, Petrology of McKinney basalt, Snake River Plain, Idaho: Geological Society of American Bulletin, v. 87, p. 1777-1792.

Lipman, P. W., 1968, Geology of the Summer Coon volcanic center, eastern San Juan Mountains, Colorado: Colorado School of Mines Quarterly, v. 63, p. 211-236.

———— 1980, Cenozoic volcanism in the western United States: Implications for continental tectonics, in Burchfiel, B. C., Oliver, J. E., and Silver, L. T., chm., Continental Tectonics: National Academy of Sciences, p. 161-174.

Lipman, P. W., Doe, B. R., Hedge, C. E., and Steven, T. A., 1978, Petrologic evolution of the San Juan volcanic field, southwestern Colorado: Pb and Sr isotope evidence: Geological Society of America Bulletin, v. 89, p. 59-82.

Lipman, P. W., and Mehnert, H. W., 1975, Late Cenozoic basaltic volcanism and development of the Rio Grande depression in the southern Rocky Mountains, in Curtis, B., ed., Cenozoic history of the southern Rocky Mountains: Geological Society of America Memoir 144, 279 p.

Lipman, P. W., Protska, H. J., and Christiansen, R. L., 1972, Cenozoic volcanism and plate-tectonic evolution of the western United States: 1. Early and middle Cenozoic: Philosophical Transactions of the Royal Society of London, ser. A, v. 271, p. 217-248.

Luttrell, G. W., Hubert, M. L., Wright, W. B., Jussen, V. M., and Swanson, R. W., 1981, Lexicon of geologic names of the United States for 1968-1975: U. S. Geological Survey Bulletin 1520, 342 p.

MacNish, R. D., 1966, The Cenozoic history of the Wet Mountain Valley: Michigan University Ph.D. dissertation, 120 p.

Mason, B., 1966, Principles of geochemistry: New York, John Wiley, 329 p.

McCarthy, T. S., and Kable, E. J. D., 1978, On the behavior of rare-earth elements during partial melting of granitic rock: Chemical Geology, v. 22, p. 21-29.

McCulloch, D. S., 1963, Late Cenozoic erosional history of Huerfano Park, Colorado: Michigan University Ph.D. dissertation, 158 p.

McDougall, I., 1976, Geochemistry and origin of basalt of the Columbia River Group, Oregon and Washington: Geological Society of America Bulletin, v. 87, p. 777-792.

McGetchen, T. R., and Silver, L. T., 1972, A crustal-upper mantle model for the Colorado Plateau based on observations of crystalline rock fragments in the Moses Rock dike: Journal of Geophysical Research, v. 77, p. 7022-7037.

Medlin, J. H., Suhr, N. H., and Bodkin, J. R., 1969, Atomic absorption analysis of silicates employing $LiBO_2$ fusion: Atomic Absorption News, v. 8, p. 25-29.

Michel-Lèvy, A., 1877, De l'emploi du microscope polarisant à lumière paralèle (Use of the polarizing microscope with parallel illumination): Annales des Mines, v. 12, p. 392-471.

Miller, C. F., 1978, Monzonitic plutons, California, and a model for generation of alkali-rich, near silica-saturated magmas: Contributions to Mineralogy and Petrology, v. 67, p. 349-355.

Miyashiro, A., 1974, Volcanic rock series in island arcs and active continental margins: American Journal of Science, v. 274, p. 321-325.

Mysen, B. O., 1979, Trace element partitioning between garnet peridotite minerals and water-rich vapor: Experimental data from 5 to 30 kb.: American Mineralogist, v. 64, p. 274-278.

Nagasawa, M., and Schnetzler, C. C., 1971, Partitioning of rare earth, alkaline, and alkaline earth elements between phenocrysts and acidic igneous magma: Geochemica et Cosmochemica Acta, v. 35, p. 953-960.

Nicholls, I. A., and Ringwood, A. E., 1973, Effect of water on olivine stability and production of SiO_2 saturated magmas in the island arc environment: Journal of Geology, v. 81, p. 285-300.

Onuma, N., Higuchi, H., Wakita, H., and Nagasawa, H., 1968, Trace element partition between two pyroxenes and the host volcanic rock: Earth and Planetary Science Letters, v. 81, p. 1665-1688.

Osborne, E. F., 1969, Experimental aspects of calcalkaline differentiation, in McBirney, A. R., ed., Proceedings of the andesite conference: Oregon Department of Geology and Mineral Industries Bulletin, v. 65, p. 33-42.

Peccerillo, A., and Taylor, S. R., 1976, Geochemistry of Eocene calc-alkaline volcanic rocks from the Kasamonu area, northern Turkey: Contributions to Mineralogy and Petrology, v. 58, p. 63-81.

Reitz, B. K., 1980, Evolution of Tertiary intrusive and volcanic rocks near Ravenna, Granite County, Montana: Kansas State University M. S. thesis, 90 p.

Ringwood, A. E., 1974, The petrological evolution of island-arc systems: Journal of the Geological Society of London, v. 130, p. 183-294.

———— 1975, Composition and petrology of the Earth's mantle: New York, McGraw-Hill, 618 p.

Robinson, P. T., Elders, W. A., and Muffler, L. J. P., 1976, Quaternary volcanism in the Salton Sea geothermal field, California: Geological Society of America Bulletin, v. 87, p. 347-360.

Schnetzler, C. C., and Philpotts, J. A., 1968, Partition coefficients of rare earth elements and barium between igneous matrix material and rock-forming phenocrysts, I., in Ahrens, L. H., ed., Origin and distribution of the elements: New York, Pergammon Press, p. 929-938.

———— 1970, Partition coefficients of rare earth elements between igneous matrix material and rock-forming phenocrysts, II.: Geochemica et Cosmochemica Acta, v. 34, p. 307-323.

Scott, G. R., and Taylor, R. B., 1975, Post-Paleocene Tertiary rocks and Quaternary volcanic ash of the Wet Mountain Valley, Colorado: U. S. Geological Survey Professional Paper 868, 15 p.

Seager, W. R., and Morgan, P., 1979, Rio Grande Rift in southern New Mexico, west Texas, and northern Chihuahua, in Reiker, R. E., ed., Rio Grande Rift: Tectonics and magmatism: American Geophysical Union, p. 87-106.

Shapiro, L., 1978, Rapid analysis of silicate, carbonate, and phosphate rocks-revised edition: U. S. Geological Survey Bulletin 1401, 76 p.

Shaw, D. M., 1970, Trace element fractionation during anatexis: Geochemica et Cosmochemica Acta, v. 34, p. 1995-2008.

Siems, P. L., 1968, Volcanic geology of the Rosita Hills and Silver Cliff district, Custer County, Colorado: Colorado School of Mines Quarterly, v. 63, p. 89-124.

Smalley, J., 1981, Geochemical investigation of the Rosita Hills volcanic complex, Custer County, Colorado: Kansas State University M. S. thesis, 115 p.

Smith, R. P., 1979, Early rift magmatism at Spanish Peaks, Colorado, in Reicker, R. E., ed., Rio Grande Rift: Tectonics and magmatism: American Geophysical Union, p. 313-322.

Spaid-Reitz, M., 1980, Petrogenesis of a bi-modal assemblage of alkali basalt and rhyolitic ignimbrite, Gravelley Range, southwest Montana: Kansas State University M. S. thesis, 94 p.

Steven, T. A., 1975, Middle Tertiary volcanic field in the southern Rocky Mountains, in Curtis, B., ed., Cenozoic history of the southern Rocky Mountains: Geological Society of America Memoir 144, 279 p.

Steven, T. A., and Epis, R. C., 1968, Oligocene volcanism in south-central Colorado: Colorado School of Mines Quarterly, v. 63, p. 241-258.

Taylor, R. B., 1974, Reconnaissance geologic map of the Deer Peak quadrangle and southern part of the Hardscrabble Mountain quadrangle, Custer and Huerfano Counties, Colorado: U. S. Geological Survey Miscellaneous Investigation Series Map I-870, scale 1:24000.

Taylor, S. R., and White, A. J. R., 1965, Geochemistry of andesites and the growth of continents: Nature, v. 208, p. 261-273.

Thompson, T. B., 1972, Sierra Blanca igneous complex, New Mexico: Geological Society of America Bulletin, v. 83, p. 2341-2356.

Thornton, C. P., and Tuttle, O. F., 1960, Chemistry of igneous rocks, part I: Differentiation index: American Journal of Science, v. 258, p. 664-684.

Turner, F. J., and Verhoogen, J., 1960, Igneous and metamorphic petrology: New York, McGraw-Hill, 649 p.

Tweto, O., 1979, Geologic map of Colorado: U. S. Geological Survey, scale 1:5000,000.

Wedepohl, K. H., exec. ed., 1978, Handbook of geochemistry: New York, Springer-Verlag, v. 5, 4400 p.

Wendtlandt, R. F., and Herrington, W. J., 1979, Rare earth partitioning between immiscible carbonate and silicate liquids and CO_2 vapor: Results and implications for the formation of light rare earth-enriched rocks: Contributions to Mineralogy and Petrology, v. 69, p. 409-419.

Williams, H., Turner, F. J., and Gilbert, C. M., 1954, Petrography: An introduction to the study of rocks in thin section (1st ed.): San Francisco, W. H. Freeman and Co., 406 p.

Wyllie, P. I., 1971, Experimental limits for melting in the Earth's crust and upper mantle, in Heacock, J., ed., The structure and properties of the Earth's crust: American Geophysical Union Monograph 14, p. 279-301.

———— 1973, Experimental petrology and global tectonics-preview: Tectonophysics, v. 17, p. 189-209.

Yoder, H. S. Jr., 1976, Generation of basaltic magma: Washington, National Academy of Sciences, 264 p.

Zielinski, R. A., and Lipman, P. W., 1976, Trace-element variation at Summer Coon volcano, San Juan Mountains, Colorado, and the origin of continental-interior andesite: Geological Society of America Bulletin, v. 87, p. 1477-1485.

APPENDIX A: Atomic absorption and emission spectrophotometry

The elements Si, Al, Fe, Ca, Mg, K, Na, and Ti were analyzed using atomic absorption and emission spectrophotometry. The method was adapted mostly from the procedures of Medlin and others (1969) and Shapiro (1978).

Sample dissolution procedure

Aliquots of 0.2000 ± 0.0002 g of powdered rock sample were thoroughly mixed with 1.20 ± 0.02 g anhydrous $LiBO_2$ flux on a weighing paper. This mixture was completely transferred to a 9-ml graphite crucible. The crucible was placed in a muffle furnace at 1000° C. for about 30 minutes, during which time fusion occurred. The crucible was removed and allowed to cool. Each bead of cooled sample-flux mixture was then transferred to a 250-ml bottle containing a teflon, magnetic stirring rod and 50 ml of about 3N HNO_3. A magnetic stirrer was used to facilitate dissolution, which usually occurred in about 1 hour. Some rhyolite samples required up to 2 hours to dissolve. Upon dissolution, the liquid was poured into a 250-ml volumetric flask, using a funnel to catch the stirring rod. The bottle and the stirrer were rinsed and the washings added to the flask, which was then brought to 250 ml with distilled deionized H_2O (< 2 mhos). The resulting solution, containing 800 ppm sample, was transferred to the original 250-ml bottle for storage.

A blank solution containing only 1.20 ± 0.02 g $LiBO_2$ was prepared in exactly the same manner as the sample solutions. This solution was used to monitor the effects of reagent impurities.

Standardization

Concentrations of major elements in the samples were determined by comparison to known concentrations in well-analyzed rocks. The United States Geological Survey (U.S.G.S.) standards RGM-1, rhyolite; BCR-1, basalt; W-1, diabase; and STM-1, nepheline syenite were used for this purpose. Concentrations of major elements in these standards are in Flanagan (1976). Powdered aliquots of these standard rocks were dissolved precisely in the same manner as the samples. The wide compositional range provided by these standard rocks bracketed the range of concentration of major elements in the samples in most cases.

Sample and standard dilution

Samples and standards were diluted from the initial 800 ppm solutions to the linear concentration range of each desired element. Three dilutions were necessary to attain optimum analytical concentrations and these are summarized in Table A-1.

Dilutions were made with a 1-percent La solution, which acts as a releasing agent for the alkaline-earth elements. The La solution was prepared by dissolving 25.4 g $LaCl_3 \cdot 6H_2O$ in 1 liter distilled de-ionized H_2O.

Determination of sample concentration

Samples were analyzed on a Perkin-Elmer model 305B spectrophotometer.

Instrumental settings of Reitz (1980) were used with minor modifications (Table A-2). Air-Acetelyne flame was used for all elements except for Si and Al for which the hotter, Nitrous oxide-Acetelyne flame was used.

Chart-output data were reduced graphically. The peak height of the blank was subtracted from all peaks of sample and standard. Concentrations of samples were determined by comparison to a calibration line constructed from concentrations of standards in a plot of peak height versus concentration. Replicate determinations were averaged and the data converted to weight percentage of oxide.

Accuracy of the analysis was monitored by simultaneously analyzing U.S.G.S. standard andesite, AGV-1. Results of AGV-1 analysis show good agreement with the recommended values of Flanagan (1976) in Table A-3.

Table A-1: Sample solutions used in atomic absorption and flame emission analyses

Initial solution	
Preparation:	Dissolve fused mixture of 0.2000 ± 0.0002 g sample and 1.20 ± 0.02 g $LiBO_2$ in 50 ml 3 N HNO_3
Solution A	
Preparation:	Dilute initial solution to 250 ml
Concentration:	800 ppm sample
Use:	Ti determination
Solution B	
Preparation:	5 ml solution A plus 10 ml La solution
Concentration:	226.6 ppm sample
Use:	Si, Al determination
Solution C	
Preparation:	3 ml solution A plus 50 ml La solution
Concentration:	45.3 ppm sample
Use:	Fe, Ca, K determination
Solution D	
Preparation:	5 ml solution C plus 25 ml La solution
Concentration:	9.1 ppm sample
Use:	Mg, Na determination

Table A-2: Perkin Elmer 305B instrument settings

Element	Wave Length	Slit	Range	Function	Burner width (in inches)	Burner heighth (in inches)	C_2H_2 (1)	N_2O (1)	air (1)
Si	251.7	3	UV	Abs.	2.5	6.0		5.3	5
Al	308.9	4	UV	Abs.	2.5	7.0		5.0	5
Fe	248.2	3	UV	Abs.	2.5	7.0	5.0		5
Ca	208.5	4	Vis.	Abs.	2.5	5.0	4.8		5
Mg	285.0	4	UV	Abs.	2.5	6.5	5.0		5
Na	292.5	4	Vis.	Abs.	2.5	8.0	4.0		5
K*	382.5	4	Vis.	Em.	2.5	8.0	6.0		
Ti	365.2	3	UV	Abs.	2.5	7.0	4.8		

* Red filter used

(1) In arbitrary flowmeter units

Table A-3: Comparison of U.S.G.S. standard andesite, AGV-1, in this study with recommended values of Flanagan (1976) (data in weight percent oxide)

	Flanagan (1976)	This study
SiO_2	59.00	59.3
Al_2O_3	17.25	17.1
Fe as Fe_2O_3	6.79	6.8
K_2O	2.89	2.9
Na_2O	4.26	4.3
CaO	4.90	5.1
MgO	1.53	1.6
TiO_2	1.04	1.0

APPENDIX B: Instrumental neutron activation analysis

Concentrations of trace elements, with the exception of Sr, were determined using instrumental neutron activation analysis (INAA). The procedure was based on that of Gordon and others (1968) and Jacobs and others (1977). Kilbane (1978) gave a detailed discussion of this technique.

Analytical procedure

Approximately 0.3 to 0.4 (± 0.0002) g of powdered rock samples were weighed precisely and placed in plastic vials. The vials were sealed with a warm soldering gun to prevent water leaks into the vial during irradiation in the reactor pool. About 100 (± 0.1) mg of Fe wire was wound spirally around the vials to serve as a neutron flux monitor.

Groups of four samples plus a primary standard (Canada Certified Reference Material Project reference soil, SO-4) were irradiated for 4 hours in a Triga Mark II experimental reactor with a flux of about 10^{13} neutrons/cm^2/sec. About four days after irradiation, samples were transferred from vials to small plastic bags (2 cm by 1 cm) and mounted in the center of 3 in. by 5 in. index cards. Iron wires were symmetrically coiled and similarly mounted.

The samples were radioassayed for gamma radiation 5, 10, and 40 days after irradiation using a 25 cm^3 Ge (Li) detector and a Canberra

model 8180 multichannel analyzer equipped with a 4096 channel memory unit. The gamma-energy spectra were recorded and partitioned into the memory such that there was a linear correlation between increasing gamma energy and increasing channel number. The correlation between gamma energy and channel number was calibrated using the radioactive sources ^{152}Eu (0.122 meV and 0.344 meV) and ^{60}Co (1.333 meV). The spectra were then transferred to magnetic storage tapes for computer processing.

Calculations

Concentrations of trace elements were determined by comparing emission rates of particular gamma-ray energies in each sample to those of Canada soil standard, SO-4. Computer output consisted of the peak area of each element, errors in computing peak areas, and sample to standard activity ratios. These ratios were corrected for variations in reactor flux and for weight differences between sample and standard. This was performed with the following equation:

$$C_s = C_{st} \text{ (St. Wt./S. Wt.) (St. Fe/S. Fe) (S./St.)}$$

Where:

C_s = concentration of element in sample

C_{st} = concentration of element in standard

St. Wt./S. Wt. = weight ratio of standard to sample

St. Fe/S. Fe = standard to sample activity ratio of Fe-wire flux monitor

S./St. = activity ratio of sample to standard

The following isotopes required further corrections because of interference by elements that emit similar gamma energies:

isotope:		interferring peak:	
^{175}Yb	396.1 kev	^{233}Th	398.5 kev
^{141}Ce	145 kev	^{59}Fe	142 kev

Tb could not be measured because of high Th interference.

Accuracy of the analyses was determined by analyzing U.S.G.S. standard basalt, BCR-1, as an unknown. The analysis of this investigation shows good agreement with the recommended values of Flanagan (1976) and with assays of other analysts (Table B-1).

Table B-1: Concentrations of trace elements in U.S.G.S. standard basalt, BCR-1, determined by INAA in this study compared to analyses by others.

	This Study	Flanagan (1976)	Smalley (1981)	Gordon and others (1968)	Koch (1978)
La	25	26	27	23	28
Ce	49	53.9	54	46	50
Sm	6.6	6.6	6.8	5.9	6.5
Eu	1.8	1.94	2.1	2.0	2.0
Yb	3.5	3.36	3.4	3.2	3.3
Lu	0.59	0.55	0.53	0.60	0.62
Ba	605	675	577	-	-
Rb	40.4	46.6	-	-	-
Sc	33	33	30	-	-
Cr	14.2	17.6	-	-	-
Hf	4.9	4.7	5.1	-	-
Th	6.9	6.0	7.2	-	-

APPENDIX C: X-ray fluorescence spectrography

X-ray fluorescence was used to determine Rb, Sr, Ba, and P in the samples. The analyses were performed by James (1980) and were reported in Kansas Geological Survey Analytical Report 80:11-1. *Concentrations of* Rb and Ba were also determined by INAA.

The analyses were completed with a Phillips 1410 wave-length dispersive spectrometer, using a LiF analyzing crystal. Instrument settings were: kilovolts = 50, milliamps = 50, baseline = 2.0, window = 2.2. U. S. Geological Survey standard rocks served as primary standards. Estimated accuracy was ± 5 percent of the amount present.

APPENDIX D: Gravimetric determinations

About 1 g of powdered rock sample was placed in a pre-ignited Pt crucible and baked at 1000° C. in a muffle furnace. After 1 hour the crucible was placed in a desiccator, allowed to cool to room temperature, and weighed. This procedure was repeated until weighings agreed to 0.0004 g. The loss of weight was reported as loss on ignition and represents the total volatile content of the sample.

APPENDIX E: Trace-element modeling equations

Equations used in this thesis to model partial melting and fractional crystallization processes are given below. Distribution coefficients that were used in these equations are given in Tables F-1 and F-2.

Concentrations of trace elements in hypothetical melts in this thesis were calculated using the aggregate, non-modal melting equation of Shaw (1970):

$$C_L/C_0 = 1/F(1 - (1 - PF/D_0)^{1/P})$$

Where:

C_L = concentration of trace element in derivative partial melt

C_0 = concentration of trace element in unmelted source rock

F = fraction of source that melted

P = proportionality constant

D_0 = bulk distribution coefficient

Because the model assumes non-modal melting, the proportionality constant represents the proportions of each phase contributing to the melt as well as the distribution coefficient of each phase. It is expressed as:

$$P = P_1K_1 + P_2K_2 + P_3K_3 + \ldots$$

Where:

P_n = proportion of phase n in the melt

K_n = distribution coefficient of a particular trace element for phase n

The bulk distribution coefficient (D_0) represents the fractionation effect of a particular trace element in a multi-phase source rock. It is expressed as:

$$D_0 = X_1K_1 + X_2K_2 + X_3K_3 + \ldots$$

Where:

X_n = the modal abundance of phase n in the source rock

K_n as previously defined

The effect of fractional crystallization on the trace-element content of the resulting liquid was predicted using the equation of Haskin and others (1970):

$$C_L/C_a = (1 - X)^{K - 1}$$

Where:

C_L = concentration of trace element in the residual liquid after crystallization and extraction of phase or phases

C_a = initial concentration of trace element in magma

X = fraction of parent magma that has crystallized and has been removed from the system

K = distribution coefficient for crystallizing phase or bulk distribution coefficient for multi-phase crystallization

APPENDIX F: Distribution coefficient data

Table F-1: Distribution coefficients used in trace-element modeling of a silica-rich magma[1]

	Quartz	Clino-pyroxene	Horn-blende	Biotite	Alkali feldspar	Plagioclase	Zircon	Garnet
Ce	0.001	0.29	0.86	0.037	0.044	0.24	2.6	0.35
Sm	0.001	0.93	4.15	0.058	0.018	0.13	3.1	2.7
Eu	0.001	0.87	3.2	0.15	1.13	2.1	3.1	1.5
Lu	0.001	1.05	2.97	0.19	0.006	0.062	323	29.6
Rb	0.001	0.038	0.011	5.5 (2.2)[2]	0.036	0.034	-	0.0085
Sr	0.001	0.10	0.058	0.12	3.9	9 (4.4)	-	0.015
Ba	0.001	0.061	0.049	8.0	6.1 (5)	0.033	-	0.017
Th	0.001	0.013	0.01	0.3	0.02	0.02	30	0.013
Cr	0.001	2	2	12	0.01	0.06	-	3.7
Sc	0.001	15	15	11	0.06	0.06	-	15
Hf	0.001	-	-	-	-	0.06	0.03	3.3

(1) Compiled from Arth and Hanson, 1975; Anderson and Cullers, 1978; and Cullers, personal communication, 1981.

(2) Parenthetical D.C. used in fractional-crystallization models if different than in partial-melting models

Table F-2: Distribution coefficients used in trace-element modeling of baslatic and intermediate-composition systems[1]

	Olivine	Clinopyroxene	Orthopyroxene	Hornblende	Plagioclase	Garnet
Ce	0.007	0.15	0.024	0.20	0.12	0.028
Nd	0.0066	0.31	-	0.33	0.081	0.068
Sm	0.0066	0.50	0.054	0.52	0.067	0.29
Eu	0.0068	0.51	0.054	0.059	0.34	0.49
Gd	0.0077	0.61	-	0.63	0.063	0.97
Dy	0.096	0.68	-	0.68	0.055	3.17
Yb	0.014	0.62	0.34	0.49	0.067	11.5
Lu	0.016	0.56	0.42	0.43	0.060	11.90
Rb	0.0098	0.031	0.001	0.29	0.071	0.042
Sr	0.014	0.012	0.017	0.46	1.83	0.012
Ba	0.001	0.001	0.001	0.42	0.023	0.002
Cr	2	5	1.8	2	0.10	2
Sc	0.003	3	1.2	10	0.035	10
Hf	0.1	0.07	0.03	-	0.1	0.3

(1) Compiled from Higuchi and Nagasawa, 1969; Nagasawa and Schnetzler, 1971; Onuma and others, 1968; Schnetzler and Philpotts, 1968, 1970; Cox and others, 1979; and Cullers (personal communication, 1981).

APPENDIX G: Petrographic descriptions

Thin sections of analyzed samples are described below. Crystallization history is based on inclusion and contact relationships among minerals.

3-3 High-potassium dacite:

This prophyritic rock contains 17 percent euhedral to subhedral plagioclase laths, 0.5 to 5.0 mm long; 6 percent euhedral to subhedral sanidine laths, 0.5 to 2.0 mm long; and 4 percent euhedral pseudohexagonal biotite, 0.2 to 1.0 mm across, in a felty groundmass of anisotropic microlites, $\leqslant$ 0.02 mm long; opaque minerals, $\leqslant$ 0.1 mm across; and apatite, $\leqslant$ 0.4 mm long. Plagioclase (Ab_{76} to Ab_{64}) is strongly zoned (both normal and oscillatory types occur), and has Carlsbad, pericline, and albite twins. Sanidine (Or_{80} to Or_{70}) is untwinned or has Carlsbad twins. Resorption of some sanidine and plagioclase occurs. Glomeroporphyritic clusters of all phenocryst phases occur up to 8.0 mm across. Microfaults offset phenocrysts of plagioclase and sanidine. Apatite and opaque minerals formed first, followed by plagioclase, and then biotite and sanidine. The fresh rock is light gray (N 7).

5-1 Latite:

This porphyritic, moderately altered rock contains 30 percent euhedral to anhedral plagioclase laths, 0.1 to 4.3 mm long; 6 percent subhedral clinopyroxene prisms, 0.1 to 1.7 mm long; and 5 percent euhedral

to subhedral biotite plates, ⩽ 0.2 to 1.0 mm across, in a felty groundmass of feldspar, ⩽ 0.05 mm long; anisotropic microlites, ⩽ 0.01 mm long; opaque minerals, ⩽ 0.1 mm across; apatite, ⩽ 0.2 mm long, crystallites, and glass. Plagioclase (Ab_{73} to Ab_{62}) often has corroded cores, is zoned (normal and oscillatory), and has Carlsbad, pericline, and albite twins. Clinopyroxene is augite. Minute opaque grains occur as: (1) complete or partial pseudomorphs after biotite, (2) rims mantling clinopyroxene, and (3) disseminations in the groundmass. Apatite and large (> 0.05 mm) opaque grains formed first, then crystallization of plagioclase, clinopyroxene, and biotite began. Late-stage hydrothermal alteration produced minute opaque minerals. The unweathered rock is olive gray (5 Y 4/1).

6-1 Shoshonite:

This porphyritic rock contains 7 percent euhedral clinopyroxene prisms, 0.5 to 1.5 mm long; 5 percent euhedral to anhedral plagioclase laths, 0.5 to 1.0 mm long; and 4 percent resorbed elongate olivine, 0.5 to 1.0 mm long, in a pilotaxitic groundmass of feldspar laths, ⩽ 0.05 mm long; anisotropic microlites, ⩽ 0.02 mm long; and opaque grains, ⩽ 0.05 mm across. Plagioclase (Ab_{52} to Ab_{47}) is unzoned and has Carlsbad, pericline, and albite twins. Clinopyroxene is augite. A few small glomeroporphyritic clusters occur up to 2.0 mm across. Opaque minerals formed first, followed by crystallization of olivine, plagioclase, and clinopyroxene. About 3 percent of the rock consists of scaly masses of secondary calcite and hematite. The fresh rock is grayish black (N 2).

6-3 Latite:

This porphyritic, moderately altered rock contains 25 percent euhedral

to subhedral plagioclase laths, 0.2 to 1.8 mm long; 4 percent euhedral to subhedral clinopyroxene prisms, 0.1 to 1.7 mm long; and 3 percent euhedral pseudohexagonal biotite, 0.3 to 1.7 mm long, in a felty groundmass of feldspar, ⩽ 0.05 mm long; anisotropic microlites, ⩽ 0.04 mm long; opaque minerals, ⩽ 0.03 mm across; apatite, ⩽ 0.2 mm long, crystallites, and glass. Plagioclase (Ab_{75} to Ab_{70}) is zoned (normal and oscillatory), may be corroded or sericitized in cores, in some cases is resorbed; and has Carlsbad, pericline and albite twins. Clinopyroxene is augite. Minute opaque minerals mantle most biotite crystals and are disseminated throughout the groundmass. Apatite and large (> 0.05 mm across) opaque minerals formed first, followed by crystallization of plagioclase, pyroxene, and biotite. Minute opaque grains resulted from secondary alteration. The fresh rock is light bluish gray (5 B 7/1).

7-1 Latite:

This porphyritic rock contains 22 percent euhedral to subhedral plagioclase laths, 0.1 to 3.7 mm long; 4 percent subhedral clinopyroxene prisms, 0.2 to 1.4 mm long; and 4 percent euhedral to subhedral biotite, 0.2 to 1.4 mm long, in a felty groundmass of feldspar, ⩽ 0.02 mm long; anisotropic microlites, ⩽ 0.02 mm long; opaque minerals, ⩽ 0.02 mm across; apatite, ⩽ 0.2 mm long; zircon, ⩽ 0.1 mm long, crystallites, and glass. Plagioclase (Ab_{75} to Ab_{68}) is zoned (normal and oscillatory), has corroded cores, and has Carlsbad, pericline, and albite twins. Clinopyroxene is diopsidic augite. Apatite and opaque minerals formed first, followed by zircon, then by plagioclase, and finally by clinopyroxene and biotite. The fresh rock is medium gray (N 5).

9-1 High-silica rhyolite

This porphyritic rock contains 13 percent euhedral or resorbed sanidine (Or_{85} to Or_{75}) glomerocrysts, 0.4 to 4.0 mm long; and 4 percent of aggregates of subhedral to anhedral quartz, < 0.02 mm across, in a flow-banded, hematitic, partly devitrified glass which includes sparse feldspar laths, ≤ 0.2 mm long. Individuals in sanidine glomerocrysts have crenulated borders and undulose extinction. The groundmass has a fibrous, spherulitic texture. Secondary quartz occurs in patches along conchoidal fractures. Sanidine formed first, the lava was extruded and quickly quenched; devitrification textures and quartz growth then occurred. The fresh roch is grayish red (5 R 4/2).

9-2 Low-silica rhyolite:

This porphyritic rock contains 25 percent euhedral to subhedral sanidine laths, 0.1 to 2.5 mm long; 2 percent elongate plagioclase laths, 0.7 to 2.5 mm long; and 1 percent subhedral oxyhornblende prisms 0.5 to 1.0 mm long, in a felty groundmass consisting of feldspar, ≤ 0.01 mm long; apatite, ≤ 0.1 mm long, crystallites, and glass. Sanidine (Or_{85} to Or_{75}) has poikilitic inclusions of glass, may be resorbed, and mantles plagioclase. Composition of plagioclase could not be determined using the Michel-Levy method. Apatite formed first, followed by amphibole and plagioclase, and then by sanidine. The fresh rock is light gray (N 7).

9-5 Latite:

This porphyritic rock contains 27 percent euhedral to subhedral plagioclase laths, 0.5 to 5.0 mm long; and 3 percent euhedral to subhedral clinopyroxene prisms, 0.2 to 0.7 mm long, in a hyalophitic groundmass of

brown glass. The brown glass surrounds phenocrysts and smaller anhedral feldspar, ⩽ 0.05 mm long; biotite, ⩽ 0.05 mm long, opaque grains, ⩽ 0.1 mm across; and apatite, ⩽ 0.2 mm long. Plagioclase (Ab_{79} to Ab_{68}) is normally zoned including concentric zones of brown glass, and has Carlsbad, pericline, and albite twins. Plagioclase phenocrysts are flow aligned in a trachytic texture. Clinopyroxene is augite. Apatite and opaque minerals formed first, followed by pyroxene, and finally by plagioclase. The fresh rock is olive black (5 Y 2/1).

10-1 Latite:

This porphyritic rock consists of 13 percent euhedral to subhedral plagioclase laths, 0.4 to 2.7 mm long; 5 percent subhedral hornblende prisms, 0.4 to 2.2 mm long; 4 percent subhedral clinopyroxene prisms, 0.4 to 1.5 mm long; and 2 percent subhedral pseudohexagonal biotite, 0.3 to 1.0 mm across, in a pilotaxitic groundmass of flow-aligned feldspar, ⩽ 0.04 mm long; opaque minerals, ⩽ 0.2 mm across; and apatite ⩽ 0.2 mm long. Plagioclase (Ab_{68} to Ab_{62}) is zoned (normal and oscillatory), may have sericitized cores, and has Carlsbad, pericline, and albite twins. Clinopyroxene is augite. Large glomeroporphyritic clusters up to 3.5 mm across contain all phenocryst phases. Apatite and opaque minerals formed first, followed by amphibole, then by pyroxene, and finally by plagioclase and biotite. The fresh rock is greenish gray (5 G 6/1).

15-3 Latite:

This porphyritic rock contains 24 percent euhedral to subhedral plagioclase laths, 0.2 to 3.6 mm long; 6 percent subhedral clinopyroxene prisms, 0.2 to 1.0 mm long; and 5 percent subhedral pseudohexagonal biotite, 0.1 to 0.7 mm across, in a pilotaxitic groundmass of feldspar laths,

$\leqslant$ 0.2 mm long; opaque grains, $\leqslant$ 0.05 mm across; apatite, $\leqslant$ 0.4 mm long, crystallites, and glass. Plagioclase (Ab_{74} to Ab_{65}) has oscillatory zones, corroded cores, and has Carlsbad, pericline, and albite twins. Clinopyroxene is diopsidic augite, and is zoned. Apatite and opaque grains formed first, followed by plagioclase and clinopyroxene, and then by biotite. The fresh rock is medium light gray (N 6).

18-2 High-silica rhyolite:

This porphyritic rock contains 11 percent euhedral or resorbed sanidine (Or_{85} to Or_{75}) glomerocrysts, 0.3 to 3.0 mm long; and traces of sanidine-mantled plagioclase, 0.5 mm long, in a flow-banded, hematitic groundmass consisting of microlites, $\leqslant$ 0.02 mm long, and devitrified glass. Individuals in sanidine glomerocrysts have crenulated borders and undulose extinction. Plagioclase and sanidine formed first, with sanidine crystallizing alone at the time of eruption. The fresh rock is medium dark gray (N 4).

20-1 High-silica rhyolite:

This porphyritic rock contains 24 percent euhedral to subhedral sanidine crystals, 0.2 to 2.5 mm long; 3 percent subhedral to anhedral plagioclase laths, 0.5 to 2.5 mm long; and traces of oxyhornblende, $\leqslant$ 1.5 mm long; and clinopyroxene, $\leqslant$ 0.8 mm long, in a felty groundmass of anisotropic grains, $\leqslant$ 0.02 mm long; opaque minerals, $\leqslant$ 0.2 mm across, and crystallites. Two types of sanidine occur: elongate laths, 1.0 to 2.5 mm long, and smaller equant crystals, 0.2 to 0.5 mm long; both types range from Or_{85} to Or_{75}. Plagioclase has albite twins and has poikilitic inclusions of brown glass; the composition could not be determined by the

Michel-Lèvy method. Plagioclase is usually mantled by sanidine. The opaque grains formed first, followed by plagioclase, then pyroxene, amphibole, and sanidine. The fresh rock is brownish gray (5 YR 4/1).

23-2 Latite:

This porphyritic rock contains 11 percent euhedral to subhedral plagioclase laths, 0.1 to 1.2 mm long; and 10 percent euhedral to subhedral oxyhornblende prisms, 0.2 to 2.0 mm long, in a felty groundmass of feldspar, ⩽ 0.04 mm long; anisotropic microlites, ⩽ 0.04 mm long; opaque grains, ⩽ 0.03 mm across; and apatite, ⩽ 0.2 mm long. Plagioclase (Ab_{74} to Ab_{48}) is zoned (oscillatory) and has Carlsbad, pericline, and albite twins. Oxyhornblende is usually mantled by minute opaque grains. Glomeroporphyritic clusters of plagioclase and of oxyhornblende occur up to 4.0 mm across. Both plagioclase and oxyhornblende show resorption effects. Apatite and opaque minerals formed first, then plagioclase, and finally oxyhornblende. The fresh rock is very light gray (N 8).

24-3 Latite:

This porphyritic rock contains 17 percent euhedral to subhedral plagioclase laths, 0.2 to 2.1 mm long; 6 percent subhedral clinopyroxene prisms, 0.2 to 1.8 mm long; and 5 percent euhedral to subhedral biotite, ⩽ 1.1 mm across, in a felty groundmass of feldspar, ⩽ 0.02 mm long; anisotropic microlites, ⩽ 0.02 mm long; apatite, ⩽ 0.1 mm long; zircon, ⩽ 0.1 mm long; opaque grains, ⩽ 0.1 mm across, and crystallites. Plagioclase (Ab_{65} to Ab_{55}) is zoned (normal and oscillatory), may be sericitized, and has Carlsbad, pericline, and albite twins. Clinopyroxene is diopsidic augite. Apatite and opaque minerals formed first, followed

by zircon, plagioclase, and finally by pyroxene and biotite. The fresh rock is medium light gray (N 6).

PETROLOGY OF THE DEER PEAK VOLCANICS, COLORADO

by

Michael J. DiMarco

B.A. State University of New York at Buffalo, 1979

AN ABSTRACT OF A MASTER'S THESIS

submitted in partial fulfillment of the

requirements for the degree

MASTER OF SCIENCE

Department of Geology

KANSAS STATE UNIVERSITY
Manhattan, Kansas

1983

ABSTRACT

The Deer Peak Volcanics represent a deeply dissected volcanic field that originated from a central-vent volcano during the Oligocene in the Wet Mountains, Colorado. From field, petrographic, major-element, and trace-element (Rb, Ba, Sr, Th, Cr, Sc, Hf, and rare-earth elements (REE)) data, five volcanic-rock types are recognized: (1) latite, (2) high-potassium dacite, (3) low-silica rhyolite, (4) high-silica rhyolite, and (5) shoshonite. Latite is the most abundant rock in the suite. High-potassium dacite and rhyolite are volumetrically minor. In most places, latite is the oldest volcanic rock, but in some localities rhyolite constitutes the basal volcanic unit. Latite erupted throughout the early and middle parts of the volcanic history at Deer Peak. High-potassium dacite and rhyolite erupted during the time interval in which latite was emplaced. Shoshonite is restricted to a small, late-stage exposure at the vent. Volcanic rocks at Deer Peak are alkali-calcic, characterized by $Na_2O + K_2O$ ranging from 6.7 to 9.9 percent by weight. The rocks are enriched in large-ion-lithophile elements (LILE) compared to most volcanic rocks in orogenic regions.

Latite (59.3 to 64.7 percent SiO_2) has highly fractionated REE patterns without Eu anomalies. Twenty percent of melting of eclogite compositionally similar to continental tholeiite can produce latite.

High-potassium dacite (66.7 percent SiO_2) and low-silica rhyolite (71.4 percent SiO_2) have fractionated REE patterns and possible small negative Eu anomalies that can be produced by 25 and 20 percent of melting, respectively, of garnet granulite. High-silica rhyolite (74.1 to 76.7 percent SiO_2), with about 74 percent SiO_2, probably formed by 20 percent of melting of feldspar-bearing rock in the upper crust. High-silica rhyolite, with greater than 75 percent SiO_2, probably originated by thermogravitational diffusion of elements in a rhyolitic magma chamber. Shoshonite (52.4 percent SiO_2) probably originated by about 2 percent of melting of upper-mantle peridotite. Fractional crystallization probably did not play an important role in the petrogenesis of the suite.

Movement along deeply penetrating fault zones associated with the development of the Wet Mountain Valley triggered magmatism at Deer Peak. Convergence at the Pacific margin may have produced a stress field that favored the development of deep-crustal faults and resulted in intermediate and felsic magmatism in the Wet Mountains area. Back-arc extension at the close of subduction-dominated tectonics may have extended deep-crustal faults into the upper mantle and initiated melting there that produced shoshonite at Deer Peak.